

Title	INTEGRAL TRANSPORT THEORY OF NEUTRON BEHAVIOUR IN HETEROGENEOUS LATTICE CELLS
Author(s)	竹田, 敏一
Citation	大阪大学, 1973, 博士論文
Version Type	VoR
URL	https://hdl.handle.net/11094/542
rights	
Note	

Osaka University Knowledge Archive : OUKA

<https://ir.library.osaka-u.ac.jp/>

Osaka University

***INTEGRAL TRANSPORT THEORY OF
NEUTRON BEHAVIOUR IN
HETEROGENEOUS LATTICE CELLS***

1973

Toshikazu TAKEDA

INTEGRAL TRANSPORT THEORY OF NEUTRON BEHAVIOUR
IN HETEROGENEOUS LATTICE CELLS

by

Toshikazu TAKEDA

A thesis submitted in partial fulfillment
of the requirements for the degree of

DOCTOR OF ENGINEERING

Department of Nuclear Engineering

Osaka University

CONTENTS

Chapter 1	Introduction	1
	References	8
Chapter 2	Improvement of the First-Flight Collision Probability Method	
§2.1	Introduction	9
§2.2	Basis of the First-Flight Collision Probability Method	12
§2.3	Effect of Anisotropic Scattering	14
§2.4	Space Dependency of the Collision Probability. .	23
§2.5	Numerical Results and Conclusions	30
	Appendices	42
	References	48
Chapter 3	Effect of Lattice Configuration	
§3.1	Introduction	49
§3.2	Disadvantage Factor in Two-Region Polygonal Cells	52
§3.3	Application to Multi-Region Polygonal Cell System	59
§3.4	Effect of Anisotropic Scattering in a Square Cell	70
§3.5	Numerical Results and Conclusions	74
	Appendices	82
	References	87

Chapter 4	Flux Calculation in Lattice Cells	
§4.1	Introduction	88
§4.2	Flux Distribution in Cluster Systems	92
§4.3	Effect of Finiteness of Cell Systems on Flux Distribution	109
§4.4	Neutron Spectra in a Resonance	122
§4.5	Numerical Results and Conclusions	126
	References	136
Chapter 5	Application to the Calculation of the Anisotropic Diffusion Coefficients	
§5.1	Introduction	138
§5.2	Derivation of the Benoist Formula of Anisotropic Diffusion Coefficient	141
§5.3	Calculation of the Diffusion Coefficients	148
§5.4	Numerical Results and Conclusions	157
	Appendices	165
	References	168
Chapter 6	Summary and Conclusions	169
	Acknowledgement	172
	List of Publications by the Author	173

CHAPTER 1

INTRODUCTION

The study of neutron behaviour in cell systems in nuclear reactors is very important in the determination of the critical condition. The equation which represents the neutron behaviour is the so-called Boltzmann equation. The equation may be written in two forms; one being the integro-differential equation and the other the integral equation.

The integro-differential equation has been treated by many authors both exactly and approximately. Exact treatments of the equation have been done by Case *et al.*⁽¹⁾ using the singular eigenfunction expansion method or the Fourier transform method, although they are limited to slab systems and cannot be adopted in practical problems. And on the other hand, approximation methods such as the P_n method⁽²⁾, the S_n method⁽³⁾ and the Monte Carlo method⁽⁴⁾ have been exploited and used in the calculation of the neutron flux for several geometries. The application of the P_n method to a highly heterogeneous system, however, has some limitation because the method requires many terms of the Legendre polynomials to express the neutron flux with strict accuracy. The treatment of such a system on the basis of the S_n method requires a large number of mesh points to express the fine structure of spatial distribution of neutrons. In the Monte Carlo method, the transport equation cannot be solved in a reasonable time

even with a high-speed computer, because the cross section varies in a complicated manner with neutron energy and the system itself is very complex in the geometrical arrangement.

On the contrary, the integral transport equation yields a better approximation in a highly heterogeneous system though it cannot be solved exactly. This comes from the fact that in the integral transport theory the boundary condition at interfaces between two different materials is unnecessary. An approximation in the integral transport theory has become known as the collision probability method. In this approximation, there are two procedures of treatment, the first-flight collision probability method and the multiple collision probability method.

The first-flight collision probability was first introduced by Chernick⁽⁵⁾ for calculating the resonance escape probability in 1955. This method has since been used in reactor cell calculations, the most successful application being found in the calculations of the fast-fission factor⁽⁶⁾, the thermal utilization⁽⁷⁾, and the resonance escape probability⁽⁵⁾. In 1963, Leslie⁽⁸⁾ combined the first-flight collision probability method and the diffusion theory to obtain the thermal spectra in lattice cells with large moderator regions. In 1964, the anisotropic diffusion coefficients in lattice cells were calculated by means of the generalized first-flight collision probability introduced by Benoist⁽⁹⁾.

On the other hand, the multiple collision probability was first derived by Stuart⁽¹⁰⁾ in 1957 to obtain the blackness of a fuel rod. Since then the method has been extended to multi-region cell problems by Amouyal *et al.*^{(11),(12)} and Müller⁽¹³⁾. It was also adopted to

calculate fast-fission factors in more heterogeneous cluster systems by Rognon⁽¹⁴⁾. Mayer⁽¹⁵⁾, in 1968, improved the method so that it could be applied to the neutron shielding problems.

The difference between the two collision probability methods comes from the use of different types of transport kernel of neutrons. In the first-flight collision probability method, the system under consideration is divided into some regions in which the neutron cross sections are constant. Thus obtained is the probability that a neutron born isotropically and uniformly in one region undergoes its first collision in a given region. This is called the first-flight collision probability. By using this probability, the average flux in each region may be obtained from simultaneous equations. In the multiple collision probability method, the neutron currents at each interface are connected by the multiple collision probability. This is the probability that a neutron injected in some region through a boundary escapes from the region through one of the boundaries after some collisions in the medium. In general, the multiple collision probability can be expressed by means of the first-flight collision probabilities.

The both collision probability methods are powerful in the treatment of cell problems or shielding problems. In the collision probability methods, however, several basic assumptions are included. Some of them prevent the methods from being applied to the analysis of fast neutron behaviour. In this thesis we will improve the collision probability method by removing the basic assumptions mainly in the first-flight collision probability method, and extend the method to apply to various problems. Since the energy dependence of the

neutron flux may be treated by dividing the energy range into many groups, the treatment in this paper is mainly concerned with one-speed problems. The extension to the multigroup theory may be done directly. The basic assumptions included in the first-flight collision probability method are the isotropy of neutron scattering and of source distribution and the flatness of neutron flux in each region.

In order to remove these assumptions, a new definition is proposed for the first-flight collision probability in Chapter 2 so that it takes into account the effects of anisotropic scattering and of the spatial change of flux distribution in each region in a cylindrical cell. This probability is obtained by expanding the scattering kernel, neutron angular flux and source term into spherical harmonics series about the neutron direction and then the neutron flux into a Legendre series about space coordinate. Making use of the new reciprocity relation and the conservation law, we introduce the probability applicable to a lattice system under the condition that all neutrons impinging on the cell boundary should reflect, with isotropic distribution, back into the original cell. In §2.3, the effect of the linearly anisotropic scattering in 2-region cells is studied particularly in detail under the assumption that all the components of neutron angular flux (flux and current etc.) are constant in each annular region. The assumption of the flat current, however, is not so good as that of the flat flux. This is based on the fact that the neutron current shows a large variation when it goes through a lattice cell, because of the strong neutron absorption in the fuel rod. In §2.4, the approximation of the flat flux and flat current in each region is improved by expanding the angular flux in a Legendre

series about the space coordinate.

Up to this point the cell boundary has been assumed to be circular (according to the Wigner Seitz cell method). However, in practice, the configuration of the cell boundary is polygonal (square, hexagonal and so on). It will be possible to estimate the difference from the exact boundary condition (effect of the lattice configuration) if we divide a cell into a large number of two dimensional regions and calculate the first-flight collision probabilities among the regions. The evaluation of the probabilities in two dimensional system, however, is very complicated. Moreover, the analytical expression of the effect of the lattice configuration is impossible to make in such a method.

In Chapter 3, the lattice configuration is treated analytically by using the multiple and the first-flight collision probability methods. In the first place derived is the analytic expression of the mono-energetic disadvantage factor in polygonal cells containing 2 regions (fuel and moderator). In view of the lattice configuration, an extended Dancoff factor is newly introduced. This factor is defined as the probability that a neutron escaping from a fuel rod makes its first collision in other fuel rods when all the materials are replaced by the moderator. In the fuel rod the blackness of the rod is used to express the flux depression as in the paper by Amouyal *et al.* Thus the effect of the lattice configuration is represented analytically by two factors. Then, we extend the method to multi-region cell problems by adopting the balance equations of neutron currents on the boundaries of each region and by obtaining the multiple collision probabilities through a variational technique. Finally a study is made of the effect of anisotropic scattering on the flux distribution

in square cells whose moderator region is thin. In the study we divide the cell into many mesh regions as in the THERMOS code⁽¹⁶⁾ and calculate isotropic and anisotropic transition probabilities among these mesh points.

In Chapter 4 we apply the first-flight collision probability to the calculation of flux distribution in lattice cells. In §4.2 the first-flight collision probabilities in a cluster system are obtained and the flux distribution in the system is calculated. The direct calculation of the first-flight collision probabilities in highly heterogeneous systems is very complicated and time-consuming, then approximations are required. In the present method both the collision probability in an annular system and the transition probability for a neutron escaping from one subcell to the other are calculated and combined. In §4.3 the effect of finiteness of cell systems in the axial direction on the flux distribution is studied. The modal expansion method is adopted for the neutron distribution in the axial direction. Then derived is a kind of first-flight collision probability which includes the modes in the axial direction as a weighting function. This probability is calculated in slab and cylindrical cells, from which the flux components in the horizontal direction are obtained. In §4.4 the neutron spectra and the resonance integral are obtained analytically in a 2-region cell containing fuel and moderator.

In Chapter 5 the anisotropic diffusion coefficients are calculated by the improved first-flight collision probability method for slab and square lattice cells with use made of the Benoist formula. In utilizing the integral transport theory, only several collisions suffered by a neutron have hitherto been considered. In this chapter

we take into consideration the effect of an infinite number of collisions of a neutron by solving simultaneous equations. Further, we consider the anisotropic scattering by means of the generalized first-flight collision probability. Then we estimate the fundamental and the additional terms in the Benoist formula. We will also discuss the difference between the experimental and theoretical values of the anisotropic diffusion coefficients.

In Chapter 6, the summary of the previous chapters is presented. Furthermore, we will discuss the possibilities of extension of the collision probability method to a complicated three-dimensional system, a multigroup theory and time-dependent problems.

References

- (1) CASE, K.M., ZWEIFEL, P.F.: "Linear Transport Theory", Addison-Wesley Publishing Co., (1967).
- (2) DAVISON, B.: "Neutron Transport Theory", Oxford University Press, (1958).
- (3) CARLSON, B.G.: LA 1891 (1955).
- (4) SPANIER, J., GEIBARD, E.M.: "Monte Carlo Principles and Neutron Transport Problem", Addison-Wesley Publishing Co., (1969).
- (5) CHERNICK, J.: "The Theory of Uranium Water Lattices", Proc. 1st International Conf. Peaceful Uses of Atomic Energy, Geneva, 5, 215 (1955).
- (6) CARLVIK, I., PERSHAGEN, B.: AE-21 (1959).
- (7) LESLIE, D.C., JONSSON, A.: Nucl. Sci. Eng., 23, 272 (1965).
- (8) LESLIE, D.C.: J. Nucl. Energy, 17, 293 (1963).
- (9) BENOIST, P.: CEA-R 2278 (1964).
- (10) STUART, G.W.: Nucl. Sci. Eng., 2, 617 (1957).
- (11) AMOUYAL, A., BENOIST, P., HOROWITZ, J.: J. Nucl. Energy, 6, 79 (1957).
- (12) AMOUYAL, A., BENOIST, P., GUIONNET, C.: CEA-1967 (1961).
- (13) MÜLLER, A., LINNARTZ, E.: Nukleonik, 5, 23 (1963).
- (14) ROGNON, J.: Nucl. Sci. Eng., 30, 109 (1967).
- (15) MAYER, L.: "Berechnung von Fluss verteilungen in Reactorrand-schichten und Zellen mit erweiterten Mehrfachstosswahrscheinlichkeiten", Doktorschrift, (1968).
- (16) HONECK, H.C.: BNL-5826, (1961).

CHAPTER 2

IMPROVEMENT OF THE FIRST-FLIGHT COLLISION PROBABILITY METHOD

§2.1 Introduction

Various characteristic factors of a cell have been calculated with the use of the first-flight collision probability based on the assumption of isotropic scattering in the system. In practice, however, appreciable anisotropic scatterings occur in the moderator or coolant composed of light nuclei. In addition, the heterogeneous structure of a system causes an anisotropic neutron distribution. One of the methods to take these effects into account is to use the usual transport cross section instead of the neutron cross section included in the collision probability calculation. The adoption of the transport cross section is, however, valid only when the anisotropic scattering is repeated infinitely in a homogeneous medium. The use of a generalized first-flight collision probability that includes the effect of anisotropic scattering has already been introduced by Takahashi^{(1),(2)} in a cylindrical cell. In the method it was assumed that flux and current are constant in each region in the system. Furthermore he assumed that a neutron reaching the cell boundary undergoes perfect reflection as he did for the problem of isotropic scattering⁽³⁾. For a lattice with a rather large pitch, this assumption would appear to be quite valid, but it is not the case for a closely packed lattice. In such a case the isotropic return boundary condition is proved to be rather good⁽⁴⁾.

Before we perform the improvement of the first-flight collision probability method, in §2.2 the basis of the method is described briefly. In §2.3 we will extend the problem to include the anisotropic scattering and introduce a new type of first-flight collision probability with a detailed example of a two-region cell. This probability can be derived when we calculate the flux originating from a source with cosine distribution in the radial direction instead of the Cartesian axis directions used in Benoist's theory⁽⁵⁾. In the probability the finiteness of anisotropic collision number in some regions and the direction of neutron path after anisotropic scattering were taken into account. Moreover, it satisfies both the usual reciprocity relation and the usual conservation law.

The assumption of the flat flux and the flat current may be improved by the increment of the number of partition. Nevertheless the improvement is very slow for the calculation of the effect of the anisotropic scattering. This is due to the fact that, from Fick's law, the assumption of flat flux in a given region is contradictory to the assumption of flat current in the region. Furthermore, different from the case of calculating the average flux for isotropic scattering, it is difficult to determine the way how to divide a cell for the case where we calculate the effect of anisotropic scattering since the current shows appreciable change through the cell. Brun and Kavenoky⁽⁶⁾ studied the anisotropic effect using the conservation law which relates the flux and current, but their method was limited up to the linearly anisotropic scattering.

Therefore, in §2.4, we will take account of the spatial dependence of the neutron angular flux in each annular region by expanding it into a Legendre series. This is an extension of the method for a slab system by Corngold⁽⁷⁾ and Carlvik⁽⁸⁾ to a cylindrical cell.

In §2.5 the effect of anisotropic scattering on the flux distribution is evaluated numerically in cylindrical lattice cells both with and without the assumption of flat flux and flat current.

§2.2 Basis of the First-Flight Collision Probability Method

In a steady state the neutron angular flux $\phi(\vec{r}, \vec{\Omega}, E)$ at position \vec{r} along direction $\vec{\Omega}$ with energy E satisfies the integral Boltzmann equation:

$$\phi(\vec{r}, \vec{\Omega}, E) = \int_0^\infty dR \, e^{-\Sigma \hat{R}} \left[\int_0^\infty dE' \int_{4\pi} d\vec{\Omega}' \Sigma_s(\vec{r}; \vec{\Omega}' \rightarrow \vec{\Omega}, E' \rightarrow E) \cdot \phi(\vec{r}, \vec{\Omega}', E') + S(\vec{r}, \vec{\Omega}, E) \right], \quad (2.1)$$

where R is the distance between points \vec{r} and \vec{r}' , $\vec{\Omega}$ is the directional vector given by $\vec{\Omega} = (\vec{r} - \vec{r}')/R$, $\Sigma \hat{R}$ is the optical distance between points \vec{r} and \vec{r}' , $\Sigma_s(\vec{r}; \vec{\Omega}' \rightarrow \vec{\Omega}, E' \rightarrow E)$ is the scattering kernel at point \vec{r}' from direction $\vec{\Omega}'$ at energy E' to direction $\vec{\Omega}$ at energy E , and $S(\vec{r}', \vec{\Omega}, E)$ is the neutron source at point \vec{r}' along the direction $\vec{\Omega}$ and with energy E . In the above equation the induced fission by neutron is neglected though it might be included in the scattering kernel. At the beginning we assume that the scattering and the source are isotropic in the laboratory system:

$$\Sigma_s(\vec{r}; \vec{\Omega}' \rightarrow \vec{\Omega}, E' \rightarrow E) = \frac{1}{4\pi} \Sigma_s(\vec{r}; E' \rightarrow E), \quad (2.2a)$$

$$S(\vec{r}, \vec{\Omega}, E) = \frac{1}{4\pi} S(\vec{r}, E). \quad (2.2b)$$

By integrating Eq. (2.1) over the whole angle of $\vec{\Omega}$, we obtain

$$\phi(\vec{r}, E) = \int \frac{d\vec{\Omega}}{4\pi} \int_0^\infty dR \, e^{-\Sigma \hat{R}} \left[S(\vec{r}, E) + \int_0^\infty dE' \Sigma_s(\vec{r}; E' \rightarrow E) \phi(\vec{r}, E') \right], \quad (2.3)$$

where $\phi(\vec{r}, E)$ is the neutron flux at point \vec{r} and with energy E , and is defined by

$$\phi(\vec{r}, E) = \int_{4\pi} d\vec{\Omega} \, \phi(\vec{r}, \vec{\Omega}, E). \quad (2.4)$$

In the next step the system under consideration is divided into several regions so as the neutron cross sections to be regarded as constants in each region. There the neutron flux $\phi(\vec{r}, E)$ is assumed to be constant and in the i-th region, for example, it is expressed by $\phi_i(E)$. Integration of Eq. (2.3) about \vec{r} over the volume V_j of the j-th region making use of the relation $d\vec{r} = R^2 dR d\vec{R}$ leads to the equation

$$\Sigma_j(E) V_j \phi_j(E) = \sum_i P_{ij}(E) V_i \left\{ S_i(E) + \int_0^\infty dE' \Sigma_{is}(E' \rightarrow E) \phi_i(E') \right\}, \quad (2.5)$$

where $\Sigma_j(E)$ is the total cross section in the j-th region and $P_{ij}(E)$ is the first-flight collision probability defined by

$$P_{ij}(E) = \frac{\Sigma_j(E)}{V_i} \int_{V_i} d\vec{r}' \int_{V_j} d\vec{r} \frac{1}{4\pi R^2} e^{-\Sigma R}. \quad (2.6)$$

In Eq. (2.6) the ranges of integration about \vec{r} and \vec{r}' are over the volumes of the j-th and the i-th regions respectively. The energy range is divided into multi-groups. The average flux in the energy group g is denoted by ϕ_i^g . Then from Eq. (2.6) we obtain the simultaneous equation

$$\Delta E_g \Sigma_j^g V_j \phi_j^g = \sum_i P_{ij}^g V_i \sum_{g'} \Delta E_{g'} \left\{ S_{ig'} S_i^g + \phi_i^{g'} \Sigma_{is}^{g' \rightarrow g} \right\}, \quad (2.7)$$

where ΔE_g and $\Delta E_{g'}$ are the energy widths of the groups g and g' and $\Sigma_{is}^{g' \rightarrow g}$ is the scattering cross section in the i-th region from group g' to g, and is defined by

$$\Sigma_{is}^{g' \rightarrow g} = \frac{\int_{g'} dE' \int_g dE \Sigma_{is}(E' \rightarrow E) \phi_i(E')}{\int_{g'} dE' \phi_i(E')}. \quad (2.8)$$

Equation (2.7) is the basic equation in the first-flight collision probability method. In the following section we will show that the assumption of isotropic scattering, Eq. (2.2a), can be removed by intro-

ducing a generalized first-flight collision probability.

§2.3 Effect of Anisotropic Scattering⁽¹¹⁾

The neutron angular flux $\phi(\vec{r}, \vec{\Omega}, E)$ is considered in a cylindrical cell with infinite axial length. The direction $\vec{\Omega}$ is expressed by two angles θ and α as shown in Fig. 2.1.

We expand the angular flux $\phi(\vec{r}, \vec{\Omega}, E)$, angular source $S(\vec{r}, \vec{\Omega}, E)$ and scattering kernel $\Sigma_s(\vec{r}, \vec{\Omega}' \rightarrow \vec{\Omega}, E' \rightarrow E)$ into spherical harmonics series about angles θ and α ⁽¹²⁾:

$$\phi(\vec{r}, \vec{\Omega}, E) = \sum_{n=0}^{\infty} \sum_{m=-n}^n \phi^{n,m}(\vec{r}, E) Y_n^m(\vec{\Omega}), \quad (2.9)$$

$$S(\vec{r}, \vec{\Omega}, E) = \sum_{n=0}^{\infty} \sum_{m=-n}^n S^{n,m}(\vec{r}, E) Y_n^m(\vec{\Omega}), \quad (2.10)$$

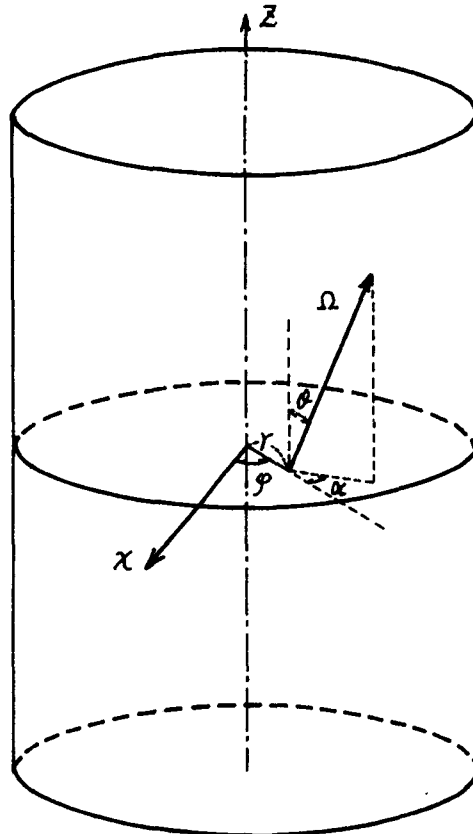


Fig. 2.1 Coordinate in a cylindrical cell

$$\Sigma_s(\vec{r}, \vec{\Omega}' \rightarrow \vec{\Omega}, E' \rightarrow E) = \sum_{n=0}^{\infty} \sum_{m=-n}^n \Sigma_s^n(\vec{r}, E' \rightarrow E) Y_n^m(\vec{\Omega}) Y_n^{m*}(\vec{\Omega}'), \quad (2.11)$$

$$\text{where } Y_n^m(\vec{\Omega}) = H_n^m P_n^m(\cos \theta) e^{im\phi}, \quad (2.12a)$$

$$H_n^m = \sqrt{\frac{(2n+1)(n-m)!}{4\pi(n+m)!}}. \quad (2.12b)$$

The average cosine of scattering angle $\bar{\mu}$ is obtained by making use of Eq. (2.11):

$$\bar{\mu} = \frac{\int_{4\pi} d\vec{\Omega}' \Sigma_s(\vec{r}, \vec{\Omega}' \rightarrow \vec{\Omega}, E' \rightarrow E) (\vec{\Omega}' \cdot \vec{\Omega})}{\int_{4\pi} d\vec{\Omega}' \Sigma_s(\vec{r}, \vec{\Omega}' \rightarrow \vec{\Omega}, E' \rightarrow E)} = \frac{\Sigma_s^1}{\Sigma_s^0}. \quad (2.13)$$

Since we are dealing with an infinitely long cylindrical cell, there remain in Eqs. (2.9)~(2.11) only the terms of which $n+m$ is an even number. The transport equation (2.1) may be rewritten in the following form:

$$\begin{aligned} \phi(\vec{r}, \vec{\Omega}, E) &= \int d\vec{r}' \int_{4\pi} d\vec{\Omega}' \frac{e^{-\widehat{\Omega}\vec{r}}}{R^2} \delta(\vec{\Omega} - \vec{\Omega}^*) \delta(\vec{\Omega}' - \vec{\Omega}^*) \\ &\cdot \left\{ S(\vec{r}, \vec{\Omega}', E) + \int_0^\infty dE' \int_{4\pi} d\vec{\Omega}'' \phi(\vec{r}, \vec{\Omega}'', E') \Sigma_s(\vec{r}, \vec{\Omega}'' \rightarrow \vec{\Omega}', E' \rightarrow E) \right\}, \end{aligned} \quad (2.14)$$

where $\vec{\Omega}^* = (\vec{r} - \vec{r}')/|\vec{r} - \vec{r}'|$, the vector along the neutron path.

Substituting Eqs. (2.9)~(2.11) into Eq. (2.14), multiplying by $Y_n^{m*}(\vec{\Omega})$, and then integrating over the whole angle of $\vec{\Omega}$, we obtain the following equation for $\phi^{n,m}$:

$$\begin{aligned} \phi^{n,m}(\vec{r}, E) &= \sum_{n'=0}^{\infty} \sum_{m'=-n'}^{n'} \int d\vec{r}' \frac{e^{-\widehat{\Omega}\vec{r}}}{R^2} Y_n^{m*}(\vec{\Omega}^*) Y_{n'}^{m'}(\vec{\Omega}^*) \\ &\cdot \left\{ S^{n',m'}(\vec{r}, E) + \int_0^\infty dE' \phi^{n',m'}(\vec{r}, E') \Sigma_s^{n'}(\vec{r}, E' \rightarrow E) \right\}. \end{aligned} \quad (2.15)$$

In order to make the anisotropic mode of collisions at the both ends of a neutron path explicit, we represent $\vec{\Omega}^*$'s in both spherical harmo-

nics functions by the angles defined at \vec{r} and \vec{r}' respectively; azimuthal angles α and α' are measured from the radial lines at the points \vec{r} and \vec{r}' respectively (see Fig. 2.2), so that $\gamma_n^m(\vec{r})$ at α and $\gamma_n^m(\vec{r}')$ at α' have not the same expression.

If we transform $\phi^{n,m}$ to

$$\phi_{(n0)}^{(0)} = \frac{\phi^{n,0}}{H_n^0}, \quad (2.16a)$$

$$\phi_{(nm)}^{(1)} = \frac{\phi^{n,m} + (-1)^m \phi^{n,-m}}{2 H_n^m}, \quad (2.16b)$$

$$\phi_{(nm)}^{(2)} = i \frac{\phi^{n,m} - (-1)^m \phi^{n,-m}}{2 H_n^m}, \quad (2.16c)$$

and use the correspondents for $S^{n,m}$, we obtain the following three equations:

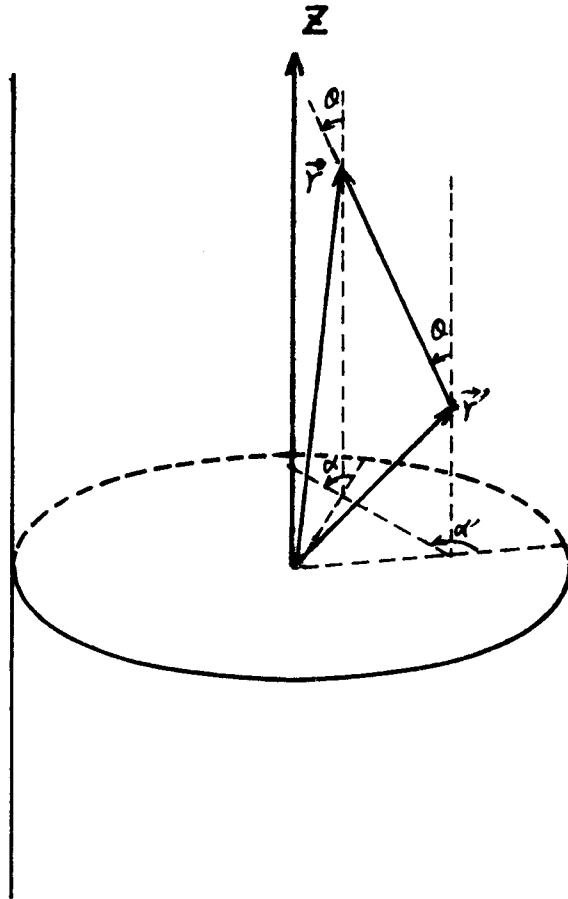


Fig. 2.2 Directions of a neutron motion at r and r'

$$\begin{aligned}
\phi \begin{pmatrix} 0 \\ 1 \\ 0 \end{pmatrix} (\vec{r}, E) &= \sum_{n=0}^{\infty} \int d\vec{r}' \frac{\bar{e}^{-\vec{\Sigma}\vec{R}}}{R^2} P_n(\cos \theta') \\
&\cdot \begin{pmatrix} P_n(\cos \theta) \\ P_n^m(\cos \theta) \cos m\alpha \\ P_n^m(\cos \theta) \sin m\alpha \end{pmatrix} (H_n^0)^2 \left\{ S^{(n0)}(\vec{r}, E) + \int_0^{\infty} dE' \phi^{(n0)}(\vec{r}, E') \Sigma_S^{n'}(\vec{r}, E' \rightarrow E) \right\} \\
&+ \sum_{n'=0}^{\infty} \sum_{n=1}^{n'} \int d\vec{r}' \frac{\bar{e}^{-\vec{\Sigma}\vec{R}}}{R^2} P_{n'}^{m'}(\cos \theta') 2 \cos m'\alpha' \\
&\cdot \begin{pmatrix} P_{n'}(\cos \theta) \\ P_{n'}^m(\cos \theta) \cos m\alpha \\ P_{n'}^m(\cos \theta) \sin m\alpha \end{pmatrix} (H_{n'}^{m'})^2 \left\{ S^{(n'm')}(\vec{r}, E) + \int_0^{\infty} dE' \phi^{(n'm')}(\vec{r}, E') \Sigma_S^{n'}(\vec{r}, E' \rightarrow E) \right\} \\
&+ \sum_{n'=0}^{\infty} \sum_{m'=1}^{n'} \int d\vec{r}' \frac{\bar{e}^{-\vec{\Sigma}\vec{R}}}{R^2} P_{n'}^{m'}(\cos \theta') 2 \sin m'\alpha' \\
&\cdot \begin{pmatrix} P_{n'}(\cos \theta) \\ P_{n'}^m(\cos \theta) \cos m\alpha \\ P_{n'}^m(\cos \theta) \sin m\alpha \end{pmatrix} (H_{n'}^{m'})^2 \left\{ S^{(n'm')}(\vec{r}, E) + \int_0^{\infty} dE' \phi^{(n'm')}(\vec{r}, E') \Sigma_S^{n'}(\vec{r}, E' \rightarrow E) \right\} .
\end{aligned}
\tag{2.17}$$

In this equation, $\phi^{(n0)}$, $\phi^{(n'm')}$ and $\phi^{(n'm)}$ are real and have clear physical meanings. For example, $\phi^{(00)}(\vec{r}, E)$ corresponds to the scalar flux at point \vec{r} , $\phi^{(11)}(\vec{r}, E)$ to the radial current and $\phi^{(21)}(\vec{r}, E)$ to the rotational current around the z-axis. The heterogeneous system is divided into many regions and it is assumed that $\phi^{(n0)}$, $\phi^{(n'm')}$ and $\phi^{(n'm)}$ are constants in each region. In the i-th region, for example, they are expressed by $\phi_i^{(n0)}$, $\phi_i^{(n'm')}$ and $\phi_i^{(n'm)}$ respectively. We introduce an operator \mathcal{H}_{ij} defined by

$$\mathcal{H}_{ij} \psi = \frac{\Sigma_j}{V_i} \int_{V_i} d\vec{r}' \int_{V_j} d\vec{r} \frac{\bar{e}^{-\vec{\Sigma}\vec{R}}}{R^2} \psi .
\tag{2.18}$$

Using this operator the following generalized collision probabilities

are defined:

$$P_{ij}^{(n'0) \rightarrow (n \begin{pmatrix} 0 \\ 1 \\ m \end{pmatrix})} = (H_n^0)^2 \mathcal{H}_{ij} P_n(\cos \theta) P_n^{(0)}(\cos \theta) \begin{pmatrix} 1 \\ \cos m \alpha \\ \sin m \alpha \end{pmatrix}, \quad (2.19)$$

$$P_{ij}^{(n'm') \rightarrow (n \begin{pmatrix} 0 \\ 1 \\ m \end{pmatrix})} = 2(H_n^{m'})^2 \mathcal{H}_{ij} P_n^{m'}(\cos \theta) P_n^{(0)}(\cos \theta) \cos m' \alpha' \begin{pmatrix} 1 \\ \cos m \alpha \\ \sin m \alpha \end{pmatrix}, \quad (2.20)$$

$$P_{ij}^{(n'm') \rightarrow (n \begin{pmatrix} 0 \\ 1 \\ m \end{pmatrix})} = 2(H_n^{m'})^2 \mathcal{H}_{ij} P_n^{m'}(\cos \theta) P_n^{(0)}(\cos \theta) \sin m' \alpha' \begin{pmatrix} 1 \\ \cos m \alpha \\ \sin m \alpha \end{pmatrix}. \quad (2.21)$$

By using Eqs. (2.19)~(2.21), Eq. (2.17) is transformed to

$$\begin{aligned} \Sigma_j(E) V_j \phi_j \left(n \begin{pmatrix} 0 \\ 1 \\ m \end{pmatrix} \right) (E) &= \sum_{i=1}^N \sum_{n'=0}^{\infty} \left[P_{ij}^{(n'0) \rightarrow (n \begin{pmatrix} 0 \\ 1 \\ m \end{pmatrix})} \left\{ S_i^{(n'0)}(E) \right. \right. \\ &+ \left. \int_0^{\infty} dE' \phi_i^{(n'0)}(E') \Sigma_{is}^{n'}(E' \rightarrow E) \right\} + \sum_{m'=1}^{n'} P_{ij}^{(n'm') \rightarrow (n \begin{pmatrix} 0 \\ 1 \\ m \end{pmatrix})} \left\{ S_i^{(n'm')}(E) + \int_0^{\infty} dE' \phi_i^{(n'm')}(E') \right. \\ &\cdot \left. \Sigma_{is}^{n'}(E' \rightarrow E) \right\} + \sum_{m'=1}^{n'} P_{ij}^{(n'm') \rightarrow (n \begin{pmatrix} 0 \\ 1 \\ m \end{pmatrix})} \left\{ S_i^{(n'm')}(E) + \int_0^{\infty} dE' \phi_i^{(n'm')}(E') \Sigma_{is}^{n'}(E' \rightarrow E) \right\} \Big], \end{aligned} \quad (2.22)$$

where N is the total number of regions included in the system, and

$\Sigma_{is}^{n'}$ is the scattering cross section of order n' in the i -th region.

If we assume that the scattering as well as the angular distribution of the source are isotropic, Eq. (2.22) reduces to the same equation as Eq. (2.5) since $P_{ij}^{(00) \rightarrow (00)}$ corresponds to the usual first-flight collision probability P_{ij} .

We now consider the case where the scattering is linearly anisotropic ($n = 0, 1$ in Eq. (2.11)), and the rotational source is zero ($S_i^{(2m)} = 0$) in Eq. (2.22) within the limit of the one-velocity theory. Since $P_{ij}^{(n'm') \rightarrow (n0)}$, $P_{ij}^{(n'm') \rightarrow (n1)}$, $P_{ij}^{(n'0) \rightarrow (n2)}$ and $P_{ij}^{(n'm') \rightarrow (n2)}$ disappear in a cylindrical system, only $\phi_i^{(0)}$ and $\phi_i^{(1)}$ remain in Eq. (2.22).

So we obtain

$$\begin{aligned} \Sigma_j V_j \phi_j^{(00)} = \sum_{i=1}^N \left[P_{ij}^{(00) \rightarrow (00)} \{ S_i^{(00)} + \Sigma_{is}^0 \phi_i^{(00)} \} V_i \right. \\ \left. + P_{ij}^{(11) \rightarrow (00)} \{ S_i^{(11)} + \Sigma_{is}' \phi_i^{(11)} \} V_i \right], \end{aligned} \quad (2.23)$$

$$\begin{aligned} \Sigma_j V_j \phi_j^{(11)} = \sum_{i=1}^N \left[P_{ij}^{(00) \rightarrow (11)} \{ S_i^{(00)} + \Sigma_{is}^0 \phi_i^{(00)} \} V_i \right. \\ \left. + P_{ij}^{(11) \rightarrow (11)} \{ S_i^{(11)} + \Sigma_{is}' \phi_i^{(11)} \} V_i \right]. \end{aligned} \quad (2.24)$$

It can be concluded from the above equations that four kinds of probabilities are necessary for the study of the effects of the forward scattering in a cell.

For simplicity we treat a cylindrical cell composed of two media under the assumption that scattering is isotropic in the inner region 1 while anisotropic (forward) scattering occurs in the external region 2.

An extension to the case of multi-region cells can easily be done.

If the distributions of sources are isotropic in the both regions

($S_i^{(11)} = 0$), we obtain from Eqs. (2.23) and (2.24)

$$\Sigma_j V_j \phi_j^{(00)} = \sum_{i=1}^2 P_{ij}^* (S_i^{(00)} + \Sigma_{is}^0 \phi_i^{(00)}) V_i \quad (2.25a)$$

where

$$P_{ij}^* = P_{ij}^{(00) \rightarrow (00)} + \frac{P_{i2}^{(00) \rightarrow (11)} \frac{\Sigma_{2s}'}{\Sigma_{2s}^0} P_{2j}^{(11) \rightarrow (00)}}{1 - P_{22}^{(11) \rightarrow (11)} \frac{\Sigma_{2s}'}{\Sigma_{2s}^0}} \quad (2.25b)$$

Thus, the problem of anisotropic scattering in the moderator can be treated with use made of the new type probability P_{ij}^* in place of the usual probability $P_{ij}^{(00) \rightarrow (00)}$ for isotropic scattering. The second term on the right-hand side of Eq. (2.25b) represents the probability with which a neutron born in the i-th region with an isotropic distribution repeats its anisotropic scattering in region 2 and, after anisotropic

escape from the region 2, collides isotropically in the j-th region.

The reciprocity relations for the four kinds of probabilities in Eq. (2.25b) are as follows:

$$\sum_i V_i P_{ij}^{(00) \rightarrow (00)} = \sum_j V_j P_{ji}^{(00) \rightarrow (00)}, \quad (2.26a)$$

$$\sum_i V_i P_{ij}^{(11) \rightarrow (00)} = -3 \sum_j V_j P_{ji}^{(00) \rightarrow (11)}, \quad (2.26b)$$

$$\sum_i V_i P_{ij}^{(11) \rightarrow (11)} = \sum_j V_j P_{ji}^{(11) \rightarrow (11)}. \quad (2.26c)$$

Here the minus sign appearing in Eq. (2.26b) denotes that the paths of neutrons traveling from the i-th region to the j-th region and the corresponding paths from the j-th region to the i-th region are mutually inverse and α is replaced by $\pi - \alpha$. The neutron conservation laws are

$$\sum_{j=1}^{\infty} P_{ij}^{(00) \rightarrow (00)} = 1, \quad (2.27a)$$

$$\sum_{j=1}^{\infty} P_{ij}^{(11) \rightarrow (00)} = 0. \quad (2.27b)$$

The first is the usual conservation law and the second means that, once the summation is made over the whole volume, the directional component of the probability no longer retains the source direction owing to the isotropy of the first collision.

We next define the probabilities $P_{sj}^{(\frac{l}{nm})}$ that a neutron with an isotropic distribution enters into a cell through a unit area of the boundary to undergo the first collision of mode $(\frac{l}{nm})$ in the j-th region:

$$P_{sj}^{(00)} = \frac{4}{\pi} \int \frac{dS}{S} \int_0^{\frac{\pi}{2}} d\theta \sin \theta \int_0^{\frac{\pi}{2}} d\varphi (\vec{n} \cdot \vec{\Omega}_s) \int_0^{R_j} dR e^{-\Sigma_j R} e^{-\widehat{\Sigma}_{R_{j+1}}} \Sigma_j, \quad (2.28a)$$

$$P_{sj}^{(11)} = -\frac{4}{\pi} \int \frac{dS}{S} \int_0^{\frac{\pi}{2}} d\theta \sin^2 \theta \int_0^{\frac{\pi}{2}} d\varphi (\vec{n} \cdot \vec{\Omega}_s) \int_0^{R_j} dR e^{-\Sigma_j R} e^{-\widehat{\Sigma}_{R_{j+1}}} \cos \alpha \Sigma_j. \quad (2.28b)$$

where \vec{n} is the unit vector inwards normal to the cell boundary S , $\vec{\Omega}_j$ the unit vector along the neutron path, $\widehat{\Sigma R}_{j+1}$ the optical distance from the cell boundary to the j -th region, and R_j the distance of the neutron path in the j -th region. The probability that a neutron starting isotropically from the cell boundary reaches again the cell boundary without collision is

$$P_{ss} = 1 - \sum_{j=1}^2 P_{sj}^{(00)} . \quad (2.29)$$

The probabilities $P_{sj}^{(00)}$ and $P_{sj}^{(11)}$ defined above may be related to the four generalized probabilities. First, $P_{ji}^{(11) \rightarrow (00)}$ may be transformed as follows:

$$\begin{aligned} P_{ji}^{(11) \rightarrow (00)} &= \frac{3 \Sigma_i}{V_j} \int_{V_j} d\vec{r} \int_{V_i} d\vec{r} \frac{e^{-\widehat{\Sigma R}}}{4\pi R^2} \sin \theta_j \cos \alpha_j \\ &= -\frac{3}{\Sigma_j V_j} \int dS \int_{2\pi} \frac{d\vec{\Omega}_s}{4\pi} (\vec{n} \cdot \vec{\Omega}_s) \sin \theta \int_0^{R_j} dR e^{-\widehat{\Sigma R}_{ij}} e^{-\Sigma_j R} \cos \alpha_j (1 - e^{-\Sigma_i R_i}), \end{aligned} \quad (2.30)$$

where $\widehat{\Sigma R}_{ij}$ is the optical distance between the i -th region and the j -th region. Summing the above equation over all i in a cell, we obtain

$$\begin{aligned} \sum_{i=1}^2 P_{ji}^{(11) \rightarrow (00)} &= \frac{3}{V_j} \int dS \int_{2\pi} \frac{d\vec{\Omega}_s}{4\pi} (\vec{n} \cdot \vec{\Omega}_s) \sin \theta \int_0^{R_j} dR \cos \alpha_j \{1 - e^{-(\Sigma_j R + \widehat{\Sigma R}_{j+1})}\} \\ &= -\frac{3}{\Sigma_j V_j} \int dS \int_{2\pi} \frac{d\vec{\Omega}_s}{4\pi} (\vec{n} \cdot \vec{\Omega}_s) \sin \theta \int_0^{R_j} dR \Sigma_j e^{-\Sigma_j R} e^{-\widehat{\Sigma R}_{j+1}} \cos \alpha_j . \end{aligned} \quad (2.31)$$

Using this equation, we may reduce Eq. (2.28b) to

$$P_{sj}^{(11)} = \frac{4 \Sigma_j V_j}{3 S} \sum_{i=1}^2 P_{ji}^{(11) \rightarrow (00)} . \quad (2.32)$$

In a similar manner, the following usual reciprocity relation can be obtained:

$$P_{sj}^{(00)} = \frac{4 \Sigma_j V_j}{S} \left(1 - \sum_{i=1}^2 P_{ji}^{(00) \rightarrow (00)} \right) . \quad (2.33)$$

Here we assumed that all the neutrons in a cell with isotropic or anisotropic source distributions are reflected back into the same cell with an isotropic distribution on the boundary instead of leaking out of the cell⁽¹³⁾. Benoist used here a distribution proportional to Ω_k as an anisotropic source on the inner boundary of a cell ($k = x, y, z$). Though he used such a means as to take into account the effect of angular distribution referred to Cartesian coordinates, his procedure is not necessarily convenient to take into consideration the tendency of distribution characterized by the boundary condition. There appears a difference between his method and ours in the details of determining the anisotropy of neutron flux distribution.

From the conservation laws (2.27 a,b), we can assume that the rate at which a neutron born in the i -th region is reflected on the boundary back into the same cell is the same as the rate of leakage from the cell:

$$1 - \sum_{k=1}^2 P_{ik}^{(00) \rightarrow (00)},$$

(for an isotropic source in the i -th region)

$$- \sum_{k=1}^2 P_{ik}^{(11) \rightarrow (00)},$$

(for an anisotropic source in the i -th region).

To take into account the effect of neutron current from other cells, we define $P_{ij}^{t(00) \rightarrow (00)}$, $P_{ij}^{t(00) \rightarrow (11)}$, $P_{ij}^{t(11) \rightarrow (00)}$ and $P_{ij}^{t(11) \rightarrow (11)}$ by adding the probability increase based on the reflection on the surface:

$$P_{ij}^{t(00) \rightarrow (00)} = P_{ij}^{(00) \rightarrow (00)} + (1 - \sum_{k=1}^2 P_{ik}^{(00) \rightarrow (00)}) \frac{P_{sj}^{(00)}}{1 - P_{ss}}, \quad (2.34)$$

$$P_{ij}^{t(00) \rightarrow (11)} = P_{ij}^{(00) \rightarrow (11)} + (1 - \sum_{k=1}^2 P_{ik}^{(00) \rightarrow (00)}) \frac{P_{sj}^{(11)}}{1 - P_{ss}}, \quad (2.35)$$

$$P_{ij}^{t(11) \rightarrow (00)} = P_{ij}^{(11) \rightarrow (00)} - \sum_{k=1}^2 P_{ik}^{(11) \rightarrow (00)} \frac{P_{sj}^{(00)}}{1 - P_{ss}}, \quad (2.36)$$

$$P_{i\downarrow}^{t(i') \rightarrow (i')} = P_{i\downarrow}^{(i') \rightarrow (i')} - \sum_{k=1}^2 P_{i\downarrow k}^{(i') \rightarrow (00)} \frac{P_{s\downarrow}^{(i')}}{1 - P_{ss}} \quad (2.37)$$

Using the above equations, a new type of first-flight collision probability for the case of anisotropic scattering and of the isotropic reflection boundary condition can be obtained:

$$P_{i\downarrow}^{t*} = P_{i\downarrow}^{t(00) \rightarrow (00)} + \frac{P_{i2}^{t(00) \rightarrow (i')} \frac{\Sigma_{2s}^1}{\Sigma_{2s}^0} P_{2\downarrow}^{t(i') \rightarrow (00)}}{1 - P_{22}^{t(i') \rightarrow (i')} \frac{\Sigma_{2s}^1}{\Sigma_{2s}^0}} \quad (2.38)$$

In Appendix 2A, we will show that Eqs. (2.25b) and (2.38) satisfy the usual reciprocity relation and the conservation law. The formulations for higher order anisotropy are written in Appendix 2B.

§2.4 Space Dependency of the Collision Probability⁽¹⁴⁾

In this section the assumption that all the components of neutron angular flux are constant in each region is improved in the case of cylindrical lattice cells. We divide a cell into N concentric annular regions and express the inner and outer radii of the i-th region by r_{i-1} and r_i respectively. Then the neutron and source distributions at radius r in the i-th region may be expanded using the Legendre functions $P_k(\frac{2r^2 - r_i^2 - r_{i-1}^2}{r_i^2 - r_{i-1}^2})$ ($k = 0, 1, 2, \dots$). In practice, the rotational source $S_i^{(2m)}$ can be assumed to be zero in each region. Then the flux $\phi_i^{(2m)}$ becomes zero. Therefore, from the beginning, we can expand the neutron flux and source only by $\cos m\alpha$ ($m=0, 1, 2, \dots$) in Eqs. (2.9) and (2.10). Namely we put the neutron angular distri-

bution and the source distribution in the i-th region in the forms:

$$\begin{aligned} \phi_i(\vec{r}, \vec{\Omega}) = & \sum_{n=0}^{\infty} \sum_{m=0}^n \sum_{k=0}^{\infty} (H_n^m)^2 \phi_i^{(n,m,k)} P_n^m(\cos \theta) \cos m \alpha \\ & \cdot P_k \left(\frac{2r^2 - r_i^2 - r_{i-1}^2}{r_i^2 - r_{i-1}^2} \right) (2 - \delta_{m0}), \end{aligned} \quad (2.39)$$

$$\begin{aligned} S_i(\vec{r}, \vec{\Omega}) = & \sum_{n=0}^{\infty} \sum_{m=0}^n \sum_{k=0}^{\infty} (H_n^m)^2 S_i^{(n,m,k)} P_n^m(\cos \theta) \cos m \alpha \\ & \cdot P_k \left(\frac{2r^2 - r_i^2 - r_{i-1}^2}{r_i^2 - r_{i-1}^2} \right) (2 - \delta_{m0}), \end{aligned} \quad (2.40)$$

where δ_{m0} is the Kronecker delta and H_n^m is defined by Eq. (2.12b).

As described in the last section, there remain in the above equations only the terms of $n+m$ even number. The scattering kernel $\Sigma_{is}(\vec{r}, \vec{\Omega}' \rightarrow \vec{\Omega})$ has no spatial dependence in a given region (for example in the i-th region) and has the same form as Eq. (2.11), which may be rewritten in the form:

$$\begin{aligned} \Sigma_{is}(\vec{r}, \vec{\Omega}' \rightarrow \vec{\Omega}) = & \sum_{n=0}^{\infty} \sum_{m=0}^n (H_n^m)^2 \Sigma_{is}^n P_n^m(\cos \theta) P_n^m(\cos \theta') \\ & \cdot \cos m(\alpha - \alpha') (2 - \delta_{m0}). \end{aligned} \quad (2.41)$$

We follow the similar procedure as in the preceding section; inserting Eqs. (2.39), (2.40) and (2.41) in the integral transport equation (2.14), multiplying the resulting equation by $P_n^m(\cos \theta) \cos m \alpha$ and integrating over the whole direction about $\vec{\Omega}$. Then we obtain

$$\begin{aligned} \sum_{k=0}^{\infty} \phi_i^{(n,m,k)} P_k \left(\frac{2r^2 - r_i^2 - r_{i-1}^2}{r_i^2 - r_{i-1}^2} \right) = & \int_0^{\infty} dR \int_{4\pi} d\vec{\Omega} P_n^m(\cos \theta) \cos m \alpha e^{-\vec{r} \cdot \vec{\Omega}} \\ & \cdot \sum_{n'=0}^{\infty} \sum_{m'=0}^{n'} \sum_{k'=0}^{\infty} (H_{n'}^{m'})^2 P_{n'}^{m'}(\cos \theta) \cos m' \alpha' P_{k'} \left(\frac{2r^2 - r_i^2 - r_{i-1}^2}{r_i^2 - r_{i-1}^2} \right) \\ & \cdot (2 - \delta_{m'0}) \left\{ S_i^{(n',m',k')} + \Sigma_{is}^{n'} \phi_i^{(n',m',k')} \right\}. \end{aligned} \quad (2.42)$$

We multiply the above equation by $P_k \left(\frac{2r^2 - r_i^2 - r_{i-1}^2}{r_i^2 - r_{i-1}^2} \right)$ and integrate about

\vec{r} over the volume of the j-th region, and obtain

$$\begin{aligned} \frac{1}{2k+1} V_j \phi_j^{(n,m,k)} &= \sum_{n'=0}^{\infty} \sum_{m'=0}^{n'} \sum_{k'=0}^{\infty} \sum_{i=1}^{\infty} \int_{V_i} d\vec{r}' \int_{V_j} d\vec{r} \frac{e^{-\vec{r}\vec{r}'}}{R^2} P_n^m(\cos\theta) \cos m\alpha \\ &\cdot P_k\left(\frac{2r^2 - r_i^2 - r_{i-1}^2}{r_i^2 - r_{i-1}^2}\right) (H_{n'}^{m'})^2 P_{n'}^{m'}(\cos\theta) \cos m'\alpha' P_{k'}\left(\frac{2r'^2 - r_i'^2 - r_{i-1}'^2}{r_i'^2 - r_{i-1}'^2}\right) \\ &\cdot (2 - \delta_{m'0}) \left\{ S_i^{(n',m',k')} + \sum_{i's} \phi_i^{(n',m',k')} \right\}, \end{aligned} \quad (2.43)$$

where V_j is the volume of the j-th region.

Here we define the following generalized first-flight collision probability:

$$\begin{aligned} P_{ij}^{(n',m',k') \rightarrow (n,m,k)} &= \frac{\sum_j}{V_i} \int_{V_i} d\vec{r}' \int_{V_j} d\vec{r} \frac{e^{-\vec{r}\vec{r}'}}{R^2} (H_{n'}^{m'})^2 P_{n'}^{m'}(\cos\theta) \cos m'\alpha' \\ &\cdot P_k\left(\frac{2r^2 - r_i^2 - r_{i-1}^2}{r_i^2 - r_{i-1}^2}\right) (2 - \delta_{m'0}) P_n^m(\cos\theta) \cos m\alpha P_{k'}\left(\frac{2r'^2 - r_i'^2 - r_{i-1}'^2}{r_i'^2 - r_{i-1}'^2}\right). \end{aligned} \quad (2.44)$$

The explicit expression for $P_{ij}^{(n',m',k') \rightarrow (n,m,k)}$ is given in Appendix

2C. In terms of the above equation, Eq. (2.43) reduces to

$$\frac{\sum_j V_j \phi_j^{(n,m,k)}}{2k+1} = \sum_{n'=0}^{\infty} \sum_{m'=0}^{n'} \sum_{k'=0}^{\infty} \sum_{i=1}^{\infty} P_{ij}^{(n',m',k') \rightarrow (n,m,k)} \frac{1}{V_i} \left\{ S_i^{(n',m',k')} + \sum_{i's} \phi_i^{(n',m',k')} \right\}. \quad (2.45)$$

In the case of isotropic scattering and isotropic source distribution it is sufficient to take account of the contribution from the factor with $(n,m) = (0,0)$. In order to consider up to the linearly anisotropic scattering, it will suffice to treat the contribution from the factors with $(n,m) = (0,0)$ and $(1,1)$. In any case the contribution from k must be considered from $k=0$ to $k=\infty$.

We calculate the generalized collision probability in lattice cells $P_{ij}^{t(n',m',k') \rightarrow (n,m,k)}$, which is the probability that a neutron starting with mode (n',m',k') from the i-th region undergoes the first collision of mode (n,m,k) in the j-th region in any cell. At first

we calculate the generalized first-flight collision probability for a neutron born in a cell to make its first collision in the nearest neighboring cell. As shown in Fig. 2.3, we divide a distance from the i -th region to the j -th region into two parts R_1 and R_2 ; R_1 being the path length in the original cell 1 and R_2 being the path length in the neighboring cell 2. The optical distances along R_1 and R_2 are denoted by $\widehat{\Sigma}R_1$ and $\widehat{\Sigma}R_2$ respectively. Then we obtain

$$P_{i,j}^{(n',m',k') \rightarrow (n,m,k)} = \frac{\Sigma_j}{V_i} \int_{V_i} d\vec{r} \int dR \int d\vec{\Omega} (H_n^{m'})^2 P_n^{m'}(\cos\theta) \cos m' \alpha' P_k \left(\frac{2r^2 - r_i^2 - r_{i-1}^2}{r_i^2 - r_{i-1}^2} \right) \cdot (2 - \delta_{m'0}) e^{-\widehat{\Sigma}R_1} e^{-\widehat{\Sigma}R_2} P_n^m(\cos\theta) \cos m \alpha P_k \left(\frac{2r^2 - r_j^2 - r_{j-1}^2}{r_j^2 - r_{j-1}^2} \right), \quad (2.46)$$

where dR is a line element in the j -th region along the direction $\vec{\Omega}$. We describe the neutron direction measured from the interface of the two cells by $\vec{\Omega}^*$ and the unit normal vector at the interface by \vec{n} .

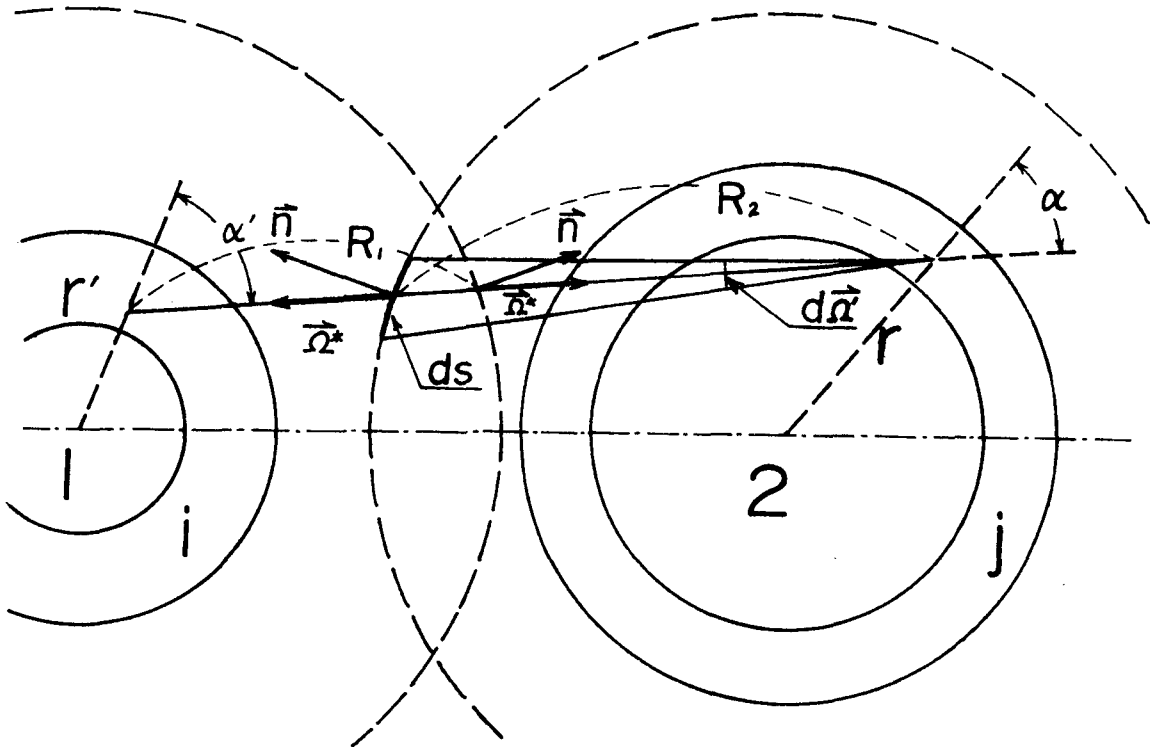


Fig. 2.3 Geometry of a first-flight of a neutron in the nearest neighboring cell

In order to calculate the above equation by using quantities evaluated only in a cell, we make the following approximation.

Inserting an identical operator

$$\frac{1}{S \int_{2\pi} d\vec{\Omega}^* (\vec{n} \cdot \vec{\Omega}^*)} \int_S dS \int_{2\pi} d\vec{\Omega}^* (\vec{n} \cdot \vec{\Omega}^*) \quad (2.47)$$

(S is the surface area of the cell per unit height) between the terms $e^{-\widehat{zR}_1}$ and $e^{-\widehat{zR}_2}$ in Eq. (2.46), the dependency of the latter term on \vec{r}' and $\vec{\Omega}$ is neglected. This is based on the assumption that all the neutrons impinging on the cell surface may return isotropically. Then we obtain

$$P_{ij}^{(n', m', k') \rightarrow (n, m, k)} = P_{is}^{(n', m', k')} P_{sj}^{(n, m, k)}, \quad (2.48)$$

where $P_{is}^{(n', m', k')}$ is the probability that a neutron starting with mode (n', m', k') in the i-th region in a cell escapes from the cell without collision, and is given by

$$P_{is}^{(n', m', k')} = \frac{1}{V_i} \int_{V_i} d\vec{r}' \int_{4\pi} d\vec{\Omega} e^{-\widehat{zR}_1} (H_{n'}^{m'})^2 P_n^{m'}(\cos \theta) \cos m' \alpha' P_k \left(\frac{2r'^2 - r_i^2 - r_{i-1}^2}{r_i^2 - r_{i-1}^2} \right) (2 - \delta_{m'0}), \quad (2.49)$$

and $P_{sj}^{(n, m, k)}$ is the probability that a neutron entering the cell 2 isotropically makes a collision of mode (n, m, k) in the j-th region, and is expressed in the form:

$$P_{sj}^{(n, m, k)} = \frac{1}{S \int_{2\pi} d\vec{\Omega}^* (\vec{n} \cdot \vec{\Omega}^*)} \int_S dS \int_{2\pi} d\vec{\Omega}^* (\vec{n} \cdot \vec{\Omega}^*) \int dR e^{-\widehat{zR}_2} P_n^m(\cos \theta) \cdot \cos m \alpha' P_k \left(\frac{2r^2 - r_j^2 - r_{j-1}^2}{r_j^2 - r_{j-1}^2} \right) \Sigma_j. \quad (2.50)$$

Equation (2.49) can be transformed into

$$P_{is}^{(n', m', k')} = \frac{1}{V_i} \int_{V_i} d\vec{r}' \int_{4\pi} d\vec{\Omega} \left(1 - \int_0^{R_1} dR \Sigma(R) e^{-\widehat{zR}} \right) (H_{n'}^{m'})^2 P_n^{m'}(\cos \theta) \cdot \cos m' \alpha' P_k \left(\frac{2r'^2 - r_i^2 - r_{i-1}^2}{r_i^2 - r_{i-1}^2} \right) (2 - \delta_{m'0})$$

$$\begin{aligned}
&= \delta_{k'0} \delta_{n'0} \delta_{m'0} - \frac{1}{V_i} \int_{V_i} d\vec{r} \int_{\text{cell 1}} d\vec{r}' \Sigma(\vec{r}) e^{-\vec{r}\vec{R}} (H_{n'}^m)^2 P_{n'}^m(\cos \theta) \\
&\cdot \cos m' \alpha' P_k \left(\frac{2r^2 - r_i^2 - r_{i-1}^2}{r_i^2 - r_{i-1}^2} \right) (2 - \delta_{m'0}) ,
\end{aligned} \tag{2.51}$$

where the integration about \vec{r} is made over the volume of the cell 1. In terms of the definition of $P_{ij}^{(n',m',k') \rightarrow (n,m,k)}$ the above equation reduces to

$$P_{is}^{(n',m',k')} = \delta_{n'0} \delta_{m'0} \delta_{k'0} - \sum_{j=1}^N P_{ij}^{(n',m',k') \rightarrow (0,0,0)} . \tag{2.52}$$

In the following the probability $P_{sj}^{(n,m,k)}$ is calculated. In a circular cylinder

$$\int_{2\pi} d\vec{\Omega}^* (\vec{n} \cdot \vec{\Omega}^*) = \pi . \tag{2.53}$$

We denote the solid angle subtended by the surface area dS at the point of collision \vec{r} in the j -th region by $d\vec{\Omega}'$. Then using the relations

$$\frac{(\vec{n} \cdot \vec{\Omega}^*)}{R_i^2} dS = d\vec{\Omega}' , \tag{2.54a}$$

$$R_i^2 dR d\vec{\Omega}^* = d\vec{r} , \tag{2.54b}$$

we have the relation

$$(\vec{n} \cdot \vec{\Omega}^*) d\vec{\Omega}^* dS dR = d\vec{\Omega}' d\vec{r} . \tag{2.55}$$

Adopting these relations we rewrite Eq. (2.50). At this point it should be noticed that, if we express the azimuthal angle by α for a neutron starting from the point \vec{r} toward the cell surface, we must replace α in equation (2.50) by $\pi - \alpha$ because the α in Eq. (2.50) is measured for a neutron directing from the cell boundary to the point \vec{r} . Then Eq. (2.50) reduces to

$$P_{sj}^{(n,m,k)} = \frac{\Sigma_j}{S\pi} \int_{V_j} d\vec{r} \int_{4\pi} d\vec{\Omega}' e^{-\vec{r}\vec{R}_i} P_n^m(\cos \theta) (-1)^m \cos m \alpha P_k \left(\frac{2r^2 - r_j^2 - r_{j-1}^2}{r_j^2 - r_{j-1}^2} \right)$$

$$\begin{aligned}
&= \frac{4 \sum_i V_i}{S} \delta_{n_0} \delta_{m_0} \delta_{k_0} - \frac{\sum_i}{S \pi} \int_{V_i} d\vec{r} \int_{+\pi} d\vec{\Omega} \int_0^{R_i} dR \Sigma(R) e^{-\vec{r} \cdot \vec{R}} \\
&\cdot P_n^m(\cos \theta) \cos m\alpha (-1)^m P_k \left(\frac{2r^2 - r_+^2 - r_{i-1}^2}{r_+^2 - r_{i-1}^2} \right) \\
&= \frac{4 \sum_i V_i}{S} \left\{ \delta_{n_0} \delta_{m_0} \delta_{k_0} - \frac{(-1)^m}{4\pi (H_n^m)^2 (2 - \delta_{m_0})} \sum_{l=1}^N P_{il}^{(n, m, k) \rightarrow (0, 0, 0)} \right\}. \quad (2.56)
\end{aligned}$$

Considering $P_{sj}^{(n, m, k)}$ in the case of $n=m=k=0$, the probability P_{ss} defined in Eq. (2.29) may be rewritten in the form:

$$P_{ss} = 1 - \sum_{j=1}^N \frac{4 \sum_i V_i}{S} \left\{ 1 - \sum_{l=1}^N P_{jl}^{(0, 0, 0) \rightarrow (0, 0, 0)} \right\}. \quad (2.57)$$

From Eqs. (2.52), (2.56) and (2.57), the generalized first-flight collision probability in lattice cells is given by

$$\begin{aligned}
P_{ij}^{t(n', m', k') \rightarrow (n, m, k)} &= P_{ij}^{(n', m', k') \rightarrow (n, m, k)} \\
&+ \left\{ \delta_{n'0} \delta_{m'0} \delta_{k'0} - \sum_{l=1}^N P_{il}^{(n', m', k') \rightarrow (0, 0, 0)} \right\} \frac{1}{1 - P_{ss}} \\
&\cdot \frac{4 \sum_i V_i}{S} \left\{ \delta_{n_0} \delta_{m_0} \delta_{k_0} - \frac{(-1)^m}{4\pi (H_n^m)^2 (2 - \delta_{m_0})} \sum_{l=1}^N P_{il}^{(n, m, k) \rightarrow (0, 0, 0)} \right\}. \quad (2.58)
\end{aligned}$$

Using this probability instead of Eq. (2.44) in Eq. (2.45), the range of summation about i is reduced to $1 \sim N$.

§2.5 Numerical Results and Conclusions

In §2.3, flat flux and flat current in each region are assumed, so that the method is suitable for a cell with a small fuel rod and thin moderator region. Takahashi's method is unsuitable for a highly heterogeneous system because the probability that a neutron born in a moderator makes its first collision in the same region is overestimated by his adoption of the perfect reflection condition on the cell boundary. We consider several cases of cylindrical cells composed of fuel and moderator regions, whose neutron cross sections and geometries are listed in Table 2.1. Suffixes 1 and 2 represent the fuel and the moderator regions respectively.

Table 2.1 Input data for two-region cylindrical cells

Case	1	2	3	4	5(6)	7
Inner radius (cm)	0.381	0.1	0.5	1.0	2.0	2.5
Outer radius (cm)	0.645	3.0	3.0	3.0	3.0	3.0
Σ_1 (cm ⁻¹)	0.78	1.0	1.0	1.0	1.0	1.0
Σ_2 (cm ⁻¹)	1.062	2.0	2.0	2.0	2.0	2.0
Σ_{1s} (cm ⁻¹)	0.387	0.5	0.5	0.5	0.5	0.5
Σ_{2s} (cm ⁻¹)	1.062	2.0	2.0	2.0	2.0(1.5)	2.0

In Table 2.2, the probabilities P_{ij}^* for an isolated cell and P_{ij}^{t*} for a lattice system evaluated from the present method are compared with those based on the use of the transport cross section in place of the total cross section. In each case, they are evaluated for three values of $\bar{\mu}$ (0, 1/3, 2/3) where $\bar{\mu}$ is the average cosine of the scattering angle in the moderator. Among the probabilities P_{ij}^* , the value of P_{11}^* for the transport approximation is independent of $\bar{\mu}$ because it contains only the cross section of the fuel element, but in the present method the value of P_{11}^* decreases with $\bar{\mu}$.

Table 22 Normalized new type collision probabilities

Case	$\bar{\mu}$	Probabilities for one cell				Probabilities for a lattice cell			
		$\dagger P_{11}^*$	P_{12}^*	P_{21}^*	P_{22}^*	P_{11}^{l*}	P_{12}^{l*}	P_{21}^{l*}	P_{22}^{l*}
1	0	0.2816	0.2401	0.09450	0.3404	0.4011	0.5989	0.2357	0.7643
	$\frac{1}{3}$	0.2709	0.2307	0.09082	0.3372	0.3981	0.6019	0.2369	0.7631
	$\frac{2}{3}$	0.2816	0.1727	0.1020	0.2511	0.4630	0.5370	0.3170	0.6830
	$\frac{2}{3}$	0.2600	0.2212	0.08707	0.3339	0.3950	0.6050	0.2381	0.7619
2	$\frac{2}{3}$	0.2816	0.09372	0.1107	0.1423	0.5920	0.4080	0.4818	0.5182
	0	0.1150	0.8800	0.000489	0.9163	0.1150	0.8850	0.000492	0.9995
	$\frac{1}{3}$	0.1147	0.8370	0.000465	0.9132	0.1147	0.8853	0.000492	0.9995
	$\frac{2}{3}$	0.1150	0.8714	0.000727	0.8754	0.1150	0.8850	0.000738	0.9993
3	$\frac{2}{3}$	0.1141	0.7675	0.000427	0.9080	0.1141	0.8859	0.000493	0.9995
	$\frac{2}{3}$	0.1150	0.7877	0.001331	0.7626	0.1150	0.8850	0.001477	0.9985
	0	0.4040	0.5934	0.008477	0.9061	0.4041	0.5959	0.008514	0.9915
	$\frac{1}{3}$	0.4004	0.5675	0.008108	0.9034	0.4004	0.5996	0.008565	0.9914
4	$\frac{2}{3}$	0.4040	0.5836	0.01251	0.8604	0.4040	0.5959	0.01277	0.9872
	$\frac{2}{3}$	0.3944	0.5249	0.007499	0.8991	0.3945	0.6055	0.008650	0.9913
	$\frac{2}{3}$	0.4040	0.5182	0.02221	0.7383	0.4051	0.5949	0.02550	0.9745
	0	0.5951	0.4042	0.02526	0.8815	0.5951	0.4049	0.02531	0.9747
5	$\frac{1}{3}$	0.5881	0.3899	0.02437	0.8796	0.5881	0.4119	0.02574	0.9742
	$\frac{2}{3}$	0.5951	0.3918	0.03673	0.8255	0.5952	0.4048	0.03795	0.9621
	$\frac{2}{3}$	0.5766	0.3663	0.02289	0.8766	0.5766	0.4234	0.02646	0.9735
	$\frac{2}{3}$	0.5951	0.3320	0.06225	0.6861	0.5989	0.4011	0.07521	0.9248
6	0	0.7641	0.2200	0.08799	0.7694	0.7648	0.2352	0.09409	0.9059
	$\frac{1}{3}$	0.7527	0.2155	0.08620	0.7687	0.7547	0.2453	0.09812	0.9019
	$\frac{2}{3}$	0.7641	0.1977	0.1186	0.6824	0.7680	0.2320	0.1392	0.8608
	$\frac{2}{3}$	0.7363	0.2090	0.08362	0.7676	0.7402	0.2498	0.1039	0.8961
7	$\frac{2}{3}$	0.7641	0.1436	0.1723	0.5123	0.7880	0.2119	0.2543	0.7457
	0	0.7641	0.2200	0.08799	0.7694	0.7648	0.2352	0.09409	0.9059
	$\frac{1}{3}$	0.7559	0.2168	0.08670	0.7688	0.7575	0.2425	0.09698	0.9030
	$\frac{2}{3}$	0.7641	0.2052	0.1094	0.7091	0.7666	0.2334	0.1245	0.8755
8	$\frac{2}{3}$	0.7453	0.2126	0.08504	0.7682	0.7482	0.2518	0.1007	0.8993
	$\frac{2}{3}$	0.7641	0.1768	0.1414	0.6135	0.7737	0.2263	0.1811	0.8189
	0	0.8068	0.1474	0.1675	0.6137	0.8156	0.1844	0.2095	0.7905
	$\frac{1}{3}$	0.7946	0.1457	0.1655	0.6134	0.8081	0.1918	0.2180	0.7820
9	$\frac{2}{3}$	0.8068	0.1209	0.2060	0.5141	0.8289	0.1711	0.2916	0.7034
	$\frac{2}{3}$	0.7800	0.1436	0.1631	0.6131	0.7992	0.2008	0.2282	0.7718
	$\frac{2}{3}$	0.8068	0.07689	0.2621	0.3546	0.8659	0.1341	0.4570	0.5430
	$\frac{2}{3}$	0.8068	0.07689	0.2621	0.3546	0.8659	0.1341	0.4570	0.5430

The values of upper rows are evaluated by the present method, lower rows by the transport approximation.

This decrease is based on the fact that a neutron which has escaped from the fuel rod has much more chances of leaking towards the void region outside the original cell by forward scattering in the moderator than in the case of isotropic scattering. For a cell with a large fuel rod, neutrons escaping from the fuel rod and suffering few collisions in the moderator have a forward angular distribution, so that the probability P_{11}^* reduces with the increase of leakage. For a cell with a large moderator region, a neutron which has suffered many collisions in the moderator will no longer retain traces of the original direction, so that the probability is nearly the same as in the case of isotropic scattering. In respect of the probability P_{21}^* , the present method yields results opposite to those based on the transport approximation. A neutron born in the moderator with uniform and isotropic distributions has much more chances (due to the larger solid angle subtended by the moderator) of remaining in the same region than proceeding towards the fuel rod, so that the anisotropic scattering in the moderator may reduce the proportion of neutrons that enter the fuel rod when the region outside the moderator is void. This is the reason why the probability P_{21}^* in the present method decreases with the average cosine of the moderator. In the transport approximation, however, the only assumption is that the cross section of the moderator reduces to $\Sigma - \bar{\mu} \Sigma_s$ (13). Thus, a larger proportion of neutrons than in the case of isotropic scattering would enter the fuel rod, and the value P_{21}^* in the transport approximation increases with the average cosine of the moderator. This is a drawback of the transport approximation, especially for a moderator of small volume and large leakage from the cell.

For a lattice system, on the other hand, the probability P_{21}^{t*}

of the present method has the same tendency as that of the transport approximation. This is due to the increase of volume of the moderator. The same is true for the probability P_{22}^{t*} . Comparing the values of P_{11}^{t*} and P_{12}^{t*} of the present method with those of the transport approximation, we may find opposing tendencies for a lattice cell.

Table 2.3 Flux ratio (\bar{P}_m / \bar{P}_f)

Average cosine	0	1/3	2/3
Case 1			
Present method	1.1405	1.1345	1.1286
Transport approx.	1.1405	1.1372	1.3330
Case 2			
Present method	1.0658	1.0650	1.0639
Transport approx.	1.0658	1.0656	1.0649
Case 3			
Present method	1.3590	1.3402	1.3137
Transport approx.	1.3590	1.3515	1.3318
Case 4			
Present method	1.8005	1.7285	1.6335
Transport approx.	1.8005	1.7611	1.6841
Case 5			
Present method	2.5855	2.3884	2.1759
Transport approx.	2.5855	2.4392	2.2848
Case 6			
Present method	2.5185	2.3953	2.2598
Transport approx.	2.5185	2.4300	2.3300
Case 7			
Present method	2.7073	2.5410	2.3751
Transport approx.	2.7073	2.5999	2.5450

In Table 2.3, moderator-to-fuel flux ratios are shown for each case in Table 1 assuming a uniform source in the moderator. In the calculation the moderator region is divided into two regions with equal volume. The results evaluated by the transport approximation are in good agreement with those of the present method only for a cell with

large moderator-to-fuel volume ratio (Case 2). With the increase of the fuel radius, the flux ratio by the present method becomes smaller than by the transport approximation for each average cosine of the scattering angle. For Case 7, this tendency is especially remarkable, and the difference of the flux ratios between the two methods reaches about 7 %. The transport approximation always underestimates the decrease of the flux ratio caused from anisotropic scattering. This approximation is equivalent to diluting the moderator with increasing $\bar{\mu}$, and in the limit of $\Sigma_m \rightarrow 0$, the fluxes in the fuel and the moderator become

$$\bar{\phi}_f = \frac{S V_m}{\Sigma_{fa} V_f}, \quad \bar{\phi}_m = S \left(P_{mn}^0 + \frac{\Sigma_{fs} V_m}{\Sigma_{fa} V_f} \right)$$

where $P_{mn}^0 = \lim_{\Sigma_m \rightarrow 0} \frac{P_{mn}}{\Sigma_m}$.

Thus it is proved that, in such a heterogeneous case or in a cell surrounded by air, the adoption of the transport cross section is not effective in taking into account the effect of anisotropic scattering. From Cases 5 and 6, we can see that the values based on the transport approximation approach to ours to some extent by the inclusion of absorption in the moderator.

Table 2.4 Values of correction $\delta(\bar{\phi}_m / \bar{\phi}_f)$ by anisotropic scattering in the moderator (Case 1)

Average cosine	1/3	2/3
Method of §2.3	-0.00566	-0.0113
Method of §2.4	-0.00609	-0.0121
Benoist's theory	-0.00675	-0.0135
Transport correction	-0.00191	-0.0028
Transport correction*	-0.0022	-0.0033

* Values listed in Ref. (14)

In Table 2.4 are shown the values of the correction $\delta(\bar{\phi}_m / \bar{\phi}_f)$

to the disadvantage factor induced by anisotropic scattering in the moderator. The results from the present method are in good agreement with those by Benoist⁽¹⁴⁾.

Next we evaluate the effect of higher order anisotropy from the method in Appendix 2B. From the discussion in Ref. (15), it is sufficient to take into account the effect up to quadratic anisotropy for the calculation of the disadvantage factor. The total cross sections used for the fuel and the moderator are both 1 cm^{-1} . The scattering cross sections used for the fuel and the moderator are 0.5537 cm^{-1} and 0.99163 cm^{-1} respectively. The average cosine (P_1 component of scattering angle) and P_2 component ($\Sigma_{fs}^1 / \Sigma_{ms}^0$) are assumed to be $2/3$ and $1/4$ respectively. The outer radius of the moderator is taken to be 3.0 cm . Using these data, the flux ratio (moderator-to-fuel flux ratio) is shown for two different fuel radii. In the calculation we divided a cell into 5 regions — 2 in the fuel and 3 in the moderator.

Table 2.5 Flux ratio for different orders of anisotropy of scattering angle

Case 1 Fuel radius 0.5 cm			
Order of anisotropy	Method		
	Present method	P_3 -approximation	P_1 -approximation
0	1.3556	1.3360	1.2292
1	1.2680	1.2126	1.1053
2	1.2794	1.2249	*
Case 2 Fuel radius 2.0 cm			
Order of anisotropy	Method		
	Present method	P_3 -approximation	P_1 -approximation
0	2.2813	2.3285	1.9946
1	2.0269	2.0395	1.7054
2	2.0620	2.0999	*

* P_1 -approximation cannot treat the second order anisotropy of scattering angle.

From Table 2.5 we can see that the linear anisotropy decreases the flux ratio evaluated in the case of isotropic scattering, but that the quadratic anisotropy acts to recover the flux ratio to some extent. These results should be contrasted with the case of slab lattice cells.

In the following the effect of variation of flux in each region is investigated. We calculate the flux distributions for two different lattice cells from the method in §2.4. The first cell (Case 1) is a closely packed lattice cell and the second (Case 2) is that with a large moderator. In both cases a cell is composed of a fuel rod and a moderator. For Case 1 the outer radii of the fuel and the moderator are 0.381 and 0.64487 cm respectively and the total and scattering cross sections of the fuel are 0.78 and 0.387 cm^{-1} and those of the moderator are 1.0618 and 1.053 cm^{-1} . For Case 2 the outer radii of the fuel and the moderator are 2.0 and 10.0 cm respectively and the total and scattering cross sections of the fuel are 0.6 and 0.35 cm^{-1} and those of the moderator are 0.3 and 0.3 cm^{-1} . The Case 1 corresponds to the Case 1 in Table 1. The Case 2 corresponds to the cell adopted by Lewis⁽¹⁶⁾. In the calculation we divide the cell of Case 1 into 2-regions and that of Case 2 into 3-regions (one fuel region and two moderator regions divided by a circle of radius 6 cm). In calculating flux distribution we assume a uniform and isotropic source per unit volume only in the moderator.

In the case of isotropic scattering, the expansion coefficients $\phi^{(0,0,k)}$ of the flux are given in Table 2.6 for each case where the upper limit of k is taken to be 0, 1, 2 or 3. For the case where the highest order of the Legendre polynomials is taken to be 3, the coefficients $\phi^{(0,0,k)}$ ($k = 0, 1, 2, 3$) can reproduce an almost continuous flux curve at interfaces. The convergency of the coefficients

Table 2.6 Legendre expansion coefficients of flux
for isotropic scattering

Upper limit of Legendre polynomials	Expansion coefficient	Case 1		Case 2		
		Fuel	Moderator	Fuel	Inner moderator	Outer moderator
0	$\phi(0,0,0)$	4.5298	5.1556	96.0	161.66	177.95
1	$\phi(0,0,0)$	4.5294	5.1654	96.0	170.68	192.10
	$\phi(0,0,1)$	0.2546	0.1316	24.34	21.66	3.49
2	$\phi(0,0,0)$	4.5292	5.1679	96.0	172.52	193.75
	$\phi(0,0,1)$	0.2532	0.1323	23.95	22.10	3.66
	$\phi(0,0,2)$	0.0401	-0.1120	3.85	-9.97	-2.26
3	$\phi(0,0,0)$	4.5292	5.1681	96.0	172.82	193.99
	$\phi(0,0,1)$	0.2531	0.1320	23.88	21.87	3.62
	$\phi(0,0,2)$	0.0399	-0.1120	3.77	-10.11	-2.25
	$\phi(0,0,3)$	0.01323	0.0306	1.05	4.56	0.34

Table 2.7 Moderator-to-fuel flux ratio
for isotropic scattering

Upper limit of Legendre polynomials	Case 1	Case 2
0	1.1382	1.7971
1	1.1404	1.9267
2	1.1410	1.9445
3	1.1412	1.9472

$\phi(0,0,k)$ is very fast for the Case 1 but not so rapid for the Case 2. This shows that the deviation of the flux from the flat flux in each region is very small for the Case 1, but is large for the Case 2.

The moderator-to-fuel flux ratio is given in Table 2.7. From this table it can be easily seen that the value of the flux ratio converges very rapidly with the increase of the number of terms in the Legendre expansion. For the ratio, it is sufficient to take into account only

the first two terms ($k = 0$ and 1).

The Legendre expansion coefficients in the case of linearly anisotropic scattering are presented in Tables 2.8 and 2.9 where the average cosines of the scattering angle $\bar{\mu}$ are taken to be $1/3$ and $2/3$ respectively. From these tables it can be seen that the convergency of the expansion coefficients $\phi^{(l,l,k)}$ ($k = 0, 1, 2, 3$) is very slow for both cases compared with that of $\phi^{(0,0,k)}$. In particular the term $\phi^{(1,1,1)}$ is nearly comparable with the term $\phi^{(1,1,0)}$ in each region. Then the flat current approximation fails to express the tendency of the current over a cell. In the case of anisotropic scattering, also, the inclusion up to the term $k=1$ yields good results for the expansion coefficients $\phi^{(0,0,0)}$ and $\phi^{(1,1,0)}$. The moderator-to-fuel flux ratio for the case of anisotropic scattering is presented in Tables 2.10 and 2.11, and shows that the error resulted from the flat flux and flat current approximation decreases with the increase of the average cosine of the scattering angle of the moderator. Thus a remarkable improvement is obtained when we include the term $k = 1$.

Table 2.8 Legendre expansion coefficients of angular flux for
linearly anisotropic scattering ($\bar{\mu} = 1/3$)

Upper limit of Legendre polynomials	Expansion coefficient	Case 1		Case 2		
		Fuel	Moderator	Fuel	Inner moderator	Outer moderator
0	$\phi(0,0,0)$	4.5305	5.1367	96.0	157.37	169.70
	$\phi(1,1,0)$	-0.2067	-0.1343	-12.43	-8.24	-1.85
1	$\phi(0,0,0)$	4.5306	5.1362	96.0	161.95	177.30
	$\phi(0,0,1)$	0.2545	0.1121	24.22	15.98	2.17
	$\phi(1,1,0)$	-0.2111	-0.1390	-13.86	-10.18	-2.17
	$\phi(1,1,1)$	-0.1422	0.1594	-10.70	6.27	2.42
2	$\phi(0,0,0)$	4.5305	5.1382	96.0	162.97	178.18
	$\phi(0,0,1)$	0.2533	0.1135	28.88	16.54	2.34
	$\phi(0,0,2)$	0.0401	-0.1027	3.80	-7.93	-1.58
	$\phi(1,1,0)$	-0.2110	-0.1392	-13.84	-10.26	-2.17
	$\phi(1,1,1)$	-0.1427	0.1621	-10.89	7.02	2.55
	$\phi(1,1,2)$	0.0261	-0.0287	1.37	-2.91	-0.46
3	$\phi(0,0,0)$	4.5305	5.1383	96.0	163.15	178.33
	$\phi(0,0,1)$	0.2532	0.1132	23.81	16.39	2.31
	$\phi(0,0,2)$	0.0399	-0.1029	3.73	-8.14	-1.57
	$\phi(0,0,3)$	0.0132	0.0287	1.05	3.96	0.15
	$\phi(1,1,0)$	-0.2110	-0.1392	-13.84	-10.26	-2.16
	$\phi(1,1,1)$	-0.1427	0.1621	-10.88	7.08	2.55
	$\phi(1,1,2)$	0.0259	-0.0293	1.33	-3.19	-0.47
	$\phi(1,1,3)$	-0.0136	0.0068	-0.88	1.48	0.10

Table 2.9 Legendre expansion coefficients of angular flux for
linearly anisotropic scattering ($\bar{\mu} = 2/3$)

Upper limit of Legendre polynomials	Expansion coefficient	Case 1		Case 2		
		Fuel	Moderator	Fuel	Inner moderator	Outer moderator
0	$\phi^{(0,0,0)}$	4.5313	5.1176	96.0	152.38	160.07
	$\phi^{(1,1,0)}$	-0.2068	-0.1352	-12.51	-8.90	-2.03
1	$\phi^{(0,0,0)}$	4.5318	5.1069	96.0	152.88	162.01
	$\phi^{(0,0,1)}$	0.2545	0.0925	24.10	10.12	0.81
	$\phi^{(1,1,0)}$	-0.2113	-0.1392	-13.94	-10.32	-2.20
	$\phi^{(1,1,1)}$	-0.1422	0.1597	-10.61	6.52	2.49
2	$\phi^{(0,0,0)}$	4.5317	5.1083	96.0	153.18	162.24
	$\phi^{(0,0,1)}$	0.2533	0.0946	23.79	10.85	0.99
	$\phi^{(0,0,2)}$	0.0401	-0.0934	3.76	-5.84	-0.89
	$\phi^{(1,1,0)}$	-0.2112	-0.1394	-13.92	-10.39	-2.20
	$\phi^{(1,1,1)}$	-0.1427	0.1621	-10.79	7.10	2.57
	$\phi^{(1,1,2)}$	0.0261	-0.0288	1.35	-2.96	-0.47
3	$\phi^{(0,0,0)}$	4.5317	5.1084	96.0	153.27	162.31
	$\phi^{(0,0,1)}$	0.2532	0.0943	23.73	10.77	0.97
	$\phi^{(0,0,2)}$	0.0399	-0.0938	3.68	-6.12	-0.89
	$\phi^{(0,0,3)}$	0.0132	0.0268	1.04	3.36	-0.04
	$\phi^{(1,1,0)}$	-0.2112	-0.1394	-13.93	-10.39	-2.19
	$\phi^{(1,1,1)}$	-0.1426	0.1622	-10.78	7.15	2.57
	$\phi^{(1,1,2)}$	0.0259	-0.0292	1.31	-3.20	-0.47
	$\phi^{(1,1,3)}$	-0.0137	0.0068	-0.87	1.47	0.11

Table 2.10 Moderator-to-fuel flux ratio for linearly
anisotropic scattering ($\bar{\mu} = 1/3$)

Upper limit of Legendre polynomials	Case 1	Case 2
0	1.1338	1.7249
1	1.1337	1.7936
2	1.1341	1.8032
3	1.1342	1.8049

Table 2.11 Moderator-to-fuel flux ratio for linearly
anisotropic scattering ($\bar{\mu} = 2/3$)

Upper limit of Legendre polynomials	Case 1	Case 2
0	1.1294	1.6407
1	1.1269	1.6559
2	1.1272	1.6585
3	1.1273	1.6593

Appendix 2A

Reciprocity Relation and Conservation Law for Eqs. (2.25b) and (2.38)

Here we verify that the new type of first-flight collision probabilities (2.25b) and (2.38) satisfy the usual reciprocity relation and the usual conservation law. First we verify the conservation law for P_{ij}^{t*} . Using the relations

$$\sum_{j=1}^2 P_{ij}^{t*} = \sum_{j=1}^2 P_{ij}^{(00) \rightarrow (00)} + \left(1 - \sum_{k=1}^2 P_{ik}^{(00) \rightarrow (00)}\right) \frac{\sum_{j=1}^2 P_{sj}^{(00)}}{\sum_{k=1}^2 P_{sk}^{(00)}} = 1, \quad (2A.1)$$

and

$$\sum_{j=1}^2 P_{2j}^{t*} = \sum_{j=1}^2 P_{2j}^{(11) \rightarrow (00)} - \sum_{k=1}^2 P_{2k}^{(11) \rightarrow (00)} \frac{\sum_{j=1}^2 P_{sj}^{(00)}}{\sum_{k=1}^2 P_{sk}^{(00)}} = 0, \quad (2A.2)$$

we obtain the conservation relation

$$\sum_{j=1}^2 P_{ij}^{t*} = \sum_{j=1}^2 P_{ij}^{(00) \rightarrow (00)} + \frac{P_{i2}^{(00) \rightarrow (11)} \frac{\sum_{25}'}{\sum_{25}^0}}{1 - P_{22}^{(11) \rightarrow (11)} \frac{\sum_{25}'}{\sum_{25}^0}} \sum_{j=1}^2 P_{2j}^{(11) \rightarrow (00)} = 1. \quad (2A.3)$$

Next we will derive the reciprocity relation for P_{ij}^* :

$$\begin{aligned} P_{ij}^* &= P_{ij}^{(00) \rightarrow (00)} + \frac{P_{i2}^{(00) \rightarrow (11)} \frac{\sum_{25}'}{\sum_{25}^0} P_{2j}^{(11) \rightarrow (00)}}{1 - P_{22}^{(11) \rightarrow (11)} \frac{\sum_{25}'}{\sum_{25}^0}} \\ &= \frac{\sum_j v_j}{\sum_i v_i} P_{ji}^{(00) \rightarrow (00)} + \frac{(-\frac{1}{3}) \frac{\sum_2 v_2}{\sum_i v_i} P_{2i}^{(11) \rightarrow (00)} \frac{\sum_{25}'}{\sum_{25}^0} (-3) \frac{\sum_j v_j}{\sum_2 v_2} P_{j2}^{(00) \rightarrow (11)}}{1 - P_{22}^{(11) \rightarrow (11)} \frac{\sum_{25}'}{\sum_{25}^0}} \end{aligned}$$

$$\begin{aligned}
&= \frac{\Sigma_i \nabla_i}{\Sigma_i \nabla_i} \left\{ P_{ji}^{(00) \rightarrow (00)} + \frac{P_{j2}^{(00) \rightarrow (11)} \frac{\Sigma_{25}'}{\Sigma_{25}''} P_{2i}^{(11) \rightarrow (00)}}{1 - P_{22}^{(11) \rightarrow (11)} \frac{\Sigma_{25}'}{\Sigma_{25}''}} \right\} \\
&= \frac{\Sigma_i \nabla_i}{\Sigma_i \nabla_i} P_{ji}^* .
\end{aligned} \tag{2A.4}$$

In a similar manner, we can verify that P_{ij}^{t*} also satisfies the same reciprocity relation as P_{ij}^* .

Appendix 2B

Formula for Higher Order Anisotropic Scattering⁽¹⁷⁾

The equations which determine the neutron flux in the case of quadratically anisotropic scattering are

$$\begin{aligned}
\Sigma_j \nabla_j \phi_j^{(00)} &= \sum_{i=1}^N \left[P_{ij}^{(00) \rightarrow (00)} \{ S_i^{(00)} + \Sigma_{is}^0 \phi_i^{(00)} \} \nabla_i \right. \\
&+ P_{ij}^{(11) \rightarrow (00)} \{ S_i^{(11)} + \Sigma_{is}^1 \phi_i^{(11)} \} \nabla_i + P_{ij}^{(20) \rightarrow (00)} \{ S_i^{(20)} + \Sigma_{is}^2 \phi_i^{(20)} \} \nabla_i \\
&\left. + P_{ij}^{(22) \rightarrow (00)} \{ S_i^{(22)} + \Sigma_{is}^2 \phi_i^{(22)} \} \nabla_i \right] ,
\end{aligned} \tag{2B.1}$$

$$\begin{aligned}
\Sigma_j \nabla_j \phi_j^{(11)} &= \sum_{i=1}^N \left[P_{ij}^{(00) \rightarrow (11)} \{ S_i^{(00)} + \Sigma_{is}^0 \phi_i^{(00)} \} \nabla_i \right. \\
&+ P_{ij}^{(11) \rightarrow (11)} \{ S_i^{(11)} + \Sigma_{is}^1 \phi_i^{(11)} \} \nabla_i + P_{ij}^{(20) \rightarrow (11)} \{ S_i^{(20)} + \Sigma_{is}^2 \phi_i^{(20)} \} \nabla_i \\
&\left. + P_{ij}^{(22) \rightarrow (11)} \{ S_i^{(22)} + \Sigma_{is}^2 \phi_i^{(22)} \} \nabla_i \right] ,
\end{aligned} \tag{2B.2}$$

$$\Sigma_j \nabla_j \phi_j^{(20)} = \sum_{i=1}^N \left[P_{ij}^{(00) \rightarrow (20)} \{ S_i^{(00)} + \Sigma_{is}^0 \phi_i^{(00)} \} \nabla_i \right.$$

$$\begin{aligned}
& + P_{ij}^{(11) \rightarrow (20)} \{ S_i^{(11)} + \sum_{is}^1 \phi_i^{(11)} \} V_i + P_{ij}^{(20) \rightarrow (20)} \{ S_i^{(20)} + \sum_{is}^2 \phi_i^{(20)} \} V_i \\
& + P_{ij}^{(12) \rightarrow (20)} \{ S_i^{(12)} + \sum_{is}^2 \phi_i^{(12)} \} V_i] ,
\end{aligned}
\tag{2B.3}$$

$$\begin{aligned}
\sum_j V_j \phi_j^{(12)} &= \sum_{i=1}^N \left[P_{ij}^{(00) \rightarrow (12)} \{ S_i^{(00)} + \sum_{is}^2 \phi_i^{(00)} \} V_i \right. \\
&+ P_{ij}^{(11) \rightarrow (12)} \{ S_i^{(11)} + \sum_{is}^1 \phi_i^{(11)} \} V_i + P_{ij}^{(20) \rightarrow (12)} \{ S_i^{(20)} + \sum_{is}^2 \phi_i^{(20)} \} V_i \\
&\left. + P_{ij}^{(12) \rightarrow (12)} \{ S_i^{(12)} + \sum_{is}^2 \phi_i^{(12)} \} V_i \right] .
\end{aligned}
\tag{2B.4}$$

In the calculation of $P_{ij}^{(\frac{k}{m}n) \rightarrow (\frac{k'}{m'}n')}$ we can use the reciprocity relations

$$\sum_i V_i P_{ij}^{(00) \rightarrow (00)} = \sum_j V_j P_{ji}^{(00) \rightarrow (00)} ,
\tag{2B.5}$$

$$\sum_i V_i P_{ij}^{(11) \rightarrow (00)} = -3 \sum_j V_j P_{ji}^{(00) \rightarrow (11)} ,
\tag{2B.6}$$

$$\sum_i V_i P_{ij}^{(11) \rightarrow (11)} = \sum_j V_j P_{ji}^{(11) \rightarrow (11)} ,
\tag{2B.7}$$

$$\sum_i V_i P_{ij}^{(20) \rightarrow (00)} = 5 \sum_j V_j P_{ji}^{(00) \rightarrow (20)} ,
\tag{2B.8}$$

$$\sum_i V_i P_{ij}^{(12) \rightarrow (00)} = \frac{5}{12} \sum_j V_j P_{ji}^{(00) \rightarrow (12)} ,
\tag{2B.9}$$

$$\sum_i V_i P_{ij}^{(20) \rightarrow (11)} = -\frac{5}{3} \sum_j V_j P_{ji}^{(11) \rightarrow (20)} ,
\tag{2B.10}$$

$$\sum_i V_i P_{ij}^{(20) \rightarrow (12)} = 12 \sum_j V_j P_{ji}^{(12) \rightarrow (20)} ,
\tag{2B.11}$$

$$\sum_i V_i P_{ij}^{(12) \rightarrow (11)} = -\frac{5}{36} \sum_j V_j P_{ji}^{(11) \rightarrow (12)} ,
\tag{2B.12}$$

$$\sum_i V_i P_{ij}^{(20) \rightarrow (20)} = \sum_j V_j P_{ji}^{(20) \rightarrow (20)} ,
\tag{2B.13}$$

$$\sum_i V_i P_{ij}^{(12) \rightarrow (12)} = \sum_j V_j P_{ji}^{(12) \rightarrow (12)} . \quad (2B.14)$$

The conservation relations are given by

$$\sum_{j=1}^{\infty} P_{ij}^{(00) \rightarrow (00)} = 1 , \quad (2B.15)$$

$$\sum_{j=1}^{\infty} P_{ij}^{(11) \rightarrow (00)} = 0 , \quad (2B.16)$$

$$\sum_{j=1}^{\infty} P_{ij}^{(20) \rightarrow (00)} = 0 , \quad (2B.17)$$

$$\sum_{j=1}^{\infty} P_{ij}^{(12) \rightarrow (00)} = 0 . \quad (2B.18)$$

The probabilities $P_{sj}^{(\ell n)}$ that a neutron entering a cell isotropically from its surface undergoes its first collision in the j-th region with modes (ℓn) are given by

$$P_{sj}^{(00)} = \frac{4 \sum_i V_i}{S} \left(1 - \sum_{i=1}^N P_{ji}^{(00) \rightarrow (00)} \right) , \quad (2B.19)$$

$$P_{sj}^{(11)} = \frac{4 \sum_i V_i}{3 S} \sum_{i=1}^N P_{ji}^{(11) \rightarrow (00)} , \quad (2B.20)$$

$$P_{sj}^{(20)} = - \frac{4 \sum_i V_i}{5 S} \sum_{i=1}^N P_{ji}^{(20) \rightarrow (00)} , \quad (2B.21)$$

$$P_{sj}^{(12)} = - \frac{48 \sum_i V_i}{5 S} \sum_{i=1}^N P_{ji}^{(12) \rightarrow (00)} . \quad (2B.22)$$

Using the above equations all the probabilities in a cylindrical cell are calculated for quadratically anisotropic scattering.

Appendix 2C

Calculation of the Generalized Collision Probability; Eq. (2.44)

We evaluate the generalized first-flight collision probability for a cylindrical cell using the same technique as Kavenoky's one⁽¹⁸⁾ adopted for the calculation of the usual first-flight collision probability. First we calculate $P_{ij}^{(n',m',k') \rightarrow (n,m,k)}$ for $i \leq j$. The region number is enumerated from the inner side of the cylindrical cell. The variables h , y and y' are taken as in Fig. 2.4. In the integration about y' over the i -th region, we concurrently sum up the values at two points A and A' located symmetrically about the h -axis. Further we express the optical distances along the paths AB and $A'B$ on the x - y plane by $\widehat{z\beta}$, and $\widehat{z\beta}_z$ respectively. Then we obtain

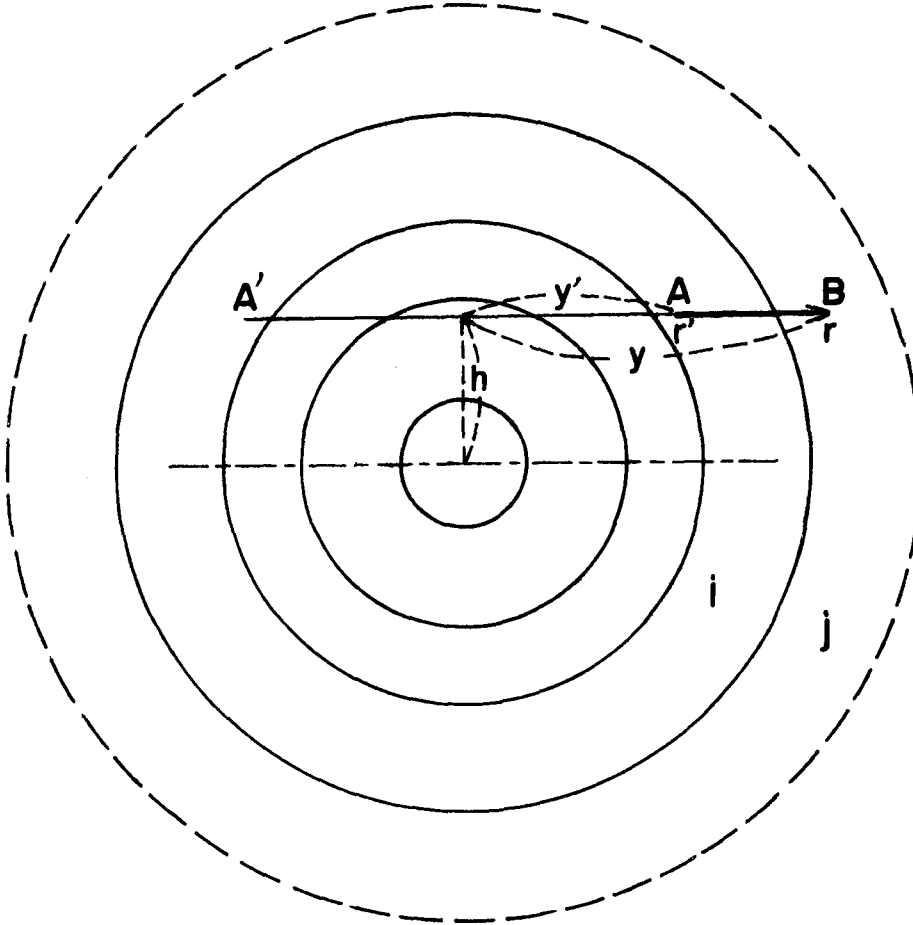


Fig. 2.4 Notations in a concentric cylindrical cell

$$\begin{aligned}
P_{ij}^{(n', m', k') \rightarrow (n, m, k)} &= \frac{8\pi \Sigma_i}{V_i} (H_{n'}^{m'})^2 \int_0^{r_i} dh \int_{\gamma_{i-1}}^{\gamma_i} dy' \int_{\gamma_{i-1}}^{\gamma_i} dy \int_0^{\frac{\pi}{2}} d\theta \left\{ \exp\left(-\frac{\widehat{\Sigma}_i}{\sin \theta}\right) \right. \\
&+ (-1)^{m'} \exp\left(-\frac{\widehat{\Sigma}_i}{\sin \theta}\right) \left. \right\} P_{n'}^{m'}(\cos \theta) \cos m' \alpha' P_k \left(\frac{2r^2 - r_i^2 - \gamma_{i-1}^2}{\gamma_i^2 - \gamma_{i-1}^2} \right) \\
&\cdot (2 - \delta_{m'0}) P_n^m(\cos \theta) \cos m \alpha P_k \left(\frac{2r^2 - r_i^2 - \gamma_{i-1}^2}{\gamma_i^2 - \gamma_{i-1}^2} \right), \quad (2C.1)
\end{aligned}$$

where y_i and y_j are given by $\sqrt{r_i^2 - k^2}$ and $\sqrt{r_j^2 - k^2}$ respectively.

For the case $m' = 0$ the integrations about dy' and dy can be achieved since the quantities r'^2 and r^2 are expressed by $h^2 + y'^2$ and $h^2 + y^2$ respectively. The integration about the polar angle θ is expressed by the Bickley function. The rational expression for the function is presented by Makino⁽¹⁹⁾.

In the calculation of $P_{ij}^{(n', m', k') \rightarrow (n, m, k)}$ for $i > j$, the following reciprocity relation can be used

$$\begin{aligned}
&(H_{n'}^{m'})^2 (2 - \delta_{m'0}) \Sigma_i V_i P_{ji}^{(n, m, k) \rightarrow (n', m', k')} \\
&= (-1)^{m+m'} (H_n^m)^2 (2 - \delta_{m0}) \Sigma_i V_i P_{ij}^{(n', m', k') \rightarrow (n, m, k)}. \quad (2C.2)
\end{aligned}$$

References

- (1) TAKAHASHI, H.: Nucl. Sci. Eng., 24, 60 (1966).
- (2) TAKAHASHI, H.: ibid., 26, 254 (1966).
- (3) TAKAHASHI, H.: J. Nucl. Energy, A12, 1 (1960).
- (4) NEWMARCH, D.A.: AEEW-R 34, (1960).
- (5) BENOIST, P.: Nucl. Sci. Eng., 34, 285 (1968).
- (6) BRUN, A.M., KAVENOKY, A.: Paper presented to ANS National
Topical Meeting, New Developments in Reactor
Mathematics and Applications. (1971).
- (7) CORNGOLD, N.: J. Nucl. Energy, 4, 293 (1957).
- (8) CARLVIK, I.: Nucl. Sci. Eng., 31, 295 (1968).
- (9) TAKEDA, T., SEKIYA, T.: J. Nucl. Sci. Technol., 8, 663 (1971).
- (10) AMYOT, L.: EUR-3937e, (1968).
- (11) HYSLOP, J.: Reactor Sci. Tech., 17, 237 (1963).
- (12) TAKEDA, T., SEKIYA, T.: To be published in J. Nucl. Energy.
- (13) HONECK, H.C.: Nucl. Sci. Eng., 18, 49 (1964).
- (14) BENOIST, P.: ibid., 30, 85 (1967).
- (15) ECCLESTON, G.W., McCORMICK, N.J.: J. Nucl. Energy, 24, 23 (1970).
- (16) LEWIS, E.E.: ibid., 23, 87 (1969).
- (17) TAKEDA, T., AZEKURA, K., SEKIYA, T.: J. Nucl. Sci. Technol.,
9, 249 (1972).
- (18) KAVENOKY, A.: CEA-N-1077, (1969).
- (19) MAKINO, K.: Nucleonik, 9, 351 (1967).

CHAPTER 3

EFFECT OF LATTICE CONFIGURATION

§3.1 Introduction

In this chapter the effect of lattice configuration on the mono-energetic disadvantage factor for closely packed lattice cell is studied. The S_n method⁽¹⁾, the collision probability method⁽²⁾, the method of Amouyal and Benoist⁽³⁾, the spherical harmonics method⁽⁴⁾, and the diffusion approximation method⁽⁵⁾ are general procedures established for obtaining the flux ratio in different lattice cells. There are drawbacks of the existing methods; the S_n and the collision probability methods usually require a large number of mesh points. On the other hand, in order to take into account the azimuthal dependence of a flux in the moderator, many higher harmonics components should be taken in the spherical harmonics.

Though this azimuthal dependence of a flux is not considered in the Amouyal-Benoist method, it still gives fairly accurate results, and has been utilized in the case of criticality calculations for several kind of lattices⁽⁶⁾. The accuracy of the method comes from its embodying the quantity representing the blackness of the fuel rod. Inside the moderator it utilizes the diffusion equation with boundary condition of no net current at the equivalent outer cell boundary and of the extrapolation distance for a black rod at the surface of the fuel rod. This condition in the moderator becomes useless for closely packed lattice cells.

Therefore we use the multiple collision probability in the moderator and derive an extended Dancoff factor which includes the effect of configuration of the lattice. Thus we correlate all the probabilities in the moderator to the extended Dancoff factor.

In §3.2 an analytic expression of the disadvantage factor is introduced in two-region cell consisting of a fuel rod and a surrounding moderator. The disadvantage factor obtained is similar to that obtained by the collision probability method, if the blackness of the fuel rod is expressed in a simplified form. The result of the present method differs from that of Amouyal and Benoist in the point that the flux ratio between the moderator and the fuel for a cell with a thin moderator includes not only a factor inversely proportional to the blackness of the fuel rod but also an additional factor proportional to the extended Dancoff factor. It would appear reasonable to assume that, for a cell including a thin moderator, the flux ratio depends directly on the extended Dancoff factor.

An extension to multi-region cell problems is done in §3.3. In this section the neutron currents on both sides of each interface are connected by the multiple collision probability. In the multiple collision probability method, it is usually assumed that the neutron angular distribution on each interface is angular independent in each half range; $\mu > 0$ or $\mu < 0$. Therefore too many increase of the number of division makes the assumption worse. In general the multiple collision probability is evaluated by assuming the flat flux in each region. This assumption is not good for a region with thickness larger than the neutron mean free path, because the neutron density shows appreciable change through the region. Therefore the usual multiple collision probability is unsatisfactory to use under the above assumption.

Then we adopt a variational technique to obtain a better estimation of the multiple collision probability. The neutron flux within each annular region is expanded into a Legendre series as done in §2.4 and the first two terms are retained in a functional. At the outermost moderator region we use the extended Dancoff factor instead of the perfect reflection condition.

In §3.4 the effect of the anisotropic scattering in a square cell with a thin moderator is investigated to estimate the accuracy of the isotropic return boundary condition. In this section we divide a cell into many square regions and calculate the flux and current at each mid-point of the square regions by using the first-flight collision probability.

In §3.5 flux distributions in both cases of two- and three-region polygonal cells are obtained and compared with the results of Amouyal-Benoist and Fukai. The effect of the anisotropic scattering in a square cell on the flux distribution is also evaluated, and is compared with the method in the preceding chapter.

§3.2 Disadvantage Factor in Two-Region Polygonal Cells⁽⁷⁾

In this section an analytic expression for the disadvantage factor in two-region cell system that includes the effect of lattice configuration is derived by improving the Amouyal-Benoist method.

To begin with, the fundamentals of the Amouyal-Benoist method are described here briefly. We utilize notations originally used: Σ_{in} is a cross section of type n which is one of t , s , c denoting total, scattering and capture respectively in the i -th region (0 = fuel rod, 1 = moderator); V_i and S_i are the volume and outer surface area of the i -th region per unit height along the axial direction. We assume that the neutron source is uniformly distributed only in the moderator and scattering is isotropic in the laboratory system.

In terms of the flux distribution $\Psi(\vec{r}_0, \vec{r}_1)$ created at a point \vec{r}_0 in the fuel by a unit source at a point \vec{r}_1 in the moderator, the thermal utilization factor can be written

$$f = \frac{\Sigma_{0c}}{V_1} \int_{V_0} d\vec{r}_0 \int_{V_1} d\vec{r}_1 \Psi(\vec{r}_0, \vec{r}_1) . \quad (3.1)$$

Using the reciprocity relation⁽⁸⁾, this reduces to

$$f = \frac{V_0 \Sigma_{0c}}{V_1 \Sigma_{1c}} \mathcal{P}_0 \mathcal{F} . \quad (3.2)$$

Here \mathcal{P}_0 is the probability that a neutron born uniformly in the fuel rod escapes from the rod directly or after some collisions in the rod, and \mathcal{F} is the probability that a neutron which has escaped from the fuel rod isotropically is captured in the moderator after suffering a number of scatterings.

If \mathcal{F}_0 represents \mathcal{F} in the case where the fuel rod is replaced by a black body, \mathcal{F} is related to \mathcal{F}_0 by

$$\mathcal{Y} = \mathcal{Y}_0 + (1 - \mathcal{Y}_0)(1 - \beta_0) \mathcal{Y} . \quad (3.3)$$

Therefore we have

$$\mathcal{Y} = \frac{\mathcal{Y}_0}{1 - (1 - \mathcal{Y}_0)(1 - \beta_0)} , \quad (3.4)$$

where β_0 is the blackness of the fuel rod, and is related to \mathcal{P}_0 by

$$\frac{S_0}{4} \beta_0 = V_0 \Sigma_{0c} \mathcal{P}_0 . \quad (3.5)$$

We assume that \mathcal{P}_1 is the probability for a neutron born uniformly in the moderator to be captured in the fuel rods in the case where the fuel is black. Then \mathcal{P}_1 is related to \mathcal{Y}_0 by

$$\mathcal{Y}_0 = \frac{4 V_1 \Sigma_{1c}}{S_0} \mathcal{P}_1 . \quad (3.6)$$

From Eqs. (3.2) through (3.6) we obtain

$$\frac{1}{f} - 1 = \frac{V_1 \Sigma_{1c}}{V_0 \Sigma_{0c} \mathcal{P}_0} + \frac{1 - \mathcal{P}_1}{\mathcal{P}_1} - \frac{4 V_1 \Sigma_{1c}}{S_0} . \quad (3.7)$$

From the above equation and the definition

$$f \equiv \frac{\phi_0 V_0 \Sigma_{0c}}{\phi_0 V_0 \Sigma_{0c} + \phi_1 V_1 \Sigma_{1c}} \quad (3.8)$$

(ϕ_i is the average flux in the i-th region), the flux ratio is given by

$$\frac{\phi_1}{\phi_0} = \frac{1}{\mathcal{P}_0} - \frac{4 V_0 \Sigma_{0c}}{S_0} + \frac{V_0 \Sigma_{0c}}{V_1 \Sigma_{1c}} \cdot \frac{1 - \mathcal{P}_1}{\mathcal{P}_1} . \quad (3.9)$$

Equation (3.9) is the result of the Amouyal-Benoist method. In their paper \mathcal{P}_0 is calculated by taking into account the first and second collisions exactly and by approximating the subsequent collisions by

uniform source distributions, and \mathcal{P}_1 is calculated by making use of the diffusion equation in the moderator.

In the following, we calculate \mathcal{P}_1 or \mathcal{P} by the multiple collision probability method. It is seen from Eq. (3.2) that, in order to obtain the flux ratio, two probabilities \mathcal{P}_0 and \mathcal{P} are necessary.

First we calculate \mathcal{P} by considering a homogeneous limit of the lattice cell. Equation (3.4) may be rewritten in the form:

$$1 - \mathcal{P} = \frac{(1 - \mathcal{P}_0)\beta_0}{1 - (1 - \mathcal{P}_0)(1 - \beta_0)} \quad (3.10)$$

When the fuel is replaced by the moderator, the above equation transforms to

$$1 - \mathcal{P}^* = \frac{(1 - \mathcal{P}_0)\beta_0^*}{1 - (1 - \mathcal{P}_0)(1 - \beta_0^*)} \quad (3.11)$$

where * indicates that the medium of the fuel rod is replaced by the moderator. From Eqs. (3.10) and (3.11), we obtain

$$1 - \mathcal{P} = \frac{1 - \mathcal{P}^*}{\frac{\beta_0^*}{\beta_0} + (1 - \mathcal{P}^*)(1 - \frac{\beta_0^*}{\beta_0})} \quad (3.12)$$

Since this relation shows that the heterogeneous value \mathcal{P} can be represented by the homogeneous values \mathcal{P}^* and β_0^* , it is sufficient that, from now on, we treat these probabilities in a homogeneous system.

We introduce an extended Dancoff factor C^* which is the sum of the probabilities for a neutron escaping from the surface of a fuel rod with isotropic distribution to make its first collision in any other fuel rod which has the same cross section as the moderator. For a neighboring fuel rod, C^* is given by^{(9),(10)}

$$\begin{aligned}
C^* &= \frac{2}{\pi^2} \int_0^{\frac{\pi}{2}} d\psi \cos \psi \int_{-\frac{\pi}{2}}^{\frac{\pi}{2}} d\theta \cos \theta \frac{a}{\sqrt{d^2 - a^2 (\sin \theta - \sin \psi)^2}} \int_0^{\frac{\pi}{2}} d\psi \sin^2 \psi \\
&\cdot e^{-\frac{\Sigma_{it} \{ \sqrt{d^2 - a^2 (\sin \theta - \sin \psi)^2} - a \cos \psi - a \cos \theta \}}{\sin \psi}} \\
&\cdot \left(1 - e^{-\frac{2a \Sigma_{it} \cos \theta}{\sin \psi}} \right), \tag{3.13}
\end{aligned}$$

where a is the fuel radius and d is the distance between the two fuel rods considered. If we assume that a uniform neutron distribution throughout the cell is created by the first collision due to a source at the surface, we have

$$\begin{aligned}
\phi^* &= \frac{\Sigma_{ic}}{\Sigma_{it}} (1 - C^*) + \frac{V_i}{V_0 + V_i} \frac{\Sigma_{is}}{\Sigma_{it}} \\
&= \frac{V_i}{V_0 + V_i} + \frac{\Sigma_{ic}}{\Sigma_{it}} \left(\frac{V_0}{V_0 + V_i} - C^* \right). \tag{3.14}
\end{aligned}$$

More rigorously, we can proceed as follows. If we represent the average fluxes in the fuel and the moderator by ϕ_0^* and ϕ_i^* respectively, and if there is a unit isotropic source directed outward at the surface of the fuel rod, ϕ_0^* and ϕ_i^* satisfy the following equations of neutron conservation:

$$V_0 \Sigma_{it} \phi_0^* = C^* + V_0 \Sigma_{is} \phi_0^* P_{00}^* + V_i \Sigma_{is} \phi_i^* P_{i0}^*, \tag{3.15a}$$

$$V_i \Sigma_{it} \phi_i^* = 1 - C^* + V_0 \Sigma_{is} \phi_0^* P_{0i}^* + V_i \Sigma_{is} \phi_i^* P_{ii}^*, \tag{3.15b}$$

where P_{ij}^* is the first-flight collision probability for a neutron born in the i -th region to undergo its first collision in the j -th region in the case of homogeneous limit. Eliminating ϕ_0^* from the above two equations, we have

$$V_i \phi_i^* = \frac{1 - C^* + \frac{\Sigma_{is}}{\Sigma_{it} - \Sigma_{is} P_{00}^*} C^* P_{0i}^*}{\Sigma_{it} - \Sigma_{is} P_{ii}^* - \frac{\Sigma_{is}^2 P_{i0}^* P_{0i}^*}{\Sigma_{it} - \Sigma_{is} P_{00}^*}} \quad (3.16)$$

Then, making use of the conservation laws:

$$P_{00}^* + P_{0i}^* = 1, \quad (3.17a)$$

$$P_{i0}^* + P_{ii}^* = 1, \quad (3.17b)$$

and the reciprocity relation:

$$V_0 P_{0i}^* = V_i P_{i0}^*, \quad (3.18)$$

the absorption ratio in the moderator is given by

$$\begin{aligned} \varphi^* = V_i \phi_i^* \Sigma_{ic} &= \frac{1 - C^* + \frac{\Sigma_{is}}{\Sigma_{it} - \Sigma_{is} P_{00}^*} C^* P_{0i}^*}{1 + \frac{\Sigma_{is} V_0}{V_i (\Sigma_{it} - \Sigma_{is} P_{00}^*)} P_{0i}^*} \\ &= \frac{V_i}{V_0 + V_i} \cdot \frac{1 - \frac{C^* \Sigma_{ic}}{\Sigma_{is} P_{0i}^*}}{1 - \frac{V_0}{V_0 + V_i} \cdot \frac{\Sigma_{ic}}{\Sigma_{is} P_{0i}^*}} \quad (3.19) \end{aligned}$$

In the case of a small absorption cross section in the moderator

($\Sigma_{ic} / \Sigma_{is} \ll 1$), we have

$$\varphi^* = \frac{V_i}{V_0 + V_i} \left\{ 1 + \left(\frac{V_0}{V_0 + V_i} - C^* \right) \frac{\Sigma_{ic}}{\Sigma_{is} P_{0i}^*} \right\} \quad (3.20)$$

Equation (3.20) reduces to Eq. (3.14) if we assume $P_{0i}^* = V_i / (V_0 + V_i)$.

Namely Eq. (3.20) embodies a more heterogeneous effect than Eq. (3.14).

Using Eqs. (3.12) and (3.19) and a relation obtained from Eqs.

(3.2) and (3.8):

$$\frac{\phi_i}{\phi_o} = \frac{1}{\rho_o \gamma} - \frac{V_o \Sigma_{oc}}{V_i \Sigma_{ic}} \quad , \quad (3.21)$$

we can obtain the flux ratio

$$\begin{aligned} \frac{\phi_i}{\phi_o} &= \frac{1}{\rho_o} \left(1 + \frac{1 - \gamma^*}{\gamma^*} \frac{\beta_o}{\beta_o^*} \right) - \frac{V_o \Sigma_{oc}}{V_i \Sigma_{ic}} \\ &= \frac{1}{\rho_o} \left(1 + \frac{C^* \Sigma_{ic} + \frac{\Sigma_{is} V_o}{V_i} P_{oi}^*}{\Sigma_{it} - C^* \Sigma_{ic} - \Sigma_{is} P_{oi}^*} \cdot \frac{\beta_o}{\beta_o^*} \right) - \frac{V_o \Sigma_{oc}}{V_i \Sigma_{ic}} \quad . \end{aligned} \quad (3.22)$$

The blackness β_o^* of the fuel rod with the same cross section as in the moderator is expressed in the form (see Appendix 3 A):

$$\beta_o^* = \frac{1}{1 + Y^*} \cdot \frac{2 a \Sigma_{ic} (1 - P_c^*)}{1 - \frac{\Sigma_{is}}{\Sigma_{it}} P_c^*} \quad , \quad (3.23)$$

where Y^* is the quantity that represents the deviation of the value of the blackness obtained by the flat flux approximation from the exact value, and P_c^* is the probability that a neutron born uniformly in the fuel rod makes its first collision within the same rod when the medium of the fuel rod is replaced by the moderator. Using Eqs. (3.5) and (3.23), Eq. (3.22) reduces to

$$\begin{aligned} \frac{\phi_i}{\phi_o} &= \frac{1}{\rho_o} + \frac{V_o \Sigma_{oc}}{V_i \Sigma_{ic}} \cdot \frac{\left(1 - \frac{\Sigma_{ic}}{\Sigma_{it}} + \frac{V_i \Sigma_{ic} C^*}{V_o \Sigma_{it} P_{oi}^*} \right) \left(1 + \frac{\Sigma_{ic} P_c^*}{\Sigma_{it} (1 - P_c^*)} \right) (1 + Y^*)}{1 - \frac{\Sigma_{ic} C^*}{\Sigma_{it} P_{oi}^*} + \frac{\Sigma_{ic} P_{oo}^*}{\Sigma_{it} P_{oi}^*}} \\ &\quad - \frac{V_o \Sigma_{oc}}{V_i \Sigma_{ic}} \quad . \end{aligned} \quad (3.24)$$

When the absorption cross section in the moderator is negligibly small, the above equation reduces to

$$\frac{\phi_1}{\phi_0} = \frac{1}{P_0} + \frac{V_0 \Sigma_{oc}}{V_1 \Sigma_{1t}} \left(\frac{V_0 + V_1}{V_0} \cdot \frac{C^*}{P_{01}^*} - 1 + \frac{P_c^*}{1 - P_c^*} - \frac{P_{00}^*}{P_{01}^*} + Y^* \right) . \quad (3.25)$$

Here the probability P_{01}^* can be assumed to be a product of two probabilities; one is a probability that a neutron born uniformly in the fuel rod with the same cross section as the moderator escapes from the rod, and the other is that a neutron which has escaped from the rod makes its first collision in the moderator. Namely it can be written in the form

$$P_{01}^* = (1 - P_c^*)(1 - C^*) . \quad (3.26)$$

Then Eq. (3.25) is written in the form

$$\frac{\phi_1}{\phi_0} = \frac{1}{P_0} + \frac{V_0 \Sigma_{oc}}{V_1 \Sigma_{1t}} \left\{ \frac{C^* V_1}{P_{01}^* V_0} + Y^* - 1 \right\} . \quad (3.27)$$

§3.3 Application to Multi-Region Polygonal Cell System⁽¹¹⁾

The method in the preceding section is applied to polygonal cell system in which each cell is divided into several concentric annular regions except an outermost moderator region. Each annular region is denoted by an integer n ($1 \leq n \leq N$) numbered from the center outwardly and the outermost moderator by M (cf. Fig. 3.1). Let us consider the n -th region and express the incoming and outgoing neutron total currents on the outer boundary by J_n^- and J_n^+ respectively and those on the inner boundary by J_{n-1}^- and J_{n-1}^+ . The inner and outer radii of the region are denoted by r_{n-1} and r_n respectively, and the surface area of the outer boundary is denoted by σ_n . The total neutron source

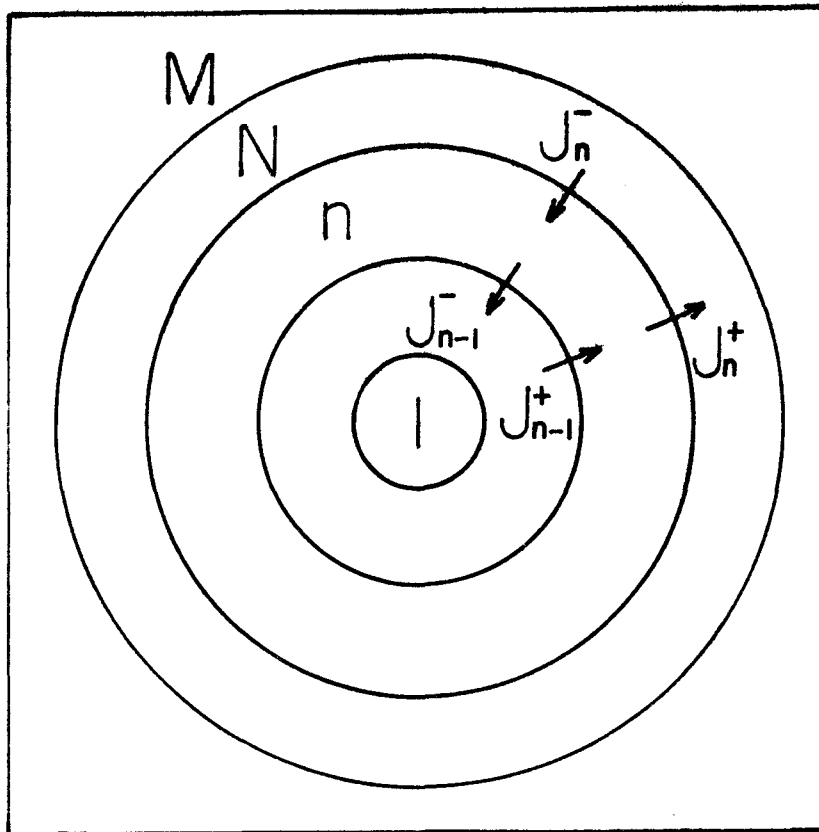


Fig. 3.1 Notations in a square cell

(source density \times volume) in the n -th region is expressed by S_n .

Then there are relations among the neutron currents: ⁽¹²⁾

$$J_n^+ = J_{n-1}^+ \mathcal{P}_n^{i0} + J_n^- \mathcal{P}_n^{o0} + S_n \mathcal{P}_n^{v0}, \quad (3.28a)$$

$$J_{n-1}^- = J_n^- \mathcal{P}_n^{oi} + J_{n-1}^+ \mathcal{P}_n^{ii} + S_n \mathcal{P}_n^{vi}, \quad (3.28b)$$

where all the probabilities \mathcal{P}_n 's defined below are to be calculated in the case where all the inner regions than the n -th region are black, and

\mathcal{P}_n^{i0} = the probability that a neutron entering the n -th region isotropically from the inner boundary escapes from the region through the outer boundary directly or after suffering some collisions in it,

\mathcal{P}_n^{o0} = the probability that a neutron entering the n -th region isotropically from the outer boundary escapes from the region through the outer boundary again directly or after some collisions in it,

\mathcal{P}_n^{v0} = the probability that a neutron born uniformly in the n -th region escapes from the region through the outer boundary.

Another three probabilities will easily be conjectured from the suffixes.

Though the probabilities \mathcal{P}_n 's include the effect of multiple collisions, we define similar probabilities P 's with the same suffixes as \mathcal{P}_n 's, by taking account of the first-flight effect only.

Equation (3.28) may be written in the matrix form:

$$\begin{pmatrix} J_n^+ \\ J_n^- \end{pmatrix} = \begin{pmatrix} \mathcal{P}_n^{i0} - \frac{\mathcal{P}_n^{oo}}{\mathcal{P}_n^{oi}} \mathcal{P}_n^{ii} & \frac{\mathcal{P}_n^{o0}}{\mathcal{P}_n^{oi}} \\ -\frac{\mathcal{P}_n^{ii}}{\mathcal{P}_n^{oi}} & 1 \end{pmatrix} \begin{pmatrix} J_{n-1}^+ \\ J_{n-1}^- \end{pmatrix} + \begin{pmatrix} \mathcal{P}_n^{v0} - \frac{\mathcal{P}_n^{oo}}{\mathcal{P}_n^{oi}} \mathcal{P}_n^{vi} \\ -\frac{\mathcal{P}_n^{vi}}{\mathcal{P}_n^{oi}} \end{pmatrix} S_n. \quad (3.29)$$

Thus, $\begin{pmatrix} J_n^+ \\ J_n^- \end{pmatrix}$ may be connected with $\begin{pmatrix} J_1^+ \\ J_1^- \end{pmatrix}$ by successive application of the above equation. Then if there are two boundary conditions on the inner- and outermost boundaries all the currents are evaluated. The average neutron flux ϕ_n in the n-th region is determined from the conservation law:

$$V_n \Sigma_{nc} \phi_n = S_n + (J_n^- + J_{n-1}^+ - J_n^+ - J_{n-1}^-), \quad (3.30)$$

where V_n and Σ_{nc} are the volume and the capture cross section of the n-th region.

In what follows, the six probabilities $P_n^{i^o}$, P_n^{oo} , P_n^{vo} , P_n^{oi} , P_n^{ii} and P_n^{vi} are calculated to determine the neutron currents.

First, we calculate the probability P_n^{oo} . Let the flux be $\phi(\vec{r})$ which is produced at position \vec{r} in the n-th region due to an isotropically injected neutron source from the outer boundary. Here we assume that all regions except the n-th region are black, namely the mean free path is zero elsewhere. The uncollided flux due to the source is denoted by $\Pi_0(\vec{r})$, then

$$\Pi_0(\vec{r}) = \frac{1}{\Omega_n \pi} \int_{\Omega_n} d\sigma \frac{(\vec{n} \cdot \vec{\Omega}^*)}{R_s^2} e^{-\hat{\Sigma} \hat{R}_s}, \quad (3.31)$$

where \vec{n} is the inward normal vector on the outer boundary of the n-th region, $\vec{\Omega}^*$ the unit directional vector along a neutron flight, and R_s and $\hat{\Sigma} \hat{R}_s$ the real and optical distances from the boundary to the point \vec{r} respectively. The integral about σ means the surface integration on the outer boundary of the n-th region. The neutron flux satisfies the integral Boltzmann equation

$$\phi(\vec{r}) = \int_{V_n} d\vec{r}' \frac{e^{-\hat{\Sigma} \hat{R}}}{4 \pi R^2} \Sigma_{ns} \phi(\vec{r}') + \Pi_0(\vec{r}). \quad (3.32)$$

We consider the functional T of the form⁽¹³⁾

$$T = 2 \int_{V_n} d\vec{r} \phi(\vec{r}) \pi_0(\vec{r}) + \int_{V_n} d\vec{r} \phi(\vec{r}) \int_{V_n} d\vec{r}' \frac{e^{-2\vec{r}\vec{r}'}}{4\pi R^2} \Sigma_{ns} \phi(\vec{r}') - \int_{V_n} d\vec{r} \phi^2(\vec{r}) . \quad (3.33)$$

This functional is stationary with respect to the variation of $\phi(\vec{r})$.

We expand the flux in the n-th annular region into a Legendre series:

$$\phi(\vec{r}) = \sum_{k=0}^K \phi_k P_k \left(\frac{2r^2 - r_n^2 - r_{n-1}^2}{r_n^2 - r_{n-1}^2} \right) , \quad (3.34)$$

where K is the upper limit of k after which terms are truncated.

By substituting Eq. (3.34) into Eq. (3.33) and using the stationary condition

$$\frac{dT}{d\phi_k} = 0 , \quad (k = 0, 1, \dots, K) \quad (3.35)$$

we have

$$\begin{aligned} & \phi_k \left[\int_{V_n} d\vec{r} P_k(r^*) \int_{V_n} d\vec{r}' \frac{e^{-2\vec{r}\vec{r}'}}{4\pi R^2} \Sigma_{ns} P_k(r'^*) - \frac{V_n}{2k+1} \right] \\ & + \sum_{k' \neq k} \phi_{k'} \left[\int_{V_n} d\vec{r} P_k(r^*) \int_{V_n} d\vec{r}' \frac{e^{-2\vec{r}\vec{r}'}}{4\pi R^2} \Sigma_{ns} P_{k'}(r'^*) \right] \\ & + \int_{V_n} d\vec{r} \pi_0(r) P_k(r^*) = 0 , \end{aligned} \quad (3.36)$$

where we used

$$r^* \equiv \frac{2r^2 - r_n^2 - r_{n-1}^2}{r_n^2 - r_{n-1}^2} ,$$

and the orthogonal relation of the Legendre polynomials:

$$\int_{V_n} d\vec{r} P_k(r^*) P_{k'}(r^*) = \begin{cases} \frac{V_n}{2k+1} & \dots \dots k = k' \\ 0 & \dots \dots k \neq k' \end{cases} . \quad (3.37)$$

If we put $K = 1$ in Eq. (3.36), it follows that

$$\phi_0 (c_n P_n^{vv} - 1) + \phi_i c_n Q_n^{vv} + \pi_{00} = 0, \quad (3.38a)$$

$$\phi_i (c_n R_n^{vv} - \frac{1}{3}) + \phi_0 c_n Q_n^{vv} + \pi_{0i} = 0, \quad (3.38b)$$

where c_n is the scattering ratio in the n-th region and

$$\pi_{00} = \frac{1}{V_n} \int_{V_n} d\vec{r} \pi_0(\vec{r}), \quad (3.39)$$

$$\pi_{0i} = \frac{1}{V_n} \int_{V_n} d\vec{r} \pi_0(r) P_i(r^*), \quad (3.40)$$

$$P_n^{vv} = \frac{\Sigma_n}{V_n} \int_{V_n} d\vec{r} \int_{V_n} d\vec{r}' \frac{e^{-\hat{z}\hat{R}}}{4\pi R^2}, \quad (3.41)$$

$$Q_n^{vv} = \frac{\Sigma_n}{V_n} \int_{V_n} d\vec{r} \int_{V_n} d\vec{r}' \frac{e^{-\hat{z}\hat{R}}}{4\pi R^2} P_i(r^*), \quad (3.42)$$

$$R_n^{vv} = \frac{\Sigma_n}{V_n} \int_{V_n} d\vec{r} \int_{V_n} d\vec{r}' \frac{e^{-\hat{z}\hat{R}}}{4\pi R^2} P_i(r^*) P_i(r'^*). \quad (3.43)$$

Using the solution of Eq. (3.38) the functional T may be reduced to the form

$$\begin{aligned} T &= V_n \left\{ \phi_0^2 (c_n P_n^{vv} - 1) + 2 \phi_0 \phi_i c_n Q_n^{vv} + 2 \phi_0 \pi_{00} \right. \\ &\quad \left. + \phi_i^2 (c_n R_n^{vv} - \frac{1}{3}) + 2 \phi_i \pi_{0i} \right\} \\ &= V_n \frac{(1 - c_n P_n^{vv}) \pi_{0i}^2 + 2 c_n Q_n^{vv} \pi_{00} \pi_{0i} + (\frac{1}{3} - c_n R_n^{vv}) \pi_{00}^2}{(1 - c_n P_n^{vv})(\frac{1}{3} - c_n R_n^{vv}) - c_n^2 (Q_n^{vv})^2}. \end{aligned} \quad (3.44)$$

The stationary value of T is given by

$$\begin{aligned} T &= \int_{V_n} d\vec{r} \phi(r) \frac{1}{\sigma_n \pi} \int_{\sigma_n} d\sigma (\vec{n} \cdot \vec{n}^*) \frac{e^{-\hat{z}\hat{R}_s}}{R_s^2} \\ &= \frac{4}{\sigma_n \Sigma_{ns}} \int_{V_n} d\vec{r} \phi(r) \Sigma_{ns} \int_{\Omega_0} \frac{d\vec{\Omega}}{4\pi} e^{-\hat{z}\hat{R}_s} = \frac{4}{\sigma_n \Sigma_{ns}} \mathcal{P}_n^{000}, \end{aligned} \quad (3.45)$$

where the integration about $\vec{\Omega}$ is performed over the domain Ω_0 corresponding to the whole angle 4π minus the solid angle subtended by the outer surface of the (n-1)-th region at each point \vec{r} . The probability \mathcal{P}_n^{ovo} is defined as that for a neutron entering the n-th region isotropically from its outer surface to escape from the region through the outer boundary after suffering some collisions in it.

In the same manner as in deriving Eq. (3.45), we obtain

$$\pi_{oo} = \frac{4}{\sigma_n} \cdot \frac{1}{V_n} \int_{V_n} d\vec{r} \int_{\Omega_0} \frac{d\vec{\Omega}}{4\pi} e^{-\vec{r}\vec{\Omega}} = \frac{4}{\sigma_n} P_n^{vo}, \quad (3.46)$$

$$\pi_{oi} = \frac{4}{\sigma_n} \cdot \frac{1}{V_n} \int_{V_n} d\vec{r} \int_{\Omega_0} \frac{d\vec{\Omega}}{4\pi} P_i(r^*) e^{-\vec{r}\vec{\Omega}} = \frac{4}{\sigma_n} Q_n^{vo}. \quad (3.47)$$

By equating Eq. (3.44) to Eq. (3.45) and making use of Eqs. (3.46) and (3.47) we get the equation

$$\mathcal{P}_n^{ovo} = \frac{4 \sum_{ns} V_n}{\sigma_n} \cdot \frac{(P_n^{vo})^2 (\frac{1}{3} - c_n R_n^{vv}) + 2 P_n^{vo} Q_n^{vo} c_n Q_n^{vv} + (1 - c_n P_n^{vv}) (Q_n^{vo})^2}{(1 - c_n P_n^{vv}) (\frac{1}{3} - c_n R_n^{vv}) - c_n^2 (Q_n^{vv})^2}. \quad (3.48)$$

The probability \mathcal{P}_n^{oo} is obtained by adding to \mathcal{P}_n^{ovo} the probability for a neutron entering the n-th region from the outer boundary to escape from the region directly through the outer boundary:

$$\mathcal{P}_n^{oo} = \mathcal{P}_n^{ovo} + P_n^{oo}. \quad (3.49)$$

This expression reduces to the well-known formula by the flat flux approximation if the quantity $Q = 0$ in Eq. (3.48). The quantity Q expresses the deviation of the flux from the flat one.

Using the same technique as in obtaining \mathcal{P}_n^{ovo} , we get

$$\mathcal{P}_n^{ovi} = \frac{4 \sum_{ns} V_n}{\sigma_{n-1}} \cdot \frac{(P_n^{vi})^2 (\frac{1}{3} - c_n R_n^{vv}) + 2 P_n^{vi} Q_n^{vi} c_n Q_n^{vv} + (1 - c_n P_n^{vv}) (Q_n^{vi})^2}{(1 - c_n P_n^{vv}) (\frac{1}{3} - c_n R_n^{vv}) - c_n^2 (Q_n^{vv})^2}. \quad (3.50)$$

Since there is no neutron which leaks directly through the inner boundary due to a source emitted from the inner boundary,

$$\mathcal{P}_n^{ii} = \mathcal{P}_n^{ivi} . \quad (3.51)$$

In the following, we calculate the probabilities (blacknesses)

β_o and β_i respectively that a neutron entering the n-th region from the outer or inner boundary is absorbed in the region when all the internal media are black. Since there are conservation laws

$$\mathcal{P}_n^{oi} + \mathcal{P}_n^{oo} + \beta_o = 1 , \quad (3.52a)$$

$$\mathcal{P}_n^{io} + \mathcal{P}_n^{ii} + \beta_i = 1 , \quad (3.52b)$$

\mathcal{P}_n^{oi} and \mathcal{P}_n^{io} are easily evaluated if β_o and β_i are known.

Substitution of Eq. (3.34) ($K = 1$) into Eq. (3.32) and integration over the volume of the n-th region after multiplying by $P_k(r^*)$ ($k = 0, 1$) lead to the equations

$$\phi_o \Sigma_n = \Sigma_n \pi_{oo} + \phi_o \Sigma_{ns} P_n^{vv} + \phi_i \Sigma_{ns} Q_n^{vv} , \quad (3.53)$$

$$\frac{\phi_i \Sigma_n}{3} = \Sigma_n \pi_{oi} + \phi_o \Sigma_{ns} Q_n^{vv} + \phi_i \Sigma_{ns} R_n^{vv} . \quad (3.54)$$

The solution of these equations is

$$\phi_o = \frac{\pi_{oo} (\frac{1}{3} - c_n R_n^{vv}) + c_n Q_n^{vv} \pi_{oi}}{(1 - c_n P_n^{vv})(\frac{1}{3} - c_n R_n^{vv}) - c_n^2 (Q_n^{vv})^2} . \quad (3.55)$$

Then the blackness β_o is calculated from the definition

$$\begin{aligned} \beta_o &= \int_{V_n} d\vec{r} \Sigma_{nc} \phi(r) = V_n \Sigma_{nc} \phi_o \\ &= V_n \Sigma_{nc} \frac{\pi_{oo} (\frac{1}{3} - c_n R_n^{vv}) + c_n Q_n^{vv} \pi_{oi}}{(1 - c_n P_n^{vv})(\frac{1}{3} - c_n R_n^{vv}) - c_n^2 (Q_n^{vv})^2} . \end{aligned} \quad (3.56)$$

In terms of Eqs. (3.46) and (3.47) and the reciprocity relations

$$V_n \sum_n P_n^{v0} = \frac{\sigma_n}{4} P_n^{0v}, \quad (3.57)$$

$$V_n \sum_n Q_n^{v0} = \frac{\sigma_n}{4} Q_n^{0v}, \quad (3.58)$$

Eq. (3.56) is transformed to

$$\beta_0 = (1 - c_n) \frac{P_n^{0v} (\frac{1}{3} - c_n R_n^{vv}) + c_n Q_n^{0v} Q_n^{vv}}{(1 - c_n P_n^{vv}) (\frac{1}{3} - c_n R_n^{vv}) - c_n^2 (Q_n^{vv})^2}. \quad (3.59)$$

In a similar manner, β_i may be calculated as follows:

$$\beta_i = (1 - c_n) \frac{P_n^{iv} (\frac{1}{3} - c_n R_n^{vv}) + c_n Q_n^{iv} Q_n^{vv}}{(1 - c_n P_n^{vv}) (\frac{1}{3} - c_n R_n^{vv}) - c_n^2 (Q_n^{vv})^2}. \quad (3.60)$$

The probabilities P_n^{v0} and P_n^{vi} are evaluated from the relations

$$\frac{\sigma_n}{4} \beta_0 = V_n \sum_{nc} P_n^{v0}, \quad (3.61)$$

$$\frac{\sigma_{n-1}}{4} \beta_i = V_n \sum_{nc} P_n^{vi}. \quad (3.62)$$

Thus all the probabilities necessary to determine the neutron currents have been calculated.

In the following, the boundary condition in the outermost moderator region is considered. To take into account the effect of the lattice configuration we adopt the concept of the extended Dancoff factor.

For the present case the extended Dancoff factor C^* is defined as the probability that a neutron emitted outwardly from the outer boundary of the N-th region undergoes its first collision at any of the regions $1 \sim N$ in another cells composed of the moderator material replaced with real media. Notations adopted in the preceding section are redefined by

φ_0 = the probability that a neutron emitted outwards from the

boundary σ_N is captured in the moderator in the case where the media of $1 \sim N$ regions become black,

\mathcal{Y}^* = the similar probability to \mathcal{Y}_0 in the meaning that the media in the regions $1 \sim N$ are replaced by the moderator,

β_0^* = the blackness of the regions $1 \sim N$ for a neutron inwardly entering the regions from the boundary σ_N , under the assumption of the isotropic distribution, to be captured in the regions $1 \sim N$ when they have the same medium as the moderator.

Using these quantities we calculate the probabilities \mathcal{P}_M^{ii} and \mathcal{P}_M^{vi} , which are necessary to relate J_N^+ and J_N^- :

$$J_N^- = J_N^+ \mathcal{P}_M^{ii} + S_M \mathcal{P}_M^{vi}. \quad (3.63)$$

From the definition of \mathcal{Y}_0 ,

$$\mathcal{P}_M^{ii} = 1 - \mathcal{Y}_0. \quad (3.64)$$

Making use of Eq. (3.11) in the case where β_0^* is very small, the probability \mathcal{P}_M^{ii} reduces to

$$\mathcal{P}_M^{ii} = 1 - \frac{\mathcal{Y}^*}{1 - \mathcal{Y}^*} \beta_0^*. \quad (3.65)$$

Here, for the calculation of β_0^* , it will be sufficient to use the flat flux approximation:

$$\beta_0^* = \frac{2 \gamma_N \Sigma_{Mc} (1 - P_c^*)}{1 - \frac{\Sigma_{Ms}}{\Sigma_M} P_c^*}, \quad (3.66)$$

where P_c^* is the probability for a neutron born uniformly in the regions $1 \sim N$ having the same property as the moderator to undergo its first collision in the regions $1 \sim N$. The quantity \mathcal{Y}^* has already been given in Eq. (3.20). Then Eq. (3.65) can be evaluated.

Next we calculate \mathcal{P}_M^{vi} . The probability \mathcal{P}_M^{vi} is related to

φ_0 by

$$\mathcal{P}_M^{vi} = \frac{\Sigma_N}{4 V_M \Sigma_{Mc}} \varphi_0 . \quad (3.67)$$

Using Eqs. (3.11) and (3.66) the above equation is reduced to the form

$$\mathcal{P}_M^{vi} = 1 - \frac{P_c^*}{1 - P_c^*} \cdot \frac{\Sigma_{ic}}{\Sigma_i} - \frac{V_i}{V_0} \beta_0^* + \frac{V_0 + V_i}{V_0} \left(\frac{V_0}{V_0 + V_i} - C^* \right) \frac{\Sigma_{ic}}{\Sigma_{is} (1 - P_c^*) (1 - C^*)} . \quad (3.68)$$

where subscript 0 corresponds to all inner regions than M and subscript 1 to the region M. Thus the boundary condition of the outermost moderator region, Eq. (3.63), is established.

The neutron flux in the moderator is determined by

$$\Sigma_{Mc} V_M \phi_M = S_M \mathcal{P}_M^{vv} + J_N^- \mathcal{P}_M^{iv} , \quad (3.69)$$

whereupon using the relations

$$\mathcal{P}_M^{iv} = \frac{\varphi^*}{1 - \varphi^*} \cdot \frac{2 r_N \Sigma_{Mc} (1 - P_c^*)}{1 - \frac{\Sigma_{Ms}}{\Sigma_M} P_c^*} , \quad (3.70)$$

and

$$\mathcal{P}_M^{vv} = \frac{P_c^*}{1 - P_c^*} \cdot \frac{\Sigma_{Mc}}{\Sigma_M} + \frac{V_i}{V_0} \beta_0^* - \frac{V_0 + V_i}{V_0} \left(\frac{V_0}{V_0 + V_i} - C^* \right) \frac{\Sigma_{Mc}}{\Sigma_{Ms} (1 - P_c^*) (1 - C^*)} , \quad (3.71)$$

we have

$$\begin{aligned} \phi_M = \frac{S_M}{V_M} \left\{ \frac{P_c^*}{1 - P_c^*} \cdot \frac{1}{\Sigma_M} + \frac{V_i}{V_0} \cdot \frac{2 r_N (1 - P_c^*)}{1 - \frac{\Sigma_{Ms}}{\Sigma_M} P_c^*} - \frac{V_0 + V_i}{V_0} \right. \\ \left. \cdot \left(\frac{V_0}{V_0 + V_i} - C^* \right) \frac{1}{\Sigma_{Ms} (1 - P_c^*) (1 - C^*)} \right\} + \frac{J_N^+}{V_M} \cdot \frac{\varphi^*}{1 - \varphi^*} \cdot \frac{2 r_N (1 - P_c^*)}{1 - \frac{\Sigma_{Ms}}{\Sigma_M} P_c^*} . \end{aligned} \quad (3.72)$$

One more boundary condition is given in the innermost region by

$$J_1^+ = J_1^- \mathcal{P}_1^{o0} + S_1 \mathcal{P}_1^{v0} . \quad (3.73)$$

Here $\mathcal{P}_i^{\circ\circ}$ corresponds to 1 minus the blackness for a neutron impinging upon the innermost region inwardly to be captured; the blackness for the central fuel rod being evaluated in Appendix 3A. Thus all the multiple collision probabilities and the boundary conditions have been obtained and the neutron currents and fluxes can be evaluated.

§3.4 Effect of Anisotropic Scattering in a Square Lattice⁽¹⁴⁾

In this section we will study the effect of anisotropic scattering on the flux ratio in a square cell containing a thin moderator. In the preceding chapter we introduced the anisotropic collision probability under the isotropic reflection condition on the lattice cell boundary. In the case of large fuel rod, however, there is no assurance of the validity of isotropic reflection condition on the cell surface. Then we divide a cell into meshes as in the THERMOS code and investigate the effect of anisotropic scattering.

We make use of the Boltzmann integral equation (2.14). Since, in this section, we take into account up to the anisotropic scattering proportional to μ (cosine of the scattering angle) and the current along the z-axis is zero for infinitely long fuel rods, the scattering kernel, flux and source are expanded as follows:

$$\Sigma_s(\vec{r}; \vec{\Omega} \rightarrow \vec{\Omega}) = \frac{1}{4\pi} \left\{ \Sigma_s^0(\vec{r}) + 3 \Sigma_s^1(\vec{r}) (\Omega_x \Omega_{x'} + \Omega_y \Omega_{y'} + \Omega_z \Omega_{z'}) \right\}, \quad (3.74)$$

$$\phi(\vec{r}, \vec{\Omega}) = \frac{1}{4\pi} \left\{ \phi^0(\vec{r}) + 3 (\phi_x^1(\vec{r}) \Omega_x + \phi_y^1(\vec{r}) \Omega_y) \right\}, \quad (3.75)$$

$$S(\vec{r}, \vec{\Omega}) = \frac{1}{4\pi} S^0(\vec{r}). \quad (3.76)$$

Three equations for flux components ϕ^0 , ϕ_x^1 and ϕ_y^1 are obtained by the integration over $d\vec{\Omega}$, and Ω_x or Ω_y multiplied integrations after the substitution of Eqs. (3.74) ~ (3.76) into Eq. (2.14):

$$\begin{aligned} \phi^0(\vec{r}) = & \int d\vec{r}' \frac{\bar{e}^{\vec{r}-\vec{r}'}}{4\pi R^2} \left[S^0(\vec{r}') + \Sigma_s^0(\vec{r}') \phi^0(\vec{r}') \right. \\ & \left. + 3 \Sigma_s^1(\vec{r}') \{ \phi_x^1(\vec{r}') \Omega_x^* + \phi_y^1(\vec{r}') \Omega_y^* \} \right], \end{aligned} \quad (3.77)$$

$$\begin{aligned}\phi'_x(\vec{r}) = & \int d\vec{r}' \frac{e^{-\hat{\Sigma}\vec{R}}}{4\pi R^2} \Omega_x^* \left[S^0(\vec{r}') + \Sigma_s^0(\vec{r}') \phi^0(\vec{r}') \right. \\ & \left. + 3 \Sigma_s^1(\vec{r}') \left\{ \phi'_x(\vec{r}') \Omega_x^* + \phi'_y(\vec{r}') \Omega_y^* \right\} \right],\end{aligned}\quad (3.78)$$

$$\begin{aligned}\phi'_y(\vec{r}) = & \int d\vec{r}' \frac{e^{-\hat{\Sigma}\vec{R}}}{4\pi R^2} \Omega_y^* \left[S^0(\vec{r}') + \Sigma_s^0(\vec{r}') \phi^0(\vec{r}') \right. \\ & \left. + 3 \Sigma_s^1(\vec{r}') \left\{ \phi'_x(\vec{r}') \Omega_x^* + \phi'_y(\vec{r}') \Omega_y^* \right\} \right].\end{aligned}\quad (3.79)$$

We can perform the integration over dz' in the volume integral dr' :

$$\begin{aligned}\phi^0(x, y) = & \frac{1}{4\pi} \iint dx' dy' \left[\left\{ S^0(x', y') + \Sigma_s^0(x', y') \phi^0(x', y') \right\} \frac{2}{\rho} K_{i1}(\tau) \right. \\ & \left. + 3 \Sigma_s^1(x', y') \left\{ (x-x') \phi'_x(x', y') + (y-y') \phi'_y(x', y') \right\} \frac{2}{\rho^2} K_{i2}(\tau) \right],\end{aligned}\quad (3.80)$$

$$\begin{aligned}\phi'_x(x, y) = & \frac{1}{4\pi} \iint dx' dy' (x-x') \left[\left\{ S^0(x', y') + \Sigma_s^0(x', y') \phi^0(x', y') \right\} \frac{2}{\rho^2} K_{i2}(\tau) \right. \\ & \left. + 3 \Sigma_s^1(x', y') \left\{ (x-x') \phi'_x(x', y') + (y-y') \phi'_y(x', y') \right\} \frac{2}{\rho^3} K_{i3}(\tau) \right],\end{aligned}\quad (3.81)$$

$$\begin{aligned}\phi'_y(x, y) = & \frac{1}{4\pi} \iint dx' dy' (y-y') \left[\left\{ S^0(x', y') + \Sigma_s^0(x', y') \phi^0(x', y') \right\} \frac{2}{\rho^2} K_{i2}(\tau) \right. \\ & \left. + 3 \Sigma_s^1(x', y') \left\{ (x-x') \phi'_x(x', y') + (y-y') \phi'_y(x', y') \right\} \frac{2}{\rho^3} K_{i3}(\tau) \right],\end{aligned}\quad (3.82)$$

where Ki_n is the Bickley function of order n ⁽¹⁵⁾, ρ the length between \vec{r} and \vec{r}' projected onto the x-y plane, and τ the optical distance along the projected length.

In the case of dividing the surface integral over $dx'dy'$ into meshes, we concisely express the mesh having the center point $x = x_i$, $y = y_j$ by ij ; Δ_{ij} is the area of the mesh ij . Thereupon we have

$$\Delta_{kl} \Sigma_{kl} \phi_{kl}^0 = \sum_{i,j} \Delta_{ij} \left[(S_{ij}^0 + \Sigma_{s,ij}^0 \phi_{ij}^0) P_{ij \rightarrow kl}^{00} \right. \\ \left. + 3 \Sigma_{s,ij}^1 (\phi_{x,ij}^1 P_{ij \rightarrow kl}^{10} + \phi_{y,ij}^1 P_{ij \rightarrow kl}^{20}) \right], \quad (3.83)$$

$$\Delta_{kl} \Sigma_{kl} \phi_{x,kl}^1 = \sum_{i,j} \Delta_{ij} \left[(S_{ij}^0 + \Sigma_{s,ij}^0 \phi_{ij}^0) P_{ij \rightarrow kl}^{10} \right. \\ \left. + 3 \Sigma_{s,ij}^1 (\phi_{x,ij}^1 P_{ij \rightarrow kl}^{11} + \phi_{y,ij}^1 P_{ij \rightarrow kl}^{12}) \right], \quad (3.84)$$

$$\Delta_{kl} \Sigma_{kl} \phi_{y,kl}^1 = \sum_{i,j} \Delta_{ij} \left[(S_{ij}^0 + \Sigma_{s,ij}^0 \phi_{ij}^0) P_{ij \rightarrow kl}^{20} \right. \\ \left. + 3 \Sigma_{s,ij}^1 (\phi_{x,ij}^1 P_{ij \rightarrow kl}^{12} + \phi_{y,ij}^1 P_{ij \rightarrow kl}^{22}) \right], \quad (3.85)$$

where $P_{ij \rightarrow kl}$'s are defined by

$$P_{ij \rightarrow kl}^{00} = \frac{\Delta_{kl} \Sigma_{kl}}{2 \pi f_{ij,kl}} K_{i1}(\tau_{ij,kl}), \quad (3.86)$$

$$P_{ij \rightarrow kl}^{10} = \frac{\Delta_{kl} \Sigma_{kl} (x_l - x_i)}{2 \pi f_{ij,kl}^2} K_{i2}(\tau_{ij,kl}), \quad (3.87)$$

$$P_{ij \rightarrow kl}^{20} = \frac{\Delta_{kl} \Sigma_{kl} (y_l - y_i)}{2 \pi f_{ij,kl}^2} K_{i2}(\tau_{ij,kl}), \quad (3.88)$$

$$P_{ij \rightarrow kl}^{11} = \frac{\Delta_{kl} \Sigma_{kl} (x_l - x_i)^2}{2 \pi f_{ij,kl}^3} K_{i3}(\tau_{ij,kl}), \quad (3.89)$$

$$P_{ij \rightarrow kl}^{22} = \frac{\Delta_{kl} \Sigma_{kl} (y_l - y_i)^2}{2 \pi f_{ij,kl}^3} K_{i3}(\tau_{ij,kl}), \quad (3.90)$$

$$P_{ij \rightarrow kl}^{12} = \frac{\Delta_{kl} \Sigma_{kl} (x_k - x_i)(y_l - y_j)}{2\pi \rho_{ij, kl}^0} K_{13}(\tau_{ij, kl}), \quad (3.91)$$

$$P_{ij \rightarrow kl}^{21} = P_{ij \rightarrow kl}^{12} . \quad (3.92)$$

$P_{ij \rightarrow kl}$'s have the following properties

$$\sum_{k,l} P_{ij \rightarrow kl}^{00} = 1 , \quad (3.93)$$

$$\sum_{k,l} P_{ij \rightarrow kl}^{10} = \sum_{k,l} P_{ij \rightarrow kl}^{20} = 0 , \quad (3.94)$$

$$\sum_{k,l} P_{ij \rightarrow kl}^{11} = \sum_{k,l} P_{ij \rightarrow kl}^{22} = \frac{1}{3} , \quad (3.95)$$

$$\sum_{k,l} P_{ij \rightarrow kl}^{12} = \sum_{k,l} P_{ij \rightarrow kl}^{21} = 0 . \quad (3.96)$$

These relations have been used to obtain $P_{ij \rightarrow kl}$'s for $i = k$ and $j = l$.

Furthermore, since there are symmetries for ϕ_{kl}^0 , $\phi_{x,kl}^1$ and $\phi_{y,kl}^1$ as shown in Table 3.1, the number of variables in a cell can be reduced.

Table 3.1 Symmetries about ϕ_{kl}^0 , $\phi_{x,kl}^1$ and $\phi_{y,kl}^1$

	Quadrant			
	1	2	3	4
ϕ_{kl}^0	+	+	+	+
$\phi_{x,kl}^1$	+	-	-	+
$\phi_{y,kl}^1$	+	+	-	-

All the values of ϕ_{kl}^0 , $\phi_{x,kl}^1$ and $\phi_{y,kl}^1$ are taken positive in the first quadrant.

§3.5 Numerical Results and Conclusions

In Table 3.2 the blackness of a cylindrical rod in the cases of scattering ratio $\Sigma_{0s} / \Sigma_0 = 0.2, 0.5$ and 0.8 is presented as a function of $x (= aZ_0, a$ is the fuel radius, Σ_0 the total neutron cross section). The value Y^* , the difference between the exact value of the blackness and that of the flat flux approximation, increases with x especially in the case of large scattering ratio. When the scattering ratio is zero, the values evaluated from Eq. (3A.9) of the present method and from Eq. (3A.10) of the flat flux approximation are identical since

Table 3.2 Values of blackness for different x (radius \times total cross section)

x	$\Sigma_{0s}/\Sigma_0=0.2$			$\Sigma_{0s}/\Sigma_0=0.5$			$\Sigma_{0s}/\Sigma_0=0.8$		
	Black- ness [†]	Black- ness ^{††}	Y^*	Black- ness [†]	Black- ness ^{††}	Y^*	Black- ness [†]	Black- ness ^{††}	Y^*
0.1	0.1449	0.1449	0.3730×10^{-4}	0.09389	0.09390	0.6068×10^{-4}	0.03899	0.03899	0.4048×10^{-4}
0.2	0.2647	0.2647	0.1305×10^{-3}	0.1769	0.1769	0.2204×10^{-3}	0.07602	0.07603	0.1532×10^{-3}
0.3	0.3644	0.3645	0.3109×10^{-3}	0.2503	0.2504	0.5449×10^{-3}	0.1112	0.1112	0.3952×10^{-3}
0.4	0.4481	0.4483	0.5801×10^{-3}	0.3153	0.3157	0.1053×10^{-2}	0.1444	0.1446	0.7970×10^{-3}
0.5	0.5182	0.5187	0.9693×10^{-3}	0.3727	0.3734	0.1821×10^{-2}	0.1759	0.1761	0.1437×10^{-2}
0.6	0.5758	0.5767	0.1587×10^{-2}	0.4226	0.4239	0.3087×10^{-2}	0.2053	0.2058	0.2547×10^{-2}
0.7	0.6249	0.6264	0.2267×10^{-2}	0.4669	0.4690	0.4552×10^{-2}	0.2330	0.2339	0.3917×10^{-2}
0.8	0.6665	0.6685	0.3035×10^{-2}	0.5058	0.5090	0.6277×10^{-2}	0.2590	0.2604	0.5625×10^{-2}
0.9	0.7018	0.7045	0.3870×10^{-2}	0.5402	0.5446	0.8228×10^{-2}	0.2833	0.2855	0.7667×10^{-2}
1.0	0.7319	0.7353	0.4753×10^{-2}	0.5705	0.5764	0.1037×10^{-1}	0.3061	0.3091	0.1003×10^{-1}
1.1	0.7576	0.7619	0.5667×10^{-2}	0.5973	0.6048	0.1266×10^{-1}	0.3273	0.3315	0.1270×10^{-1}
1.2	0.7798	0.7849	0.6598×10^{-2}	0.6210	0.6303	0.1508×10^{-1}	0.3471	0.3525	0.1565×10^{-1}
1.3	0.7989	0.8249	0.7534×10^{-2}	0.6420	0.6532	0.1758×10^{-1}	0.3656	0.3725	0.1887×10^{-1}
1.4	0.8154	0.8223	0.8465×10^{-2}	0.6606	0.6739	0.2015×10^{-1}	0.3828	0.3913	0.2232×10^{-1}
1.5	0.8298	0.8376	0.9385×10^{-2}	0.6772	0.6926	0.2275×10^{-1}	0.3988	0.4092	0.2599×10^{-1}
1.6	0.8424	0.8511	0.1029×10^{-1}	0.6920	0.7095	0.2537×10^{-1}	0.4137	0.4261	0.2985×10^{-1}
1.7	0.8534	0.8629	0.1117×10^{-1}	0.7052	0.7249	0.2800×10^{-1}	0.4276	0.4421	0.3389×10^{-1}
1.8	0.8630	0.8734	0.1202×10^{-1}	0.7170	0.7389	0.3061×10^{-1}	0.4406	0.4573	0.3807×10^{-1}
1.9	0.8715	0.8827	0.1285×10^{-1}	0.7276	0.7518	0.3320×10^{-1}	0.4526	0.4718	0.4240×10^{-1}
2.0	0.8790	0.8910	0.1365×10^{-1}	0.7371	0.7635	0.3576×10^{-1}	0.4638	0.4855	0.4684×10^{-1}
2.2	0.8916	0.9051	0.1516×10^{-1}	0.7534	0.7842	0.4076×10^{-1}	0.4839	0.5110	0.5604×10^{-1}
2.4	0.9016	0.9166	0.1655×10^{-1}	0.7668	0.8017	0.4557×10^{-1}	0.5012	0.5341	0.6559×10^{-1}
2.6	0.9096	0.9259	0.1783×10^{-1}	0.7778	0.8168	0.5020×10^{-1}	0.5162	0.5552	0.7546×10^{-1}
2.8	0.9162	0.9336	0.1900×10^{-1}	0.7869	0.8299	0.5462×10^{-1}	0.5292	0.5745	0.8562×10^{-1}
3.0	0.9216	0.9401	0.2008×10^{-1}	0.7945	0.8412	0.5886×10^{-1}	0.5402	0.5922	0.9609×10^{-1}
3.2	0.9260	0.9455	0.2110×10^{-1}	0.8006	0.8511	0.6316×10^{-1}	0.5492	0.6084	0.1079×10^0
3.4	0.9297	0.9501	0.2199×10^{-1}	0.8061	0.8600	0.6685×10^{-1}	0.5576	0.6235	0.1181×10^0
3.6	0.9328	0.9541	0.2280×10^{-1}	0.8108	0.8678	0.7033×10^{-1}	0.5648	0.6374	0.1284×10^0
3.8	0.9355	0.9575	0.2355×10^{-1}	0.8149	0.8749	0.7363×10^{-1}	0.5710	0.6503	0.1388×10^0
4.0	0.9378	0.9605	0.2423×10^{-1}	0.8184	0.8812	0.7674×10^{-1}	0.5764	0.6623	0.1491×10^0

† based on the present method

†† based on the flat flux approximation

a neutron that suffers one collision is captured and does not contribute to the neutron distribution. The comparison of the values from Eq. (3A.9) with those from curves obtained in Ref. (13) attests to the accuracy of Eq. (3A.9)

The form of Eq. (3.27) is very similar to that of Eq. (3B.7) obtained from the collision probability method. The main difference is that the effect of the deviation from the constant flux is taken into account in Eq. (3.27). Thus we can apply Eq. (3.27) to closely packed lattices where accuracy of the Amouyal-Benoist method can be considered to be poor. The form of Eq. (3.27) also verifies Fukai's result⁽²⁾ by the collision probability method that the absorption ratio of the moderator has little effect on the flux ratio in a lattice if the absorption is small.

The extended Dancoff factor depends directly on the flux ratio, which was not contained in the Amouyal-Benoist theory. The extended Dancoff factor C^* , necessary to evaluate the flux ratio, is easily

Table 3.3 Convergency of the extended Dancoff factor in square lattices

Fuel radius: 1.0 cm, Pitch: 2.50663 cm

d*	Total cross section of the moderator	
	0.5 cm ⁻¹	1.0 cm ⁻¹
1	0.04984	0.04450
$\sqrt{2}$	0.01778	0.00880
2	0.00523	0.00118
$\sqrt{5}$	0.00332	0.00055
$2\sqrt{2}$	0.00114	0.00009
3	0.00085	0.00005
$\sqrt{10}$	0.00064	0.00003
$\sqrt{13}$	0.00031	0.00001
$3\sqrt{2}$	0.00011	0.00000
C^*	0.33401	0.22324

d*: Distance between the original rod and the rod considered in unit of pitch

calculated since the shadowing effect by intermediate fuel rods need not be considered. In Table 3.3 is given the convergency of the extended Dancoff factor. These values indicate that, in the calculation of the extended Dancoff factor for a square lattice, it will suffice to take into account the 48 fuel rods immediately surrounding a fuel rod.

In Table 3.4 are given the values of the flux ratio in two-region square cells for the input data used in Ref. (2) (here $l_0 = 2a\Sigma_0$, $l_1 = 2a\Sigma_1 V_1/V_0$). The absorption in the moderator is neglected. The values by Fukai can be considered to be rather correct since he divided a cell into many shells. The results obtained by the present method (Eq. (3.27)) are in good agreement with Fukai's values. They

Table 3.4 Calculated results of flux ratios in square lattices

Case	V_1/V_0	l_1	l_0	Σ_{0a}/Σ_{0t}	ϕ_1/ϕ_0		
					Present method	Fukai†	Amouyal††
1	1	1.0	0.5	0.1	1.224	1.240	1.219
2				0.2	1.199	1.213	1.195
3				0.5	1.125	1.134	1.122
4				0.75	1.062	1.067	1.061
5				0.9	1.025	1.027	1.025
6	1	2.0	0.5	0.1	1.229	1.239	1.207
7				0.2	1.204	1.213	1.184
8				0.5	1.128	1.133	1.115
9				0.75	1.064	1.067	1.058
10				0.9	1.026	1.027	1.023
11	1	1.0	1.0	0.1	1.468	1.502	1.459
12				0.2	1.417	1.447	1.408
13				0.5	1.262	1.282	1.256
14				0.75	1.132	1.142	1.129
15				0.9	1.053	1.057	1.052
16	1	2.0	1.0	0.1	1.479	1.493	1.434
17				0.2	1.426	1.439	1.386
18				0.5	1.268	1.277	1.242
19				0.75	1.135	1.139	1.122
20				0.9	1.054	1.056	1.049

† Values based on multi-shell collision probabilities

†† Values listed in Ref. (2)

represent an improvement over the Amouyal-Benoist method. Since the contribution of Y^* in Eq. (3.27) is very small ($Y^* = 0.000021$ for cases (1) \sim (5) and (11) \sim (15) and $Y^* = 0.000088$ for cases (6) \sim (10) and (16) \sim (20)), we can calculate the flux ratio from the equation

$$\frac{\phi_1}{\phi_0} = \frac{1}{P_0} + \frac{V_0 \Sigma_{0c}}{V_1 \Sigma_{1c}} \left\{ \frac{C^* V_1}{(1 - P_c^*)(1 - C^*) V_0} - 1 \right\}.$$

This equation is simpler than the result by the collision probability method, Eq. (3B.7), which requires taking account of the shadowing effect in the calculation of P_{01} . Moreover, the effect of difference in lattice configuration is easily taken into account by the factor C^* . The above equation is very suitable for a series of flux calculations where it is only the cross section of the fuel rod that changes, since only one calculation of C^* is required. Thus the present method should be particularly suitable for calculating the resonance absorption.

In Table 3.5 are presented the flux ratios evaluated by the above

Table 3.5 Flux ratios for various lattice pitches in square lattices

Σ_{0t} : 0.7221 cm⁻¹, Σ_{0c} : 0.3230 cm⁻¹
 Σ_{1t} : 0.3721 cm⁻¹, Σ_{1c} : 0.3118 $\times 10^{-3}$ cm⁻¹
 Fuel radius: 1.5 cm

Pitch (cm)	3.2	3.5	4	5	10	20
ϕ_1 / ϕ_0	1.642	1.606	1.592	1.604	1.684	1.727

equation for square lattices of various pitches. The ratio does not increase monotonously with lattice pitch, but has a minimum point, as pointed by Fukai⁽¹⁶⁾. The ratio rises in level with decreasing

moderator thickness. This is attributed to the increase brought thereby to the coefficient $C^* V_1 / (1 - P_c^*)(1 - C^*) V_0$ in the above equation.

In Table 3.6 the flux ratio by the present method in a two-region square cell is compared with values of the collision probability method and of Carlvik's numerical method⁽¹⁷⁾. Good agreement is seen between the present method and the Carlvik's method. The first-flight collision probability method with the perfect reflection condition overestimates the value appreciably.

Next as an application of the method in §3.3 we calculate the flux distribution in a three-region square cell. Outer radii of the central region (region 1) and the intermediate region (region 2) are taken to be 1.0 and 1.5 cm respectively. The outermost region 3 is a moderator and arranged in a square lattice with a lattice pitch 4.0 cm. In the system we adopt two cases of neutron cross sections in

Table 3.6 Disadvantage factor in a square lattice cell with two regions

volume ratio 1.865
 fuel radius 0.381 cm
 distance between adjacent fuel rods 1.143 cm
 total cross section of the fuel 0.78 cm⁻¹
 scattering cross section of the fuel 0.387 cm⁻¹
 total cross section of the moderator 1.0618 cm⁻¹
 scattering cross section of the moderator 1.053 cm⁻¹

Methods	$\bar{\phi}_m / \bar{\phi}_f$
Present method	1.1498
Carlvik's method	1.150 ± 0.005
Two-region collision probability method (isotropic reflection condition)	1.1407
Two-region collision probability method (perfect reflection condition)	1.2843

each region. For both cases the total cross sections of the both regions 1 and 3 are 1.0 cm^{-1} and the scattering cross sections of these regions are 0.5 and 0.9999 cm^{-1} respectively. In the first case, the total and scattering cross sections of the region 2 are taken to be 1.0 and 0.5 cm^{-1} . In the second case, those of the region 2 are taken to be 1.0 and 0.8 cm^{-1} respectively. In the calculation of the flux distributions for both cases we consider a uniform and isotropic source per unit volume only in the moderator. Values of the currents at interfaces of each region are presented in Table 3.7 for both cases. The neutron currents for the case 1 show strong anisotropy, large difference between inward and outward currents, at each interface. This is due to the strong absorption in the regions 1 and 2. For such a heterogeneous system the present method is powerful since it takes into account the spatial change of neutron flux in each region. Comparing the currents for both cases it can be seen that, in the case 2, the outward neutron currents J_1^+ , J_2^+ show larger increase than those in the case 1. This is based on the fact that neutrons which have arrived at the inner regions from the moderator will have more chances to escape from the inner regions outwardly in the case 2 than in the

Table 3.7 Neutron currents at each interface

Currents	Case 1	Case 2
J_1^+	2.6660	4.2246
J_1^-	6.2069	9.8355
J_2^+	3.1409	6.3459
J_2^-	12.0682	15.2720

Case 1. Therefore the neutron flux for the case 2 approaches to flat one. This is easily seen from Table 3.8 where the neutron average flux in each region is shown. Since the effect of the lattice configuration is taken into account by the extended Dancoff factor, this method can be used to calculate neutron flux distributions for closely packed lattices. The flux distributions based on the flat flux approximation are shown in Table 3.9. Comparing Tables 3.8 and 3.9, it can be seen that the flat flux approximation leads to flatter

Table 3.8 Neutron flux in each region

Region number	Case 1	Case 2
1	2.2542	3.5720
2	2.7433	4.2210
3	4.5997	5.9600

Table 3.9 Neutron flux in each region based on the flat flux approximation

Region number	Case 1	Case 2
1	2.2973	3.6262
2	2.7088	4.1127
3	4.5629	5.8441

Table 3.10 Moderator-to-fuel flux ratio in a square cell for anisotropic scattering

$\Sigma_{ot} : 1.0 \text{ cm}^{-1}$, $\Sigma_{os} : 0.5 \text{ cm}^{-1}$
 $\Sigma_{ft} : 2.0 \text{ cm}^{-1}$, $\Sigma_{fs} : 2.0 \text{ cm}^{-1}$
 Pitch : 3.5 cm

$\bar{\mu}$	Present method	Method in Chap. 2
0	1.6651	1.6734
1/3	1.5446	1.5654
2/3	1.4401	1.4578

flux distribution.

Next we evaluate the effect of anisotropic scattering in a square cell by the method in §3.4. We take 36 mesh points in $1/8$ of a cell. Thus direct flights of neutrons among the meshes in the original and the first and second nearest neighboring cells have been taken into consideration. The ratios of average flux in the moderator to that in the fuel are shown in Table 3.10 for three values of the average cosine of the scattering angle $\bar{\mu}$ in the moderator. The average cosine for the fuel is zero in all cases. Good agreement is obtained between the results of the present method and those in the preceding chapter, which proves the validity of the "white" or isotropic return condition on the cell boundary in the case of anisotropic scattering.

Appendix 3A

Determination of the Blackness of a Fuel Rod

In Ref. (13), the blackness was calculated by Stuart based on a variational method. Here we use his method by choosing a trial function of the fuel flux in a form of a quadratic function about r . We now describe it briefly.

From Eq. (3.33) we obtain a functional

$$T = \frac{\left(\int_{V_0} d\vec{r} \pi_0(\vec{r}) \varphi(\vec{r}) \right)^2}{\int_{V_0} d\vec{r} \varphi^2(\vec{r}) - \int_{V_0} d\vec{r} \int_{V_0} d\vec{r}' \varphi(\vec{r}) \varphi(\vec{r}') \frac{\Sigma_{os} e^{-\Sigma_{ot}R}}{4\pi R^2}} \quad (3A.1)$$

The stationary value of T is given by

$$|T| = \frac{4}{S_0 \Sigma_{os}} \left\{ \frac{4 V_0 \Sigma_{ot}}{S_0} (1 - P_c) - \beta_0 \right\} \quad (3A.2)$$

If we choose a trial function of the flux in the fuel such as

$$\varphi(\vec{r}) = 1 + b r^2 \quad (3A.3)$$

and eliminate the constant b by the relation $dT/db = 0$ about T in

Eq. (3A.1), we obtain

$$T = \left(\frac{4}{S_0} \right)^2 V_0 \frac{\frac{4}{3} (1 - P_c)^2 \left(1 - \frac{\Sigma_{os}}{\Sigma_{ot}} R_c \right) - (1 - Q_c) \left(1 + \frac{\Sigma_{os}}{\Sigma_{ot}} Q_c P_c - \frac{\Sigma_{ot} + \Sigma_{oc}}{\Sigma_{ot}} P_c - \frac{\Sigma_{os} - \Sigma_{oc}}{\Sigma_{ot}} Q_c \right)}{\frac{4}{3} \left(1 - \frac{\Sigma_{os}}{\Sigma_{ot}} P_c \right) \left(1 - \frac{\Sigma_{os}}{\Sigma_{ot}} R_c \right) - \left(1 - \frac{\Sigma_{os}}{\Sigma_{ot}} Q_c \right)^2} \quad (3A.4)$$

Here Q_c is the probability that a neutron born in the fuel rod with a source distribution proportional to r^2 undergoes its first collision in the same rod; R_c is the probability that a neutron born in the fuel rod with r^2 source distribution undergoes its first collision in the same rod with a weight proportional to r^2 , which is normalized by

dividing with the r^4 integral:

$$Q_c = \frac{1}{\int_{V_0} d\vec{r} r^2} \int_{V_0} d\vec{r} r^2 \int_{V_0} d\vec{r}' \frac{\Sigma_{ot} \bar{e}^{-\Sigma_{ot} R}}{4\pi R^2} \quad , \quad (3A.5)$$

$$R_c = \frac{1}{\int_{V_0} d\vec{r} r^4} \int_{V_0} d\vec{r} r^2 \int_{V_0} d\vec{r}' r'^2 \frac{\Sigma_{ot} \bar{e}^{-\Sigma_{ot} R}}{4\pi R^2} \quad . \quad (3A.6)$$

The behaviours of Q_c and R_c versus x (= fuel radius \times cross section) are shown in Fig. 3.2 together with that of P_c . Approximate expressions for them are given by

$$1 - Q_c = \begin{cases} \frac{1}{1 + 1.19958x - 0.0382635x^2 + 0.001313x^3} & \text{for } 0 \leq x \leq 5 \\ \frac{1}{1 + 1.16635x - 0.0289544x^2 + 0.0007802x^3} & \text{for } 5 \leq x \leq 10 \\ \frac{1}{x} - \frac{4}{3x^2} + \frac{3}{2x^3} & \text{for } 10 \leq x \end{cases} \quad (3A.7)$$

$$1 - R_c = \begin{cases} \frac{1}{1 + 0.849485x - 0.0992105x^2 + 0.0140285x^3} & \text{for } 0 \leq x \leq 3 \\ \frac{1}{1.2932177 + 0.5750779x + 0.00575329x^2 - 0.000554036x^3} & \text{for } 3 \leq x \leq 10 \\ \frac{3}{2x} - \frac{2}{x^2} + \frac{3}{2x^3} + \frac{15}{4x^5} & \text{for } 10 \leq x \end{cases} \quad (3A.8)$$

The error of each expression is smaller than 0.1 %.

From Eqs. (3A.2) and (3A.4), we obtain

$$\beta_o = 2a\Sigma_{oc} \frac{\frac{4}{3}(1-P_c)(1-\frac{\Sigma_{os}}{\Sigma_{ot}}R_c) - \frac{\Sigma_{oc}}{\Sigma_{ot}}(1-P_c) - \frac{\Sigma_{os}}{\Sigma_{ot}}(1-Q_c)^2}{\frac{4}{3}(1-\frac{\Sigma_{os}}{\Sigma_{ot}}P_c)(1-\frac{\Sigma_{os}}{\Sigma_{ot}}R_c) - (1-\frac{\Sigma_{os}}{\Sigma_{ot}}Q_c)^2} \quad . \quad (3A.9)$$

If we let $P_c = Q_c = R_c$, we have

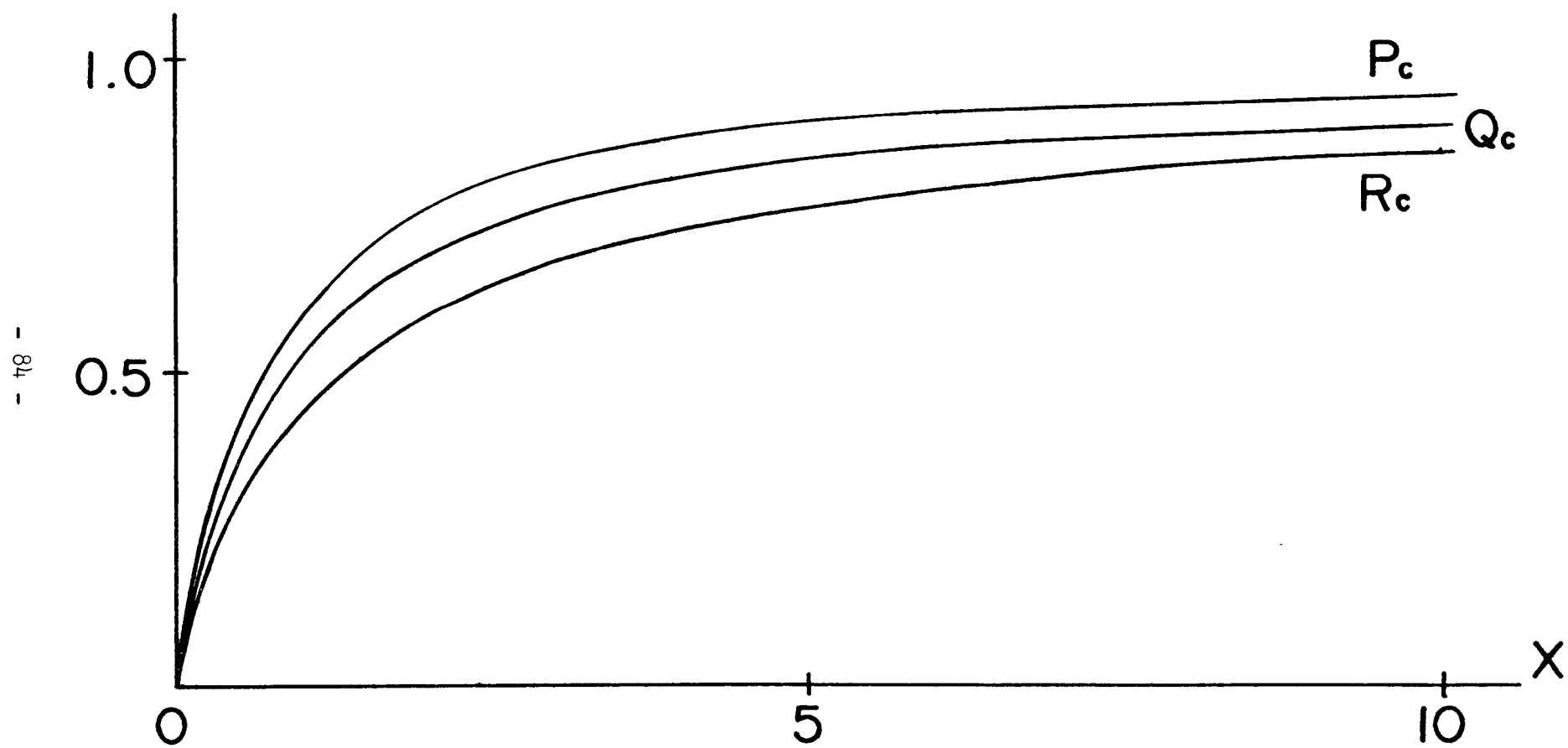


Fig. 3.2 Curves for P_c , Q_c and R_c vs. x (= radius \times total cross section)

$$\beta'_0 = 2 a \Sigma_{oc} \frac{1 - P_c}{1 - \frac{\Sigma_{os}}{\Sigma_{ot}} P_c} , \quad (3A.10)$$

and this is the form which could be obtained easily by the flat flux approximation. From the definition of Y^* we obtain

$$Y^* = \frac{\beta'_0}{\beta_0} - 1 . \quad (3A.11)$$

Appendix 3B

Flux Ratio Based on the Collision Probability Method

In the case where the moderator contains a uniform source Q , the neutron conservation in each region may be expressed by

$$V_0 \Sigma_{ot} \phi_0 = V_0 \Sigma_{os} \phi_0 P_{00} + V_1 \Sigma_{1s} \phi_1 P_{10} + P_{10} Q , \quad (3B.1)$$

$$V_1 \Sigma_{1t} \phi_1 = V_0 \Sigma_{0s} \phi_0 P_{01} + V_1 \Sigma_{1s} \phi_1 P_{11} + P_{11} Q . \quad (3B.2)$$

From the above equations, flux ratio is given by

$$\frac{\phi_1}{\phi_0} = \frac{\Sigma_{os}}{\Sigma_{ot}} - \frac{V_0 \Sigma_{oc}}{V_1 \Sigma_{1t}} + \frac{\Sigma_{oc}}{\Sigma_{ot} P_{01}} . \quad (3B.3)$$

We introduce the quantity

$$\beta'_0 = \frac{1 - P_c}{1 - \frac{\Sigma_{os}}{\Sigma_{ot}} P_c} , \quad (3B.4)$$

where ' denotes that the quantity is expressed in terms of the first-flight collision probability. Then Eq. (3B.3) becomes

$$\frac{\phi_i}{\phi_o} = \frac{1}{\mathcal{P}_o'} + \frac{\Sigma_{oc}}{\Sigma_{ot}} \left(\frac{1}{P_{oi}} - \frac{1}{1-P_c} \right) - \frac{V_o \Sigma_{oc}}{V_i \Sigma_{it}} , \quad (3B.5)$$

where P_c is the probability for a neutron born uniformly in the fuel rod to undergo its first collision in the same rod. We put

$$P_{oi} = (1 - P_c)(1 - C') , \quad (3B.6)$$

where C' is the sum of the probabilities for a neutron emitted isotropically from a fuel rod to collide in any fuel rod other than the original rod. Then Eq. (3B.5) reduces to

$$\frac{\phi_i}{\phi_o} = \frac{1}{\mathcal{P}_o'} + \frac{\Sigma_{oc} C'}{\Sigma_{ot} P_{oi}} - \frac{V_o \Sigma_{oc}}{V_i \Sigma_{it}} . \quad (3B.7)$$

This corresponds to Eq. (3.27) in the case where $Y^* = 0$, $C^*/P_{oi}^* \Sigma_{it} = C'/P_{oi} \Sigma_{ot}$ and $\mathcal{P}_o = \mathcal{P}_o'$.

References

- (1) THIE, J.A.: Nucl. Sci. Eng., 9, 286 (1961).
- (2) FUKAI, Y.: J. Nucl. Energy, Pt A/B, 18, 241 (1964).
- (3) AMOUYAL, A., BENOIST, P., HOROWITZ, J.: ibid., 6, 79 (1957).
- (4) DUDLEY, T.E., DAITCH, P.B.: Nucl. Sci. Eng., 25, 75 (1966).
- (5) ZWEIFEL, P.F., MANNAN, M.A.: J. Nucl. Energy, 21, 1 (1967).
- (6) STRAWBRIDGE, L.E., BARRY, R.F.: Nucl. Sci. Eng., 23, 58 (1965).
- (7) TAKEDA, T., SEKIYA, T.: J. Nucl. Sci. Technol., 8, 539 (1971).
- (8) CASE, K.M., DE HOFFMANN, F., PLACZEK, G.: "Introduction to the Theory of Neutron Diffusion", Vol. 1, (1953), Los Alamos Sci. Lab.
- (9) THIE, J.A.: Nucl. Sci. Eng., 5, 75 (1959).
- (10) CARLVIK, I., PERSHAGEN, B.: AE-16, (1959).
- (11) TAKEDA, T., SEKIYA, T.: Technol. Report, Osaka Univ., 22, 345 (1972).
- (12) MÜLLER, A., LINNARTZ, E.: Nukleonik, 5, 23 (1963).
- (13) STUART, G.W.: Nucl. Sci. Eng., 2, 617 (1957).
- (14) TAKEDA, T., NAKAMURA, K., SEKIYA, T.: J. Nucl. Sci. Technol., 9, 53 (1972).
- (15) BICKLEY, W.G., NAYLER, J.: Phil. Mag., 20, Ser. 7, 343 (1935).
- (16) FUKAI, Y.: J. Nucl. Sci. Technol., 3, 4 (1966).
- (17) FUKAI, Y.: private communication, (1971).

CHAPTER 4

FLUX CALCULATION IN LATTICE CELLS

§4.1 Introduction

In this chapter the usual first-flight collision probability method is applied to the calculation of the neutron distributions in various cell systems. In a highly heterogeneous system such as pressurized heavy water reactor, the calculation method based on the first-flight collision probability is very useful. In such a heterogeneous system, however, it is very hard to take into account the deviation from the flat flux (see §2.4), and we are obliged to assume flat flux within each region. Thus it is necessary to divide the system into the largest number of regions by possibly diminishing the size of each region. It takes very long to evaluate numerically the exact collision probabilities between many regions.

In §4.2, therefore, we introduce a new approximate expression for the first-flight collision probability for cluster systems. First, we obtain an approximation of the probability in an annular system. This corresponds to an improvement of the Bonalumi approximation^{(1)~(3)}, and the numerical results are compared with those of Bonalumi's, though our expression coincides with his result in a system containing only two regions.

In a cluster system, we must divide the system into many ring regions in each of which several fuel rods are included. By using

Leslie's method⁽⁴⁾, collision probabilities between different rings are calculated by replacing the heterogeneous rings by annular domains having equivalent homogeneous cross sections. His method requires a knowledge of the collision probabilities among fuel, cladding and coolant in the same ring when the inner domain is void. But he did not take rigorous account of the existence of the void region. To remedy this shortcoming, we introduce the transition probability for a neutron escaping from one subcell to collide in another subcell when the internal medium is void. The transition probability between two adjacent subcells corresponds to a principal constituent of the Dancoff factor^{(5)~(7)} in the case where the medium between the subcells is empty. Combining the collision probability in an annular system with the transition probability between subcells and using Leslie's method, we obtain the collision probability in a cluster system.

As an application of this method, we treat a hexagonal cluster containing 7 fuel rods without cladding and a square cluster containing 28 fuel rods with cladding. Our numerical results for collision probabilities in annular and cluster systems show good agreement with the results obtained by the exact method.

In this section, we assume the infinite extension of the system in the axial direction. Usually the buckling approximation is used to take into account the finiteness of the system. This approximation comes from the fundamental diffusion theory; the flux distribution in the axial direction is assumed to be $\sin Bz$, then the pseudo absorption in the system increases by DB^2 . This approximation, however, implies the use of the P_1 theory in the whole three dimensions; there is no theoretical justification that the pseudo absorption may be applied to

the first-flight collision probability method in reduced two dimensional systems.

In §4.3 we calculate the first-flight collision probability for finite slab and cylindrical systems directly, assuming the flux distribution in the axial direction of the type $\sin B_m z$ ⁽⁸⁾. Generally the integral included in the calculation of the first-flight collision probability is sixfold. In such a case the numerical evaluation of the probability is impossible and the Monte Carlo method is usually adopted⁽⁹⁾. In the present method the integral is reduced to threefold. Then the first-flight collision probability is evaluated directly from the expression obtained. In a slab system the first-flight collision probability that a neutron born in a region makes its first collision in a given region in the lattice cells is obtained by summing the probabilities that the neutron undergoes its first collision in the original cell and in the next neighboring cell and so on. In the cylindrical cell, however, this is not the case. The first-flight collision probabilities in one cell are calculated directly. Next it is assumed that the spatial distribution of an escaping neutron from the original cell is proportional to $\sin Bz$ and isotropic. Under the above assumption with the isotropic return condition on the cell boundary, the first-flight collision probabilities in the lattice cells are obtained.

The methods described up to now could be extended to the multi-group theory. But the resonance region need to be particularly treated because of the rapid change of neutron cross section with energy.

Then, in §4.4, the neutron spectra and the resonance integral for an isolated wide resonance are calculated analytically for a two-region cell. The resonance integrals in homogeneous system have been calculated by many authors through various analytic treatments (for example,

Goldstein's λ method^{(10)~(13)}, Chernick's improved W.R. approximation⁽¹⁴⁾, and Spinney's N.R. approximation⁽¹⁵⁾). They have also improved the methods in order to treat the resonance integral in heterogeneous systems. The usual treatment of the resonance absorption, however, involves the assumption that the spectrum is symmetric about the energy of the resonance peak. This assumption of flux recovery is proved to be incorrect for a large wide resonance. Even if we take into account the flux depression — the moderator correction — by repeating iteratively Goldstein's method, the improvement is very slow⁽¹⁶⁾. Furthermore the neutron spectra far below the resonance energy cannot be expressed correctly in the method.

Therefore, in the equation of neutron balance in a cell, we use the Greuling-Goertzel approximation⁽¹⁷⁾ for the slowing down kernel in the moderator by assuming the known flux in the fuel. After two iterations about the neutron fluxes, we obtain the resonance integral and analytic expressions for fluxes in the fuel and the moderator. The neutron spectra obtained show the exact neutron behaviour far below the resonance. The correction to the constant flux in the fuel rod could easily be taken into account by the method in §2.4.

§4.2 Flux Distribution in Cluster Systems⁽¹⁸⁾

In this section we derive a new calculational method of the first-flight collision probability in cluster systems. To begin with, we will derive an approximate expression for the collision probability in an annular system. The collision probability that a neutron born uniformly and isotropically in a cylindrical rod makes its first collision within the same rod has been evaluated by Case et al.⁽¹⁹⁾, and may be written in the following form:

$$P_c(a\Sigma) = 1 - \frac{1}{2a\Sigma} + \frac{2}{\pi a\Sigma} \int_0^{\frac{\pi}{2}} d\varphi \cos \varphi K_{i3}(2a\Sigma \cos \varphi), \quad (4.1)$$

where a and Σ are the radius and the total cross section of the rod, and $K_{i3}(x)$ is the Bickley function, and is given in terms of the polar angle θ between the axis of the cylinder and the direction of the neutron path:

$$K_{i3}(x) = \int_0^{\frac{\pi}{2}} d\theta \sin^2 \theta e^{-\frac{x}{\sin \theta}}. \quad (4.2)$$

We calculate the probability P_{ii} in an annular region for a neutron born in the i -th region, and having a uniform and isotropic distribution, to undergo its first collision in the same region^{(20),(21)}. Using the notations in Fig. 4.1, we obtain

$$\begin{aligned} P_{ii} = & \frac{2r_i}{V_i} \int_0^{\frac{\pi}{2}} d\theta \sin \theta \left[\int_{\varphi_i^1}^{\frac{\pi}{2}} d\varphi \cos \varphi \int_0^{x_i'} dl \left\{ 1 - e^{-\frac{l z_i}{\sin \theta}} \right\} \right. \\ & + \int_{\varphi_i^2}^{\varphi_i^1} d\varphi \cos \varphi \int_0^{x_i} dl \left\{ \left(1 - e^{-\frac{l z_i}{\sin \theta}} \right) + \left(1 - e^{-\frac{(x_i-l) z_i}{\sin \theta}} \right) \right. \\ & \quad \left. \left. + e^{-\frac{l z_i + x_{i-1} z_{i-1}}{\sin \theta}} \left(1 - e^{-\frac{x_i z_i}{\sin \theta}} \right) \right\} \right. \\ & \left. + \int_{\varphi_i^3}^{\varphi_i^2} d\varphi \cos \varphi \int_0^{x_i} dl \left\{ \left(1 - e^{-\frac{l z_i}{\sin \theta}} \right) + \left(1 - e^{-\frac{(x_i-l) z_i}{\sin \theta}} \right) \right\} \right] \end{aligned}$$

$$\begin{aligned}
& + e^{-\frac{l \Sigma_i + 2X_{i-1} \Sigma_{i-1} + X'_{i-2} \Sigma_{i-2}}{\sin \theta}} (1 - e^{-\frac{X_i \Sigma_i}{\sin \theta}}) \} \\
& + \dots \} \\
= & \frac{2r_i}{V_i} \int_0^{\frac{\pi}{2}} d\theta \sin \theta \left\{ \int_{\varphi_i^1}^{\frac{\pi}{2}} d\varphi \cos \varphi \int_0^{X_i'} d\ell (1 - e^{-\frac{l \Sigma_i}{\sin \theta}}) \right. \\
& \quad \left. + 2 \int_0^{\varphi_i^1} d\varphi \cos \varphi \int_0^{X_i} d\ell (1 - e^{-\frac{l \Sigma_i}{\sin \theta}}) \right. \\
& + \frac{2r_i}{V_i \Sigma_i} \int_0^{\frac{\pi}{2}} d\theta \sin^2 \theta \int_{\varphi_i^2}^{\varphi_i^1} d\varphi \cos \varphi e^{-\frac{X'_{i-1} \Sigma_{i-1}}{\sin \theta}} \left\{ 1 - e^{-\frac{X_i \Sigma_i}{\sin \theta}} \right\}^2 \\
& + \frac{2r_i}{V_i \Sigma_i} \int_0^{\frac{\pi}{2}} d\theta \sin^2 \theta \int_{\varphi_i^3}^{\varphi_i^2} d\varphi \cos \varphi e^{-\frac{X_{i-2} \Sigma_{i-2}}{\sin \theta}} \left\{ e^{-\frac{X_{i-1} \Sigma_{i-1}}{\sin \theta}} \right. \\
& \quad \left. \cdot (1 - e^{-\frac{X_i \Sigma_i}{\sin \theta}}) \right\}^2 \\
& + \dots ,
\end{aligned} \tag{4.3}$$

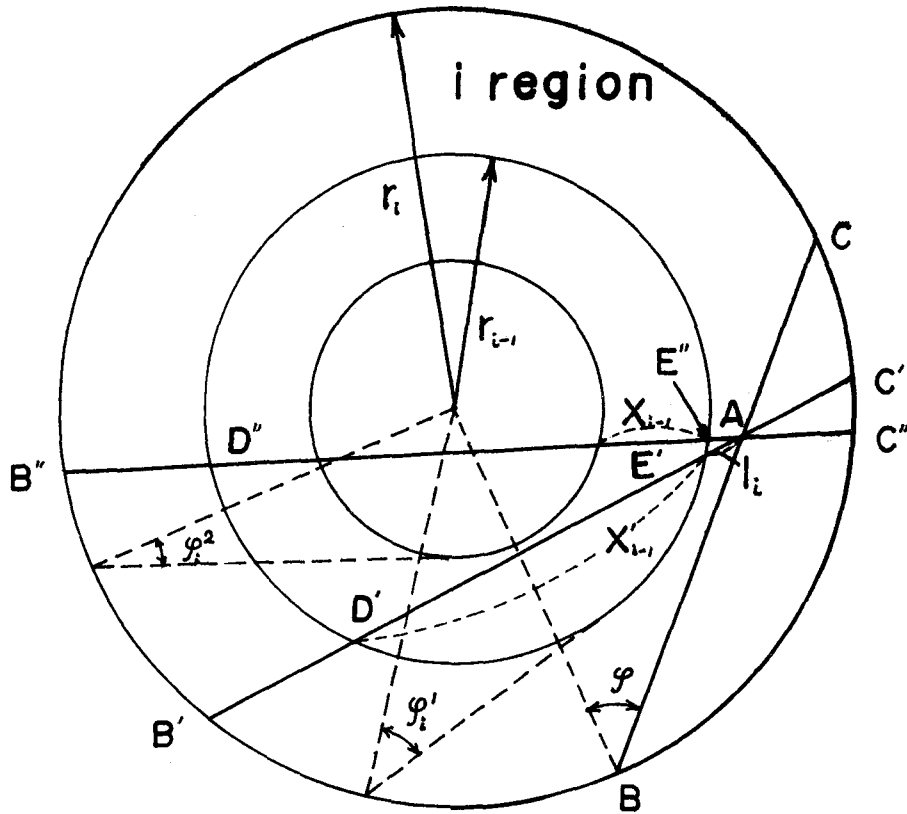


Fig. 4.1 Neutron path in an annular system

where X_i is the projection of a chord length in the i -th region onto the radial plane, along which a neutron starting from the outer boundary of the i -th region travels till it reaches the inner boundary of the region. And X_i' is the similar length along which a neutron starting from the outer boundary of the i -th region travels till it reaches again the outer boundary of the same region without passing any internal region. We denote the P_{ii} for the case where $\Sigma_{i-1} = \Sigma_{i-2} = \dots = 0$ by P_{ii}^0 . When we let $\Sigma_j = 0$ for $j \leq i-1$ in Eq. (4.3), and use the relation

$$r_i \int_0^{\varphi_i'} d\varphi_i \cos \varphi_i = r_{i-1} \int_0^{\frac{\pi}{2}} d\varphi_{i-1} \cos \varphi_{i-1},$$

we have the expression

$$\begin{aligned} P_{ii}^0 = & 1 - \frac{2r_i}{V_i \Sigma_i} \int_0^{\frac{\pi}{2}} d\varphi_i \cos \varphi_i \int_0^{\frac{\pi}{2}} d\theta \sin^2 \theta \left(1 - e^{-\frac{2r_i \Sigma_i \cos \varphi_i}{\sin \theta}} \right) \\ & + \frac{2r_{i-1}}{V_i \Sigma_i} \int_0^{\frac{\pi}{2}} d\varphi_{i-1} \cos \varphi_{i-1} \int_0^{\frac{\pi}{2}} d\theta \sin^2 \theta e^{-\frac{2\Sigma_i X_i}{\sin \theta}} \\ & \cdot \left(1 - e^{-\frac{2r_{i-1} \Sigma_i \cos \varphi_{i-1}}{\sin \theta}} \right). \end{aligned} \quad (4.4)$$

Now we adopt an approximation by which we replace the integrand of the last term of Eq. (4.4) by the product of each average using Eq. (4.1):

$$\begin{aligned} P_{ii}^0 = & 1 - \frac{1}{1 - \alpha_i^2} \left[1 - P_c(r_i \Sigma_i) \right. \\ & \left. - \alpha_i^2 \left\{ 1 - P_c(r_{i-1} \Sigma_i) \right\} (1 - H_{i-1,i})^2 \right], \end{aligned} \quad (4.5)$$

where $\alpha_i = r_{i-1}/r_i$ and $H_{i-1,i}$ is the probability for a neutron emitted isotropically from the outer boundary of the region $i-1$ to undergo its first collision in the region i :

$$H_{i-1,i} = \frac{4}{\pi} \int_0^{\frac{\pi}{2}} d\varphi_{i-1} \cos \varphi_{i-1} \int_0^{\frac{\pi}{2}} d\theta \sin^2 \theta \left(1 - e^{-\frac{X_i \Sigma_i}{\sin \theta}} \right). \quad (4.6)$$

Substituting Eq. (4.5) into Eq. (4.3) and transforming the range of integrals about φ from 0 to $\pi/2$ by using the relation

$$\begin{aligned} r_i \int_{\varphi_{i-1}}^{\varphi_i} d\varphi_i \cos \varphi_i &= r_{i-1} \int_0^{\frac{\pi}{2}} d\varphi_{i-1} \cos \varphi_{i-1} \\ &- r_{i-2} \int_0^{\frac{\pi}{2}} d\varphi_{i-2} \cos \varphi_{i-2}, \quad (i = \text{integer}), \end{aligned}$$

it follows that

$$\begin{aligned} P_{ii}^0 - P_{ii} &= \frac{2 r_{i-1}}{\Sigma_i V_i} \int_0^{\frac{\pi}{2}} d\varphi_{i-1} \cos \varphi_{i-1} \int_0^{\frac{\pi}{2}} d\theta \sin^2 \theta (1 - e^{-\frac{\chi'_{i-1} \Sigma_{i-1}}{\sin \theta}}) (1 - e^{-\frac{\chi_i \Sigma_i}{\sin \theta}})^2 \\ &+ \frac{2 r_{i-2}}{\Sigma_i V_i} \int_0^{\frac{\pi}{2}} d\varphi_{i-2} \cos \varphi_{i-2} \int_0^{\frac{\pi}{2}} d\theta \sin^2 \theta \left[(1 - e^{-\frac{\chi'_{i-2} \Sigma_{i-2}}{\sin \theta}}) - (1 - e^{-\frac{\chi'_{i-1} \Sigma_{i-1}}{\sin \theta}}) \right] \\ &\quad \cdot e^{-\frac{\chi_{i-1} \Sigma_{i-1}}{\sin \theta}} (1 - e^{-\frac{\chi_i \Sigma_i}{\sin \theta}}) \\ &+ \frac{2 r_{i-3}}{\Sigma_i V_i} \int_0^{\frac{\pi}{2}} d\varphi_{i-3} \cos \varphi_{i-3} \int_0^{\frac{\pi}{2}} d\theta \sin^2 \theta \left[(1 - e^{-\frac{\chi'_{i-3} \Sigma_{i-3}}{\sin \theta}}) - (1 - e^{-\frac{\chi'_{i-2} \Sigma_{i-2}}{\sin \theta}}) \right] \\ &\quad \cdot e^{-\frac{\chi_{i-1} \Sigma_{i-1} + \chi_{i-2} \Sigma_{i-2}}{\sin \theta}} (1 - e^{-\frac{\chi_i \Sigma_i}{\sin \theta}}) \\ &+ \dots \end{aligned} \quad (4.7)$$

Following the same process as in deriving Eq. (4.5), we obtain

$$\begin{aligned} P_{ii}^0 - P_{ii} &= \frac{V_{i-1,t} \Sigma_{i-1}}{\Sigma_i V_i} \{ 1 - P_c(\Sigma_{i-1}, r_{i-1}) \} H_{i-1,i}^2 \\ &+ \frac{V_{i-2,t}}{\Sigma_i V_i} \left[\Sigma_{i-2} \{ 1 - P_c(\Sigma_{i-2}, r_{i-2}) \} - \Sigma_{i-1} \{ 1 - P_c(\Sigma_{i-1}, r_{i-1}) \} \right] H_{i-2,i}^2 \\ &+ \frac{V_{i-3,t}}{\Sigma_i V_i} \left[\Sigma_{i-3} \{ 1 - P_c(\Sigma_{i-3}, r_{i-3}) \} - \Sigma_{i-2} \{ 1 - P_c(\Sigma_{i-2}, r_{i-2}) \} \right] H_{i-3,i}^2 \\ &+ \dots, \end{aligned} \quad (4.8)$$

where $V_{j,t} = \pi r_j^2$ and $H_{j,i}$ is the probability that a neutron emitted isotropically from the outer boundary of the j -th region undergoes its

first collision in the i-th region.

In Bonalumi's approximation, P_{ii}^0 is identical with Eq. (4.5).

But he made the following approximation for $P_{ii}^0 - P_{ii}$:

$$\begin{aligned}
 P_{ii}^0 - P_{ii} &= \frac{2r_i}{\Sigma_i V_i} \int_{y_i^2}^{y_i^1} d\varphi \cos \varphi \int_0^{\frac{\pi}{2}} d\theta \sin^2 \theta \left(1 - e^{-\frac{X'_{i-1} \Sigma_{i-1}}{\sin \theta}}\right) \left(1 - e^{-\frac{X_i \Sigma_i}{\sin \theta}}\right)^2 \\
 &+ \frac{2r_i}{\Sigma_i V_i} \int_{y_i^3}^{y_i^2} d\varphi \cos \varphi \int_0^{\frac{\pi}{2}} d\theta \sin^2 \theta \left(1 - e^{-\frac{X'_{i-2} \Sigma_{i-2} + 2X_{i-1} \Sigma_{i-1}}{\sin \theta}}\right) \left(1 - e^{-\frac{X_i \Sigma_i}{\sin \theta}}\right)^2 \\
 &+ \dots \\
 &= \frac{2r_i}{\Sigma_i V_i} \left[\int_{y_i^2}^{y_i^1} d\varphi \cos \varphi \int_0^{\frac{\pi}{2}} d\theta \sin^2 \theta \left(1 - e^{-\frac{X'_{i-1} \Sigma_{i-1}}{\sin \theta}}\right) \left(1 - e^{-\frac{X_i \Sigma_i}{\sin \theta}}\right) \right. \\
 &+ \int_{y_i^3}^{y_i^2} d\varphi \cos \varphi \int_0^{\frac{\pi}{2}} d\theta \sin^2 \theta \left(1 - e^{-\frac{X'_{i-2} \Sigma_{i-2} + 2X_{i-1} \Sigma_{i-1}}{\sin \theta}}\right) \left(1 - e^{-\frac{X_i \Sigma_i}{\sin \theta}}\right) \\
 &+ \dots \left. \right] H_{i-1,i} \\
 &= \sum_{m=1}^{i-1} P_{i,m} H_{i-1,i} \quad (4.9)
 \end{aligned}$$

It is seen that Bonalumi's approximation neglects the azimuthal dependence of $H_{i-1,i}$ in addition to our approximation of replacing the integrand by the product of each average. The former approximation will not be valid when the system contains a region of small thickness or small neutron cross section.

Next we introduce an approximate expression for P_{ij} ($i < j$), which is composed of two different probabilities P'_{ij} and P''_{ij} , where P'_{ij} is the first-flight collision probability for a neutron born in the i-th region to collide in the j-th region without passing the inner regions of i, and P''_{ij} is that for a neutron to collide in the j-th region after passing the inner regions of i:

$$\begin{aligned}
P'_{i,j} &= \frac{2r_i}{\Sigma_i V_i} \left\{ \int_{y'_i}^{\frac{\pi}{2}} d\varphi \cos \varphi \int_0^{\frac{\pi}{2}} d\theta \sin^2 \theta \left(1 - e^{-\frac{X'_i \Sigma_i}{\sin \theta}} \right) \right. \\
&\quad \cdot e^{-\frac{X_{i+1} \Sigma_{i+1} + X_{i+2} \Sigma_{i+2} + \dots + X_{j-1} \Sigma_{j-1}}{\sin \theta}} \left(1 - e^{-\frac{X_j \Sigma_j}{\sin \theta}} \right) \\
&\quad \left. + \int_0^{y'_i} d\varphi \cos \varphi \int_0^{\frac{\pi}{2}} d\theta \sin^2 \theta \left(1 - e^{-\frac{X_i \Sigma_i}{\sin \theta}} \right) e^{-\frac{X_{i+1} \Sigma_{i+1} + \dots + X_{j-1} \Sigma_{j-1}}{\sin \theta}} \left(1 - e^{-\frac{X_j \Sigma_j}{\sin \theta}} \right) \right\} \\
&= \frac{1}{1 - \alpha_i^2} \left\{ 1 - P_c(r_i \Sigma_i) \right\} H_{i,j} - \frac{\pi r_{i-1}}{2 \Sigma_i V_i} \left\{ H_{i-1,j} - H_{i-1,j}(2 \Sigma_i) \right\} \\
&\quad - \frac{\alpha_i^2}{1 - \alpha_i^2} \left\{ 1 - P_c(r_{i-1} \Sigma_i) \right\} H_{i-1,j}(2 \Sigma_i),
\end{aligned} \tag{4.10}$$

$$\begin{aligned}
P''_{i,j} &= \frac{2r_i}{\Sigma_i V_i} \left\{ \int_{y_i^2}^{y_i^1} d\varphi \cos \varphi \int_0^{\frac{\pi}{2}} d\theta \sin^2 \theta \left(1 - e^{-\frac{X_i \Sigma_i}{\sin \theta}} \right) \right. \\
&\quad \cdot e^{-\frac{X'_{i-1} \Sigma_{i-1} + X_i \Sigma_i + \dots + X_{j-1} \Sigma_{j-1}}{\sin \theta}} \left(1 - e^{-\frac{X_j \Sigma_j}{\sin \theta}} \right) \\
&\quad + \int_{y_i^3}^{y_i^2} d\varphi \cos \varphi \int_0^{\frac{\pi}{2}} d\theta \sin^2 \theta \left(1 - e^{-\frac{X_i \Sigma_i}{\sin \theta}} \right) e^{-\frac{2X_{i-1} \Sigma_{i-1} + X'_{i-2} \Sigma_{i-2} + X_i \Sigma_i + \dots + X_{j-1} \Sigma_{j-1}}{\sin \theta}} \\
&\quad \cdot \left(1 - e^{-\frac{X_j \Sigma_j}{\sin \theta}} \right) \\
&\quad + \int_{y_i^4}^{y_i^3} d\varphi \cos \varphi \int_0^{\frac{\pi}{2}} d\theta \sin^2 \theta \left(1 - e^{-\frac{X_i \Sigma_i}{\sin \theta}} \right) \\
&\quad \cdot e^{-\frac{2X_{i-1} \Sigma_{i-1} + 2X_{i-2} \Sigma_{i-2} + X'_{i-3} \Sigma_{i-3} + X_i \Sigma_i + \dots + X_{j-1} \Sigma_{j-1}}{\sin \theta}} \left(1 - e^{-\frac{X_j \Sigma_j}{\sin \theta}} \right) \\
&\quad + \dots \left. \right\} \\
&= \frac{1}{\Sigma_i V_i} \left[\frac{\pi r_{i-1}}{2} - \Sigma_{i-1} V_{i-1,t} \left\{ 1 - P_c(\Sigma_{i-1} r_{i-1}) \right\} \left\{ H_{i-1,j} - H_{i-1,j}(2 \Sigma_i) \right\} \right] \\
&\quad + \frac{V_{i-2,t}}{\Sigma_i V_i} \left[\Sigma_{i-1} \left\{ 1 - P_c(\Sigma_{i-1} r_{i-2}) \right\} - \Sigma_{i-2} \left\{ 1 - P_c(\Sigma_{i-2} r_{i-2}) \right\} \right]
\end{aligned}$$

$$\begin{aligned}
& \cdot \left[H_{i-2,j}(2\Sigma_{i-1}) - H_{i-2,j}(2\Sigma_{i-1}, 2\Sigma_i) \right] \\
& + \frac{V_{i-3,j}}{\Sigma_i V_i} \left[\Sigma_{i-2} \{1 - P_c(\Sigma_{i-2} r_{i-3})\} - \Sigma_{i-3} \{1 - P_c(\Sigma_{i-3} r_{i-3})\} \right] \\
& \cdot \left[H_{i-3,j}(2\Sigma_{i-2}, 2\Sigma_{i-1}) - H_{i-3,j}(2\Sigma_{i-2}, 2\Sigma_{i-1}, 2\Sigma_i) \right] \\
& + \dots, \tag{4.11}
\end{aligned}$$

where $H_{i-1,j}(2\Sigma_i)$ is the value of $H_{i-1,j}$ when the neutron cross section in the i -th region is $2\Sigma_i$ and $H_{i-2,j}(2\Sigma_{i-1}, 2\Sigma_i)$ is the value of $H_{i-2,j}$ when the neutron cross sections in the regions $i-1$ and i are $2\Sigma_{i-1}$ and $2\Sigma_i$ respectively. The collision probabilities $P_{ji}(j > i)$ are evaluated with the aid of the reciprocity relation

$$\Sigma_i V_i P_{i,j} = \Sigma_j V_j P_{j,i}.$$

When we apply the isotropic reflection condition on the cell boundary, the first-flight collision probabilities P_{ij}^t in lattice cells containing N annular regions acquire the form⁽²²⁾,

$$P_{i,j}^t = P_{i,j} + \left(1 - \sum_{k=1}^N P_{i,k}\right) \frac{P_{s,j}}{\sum_{k=1}^N P_{s,k}}, \tag{4.12a}$$

where

$$P_{s,j} = \frac{4 \Sigma_j V_j}{S} \left(1 - \sum_{k=1}^N P_{j,k}\right), \tag{4.12b}$$

and S is the surface area of the cell boundary.

In what follows, we have introduced the first-flight collision probabilities between annular regions. To treat a cluster system by Leslie's formula, it is necessary to obtain the collision probabilities between subregions (fuel, cladding or coolant) in a ring possessing an internal void. To calculate these probabilities we derive the first-flight collision probabilities between neighboring subcells and between subcells separated from one another by a void region between them.

Firstly, we derive the probability Λ_{1a} for a neutron emitted isotropically from the surface of the fuel rod 1 to reach the fuel rod 2 (see Fig. 4.2, where a means the radius of the rods). Here it is assumed that the fuel rods are black and the medium between the rods is void. When a point A is on $\widehat{PBP'}$, namely, $|\alpha| < \alpha_0$, a neutron starting from the point A with azimuthal angle φ may strike the fuel rod 2 if $\varphi_1 < \varphi < \varphi_2$ (φ is measured clockwise). When A is outside $\widehat{PBP'}$, i.e. when $|\alpha|$ is between α_0 and $\pi/2$, only the neutron with the condition $\varphi_1 < \varphi < \pi/2$ may enter the fuel rod 2. So we obtain

$$\begin{aligned}
 \Lambda_{1a} &= \frac{1}{\int_{2\pi} d\vec{\Omega} (\vec{n} \cdot \vec{\Omega})} \cdot \frac{1}{2S_0} \int_{(\text{semi-surface})} dS_0 \int_{(\text{solid angle glancing the fuel rod 2})} d\vec{\Omega} (\vec{n} \cdot \vec{\Omega}) \\
 &= \frac{1}{2\pi} \left[\int_0^{\alpha_0} d\alpha \int_{\varphi_1(\alpha)}^{\varphi_2(\alpha)} d\varphi \cos \varphi + \int_{\alpha_0}^{\pi/2} d\alpha \int_{\varphi_1(\alpha)}^{\pi/2} d\varphi \cos \varphi \right] \\
 &= \frac{1}{4\pi} \int_{-\pi/2}^{\pi/2} d\varphi \cos \varphi \int_{-\pi/2}^{\pi/2} d\theta \cos \theta \frac{a}{\sqrt{d^2 - a^2 (\sin \theta - \sin \varphi)^2}} \\
 &= \frac{1}{2\pi} \left\{ 2 \sin^{-1} \frac{2a}{d} + \frac{d}{a} \left(\sqrt{1 - \frac{4a^2}{d^2}} - 1 \right) \right\}, \tag{4.13}
 \end{aligned}$$

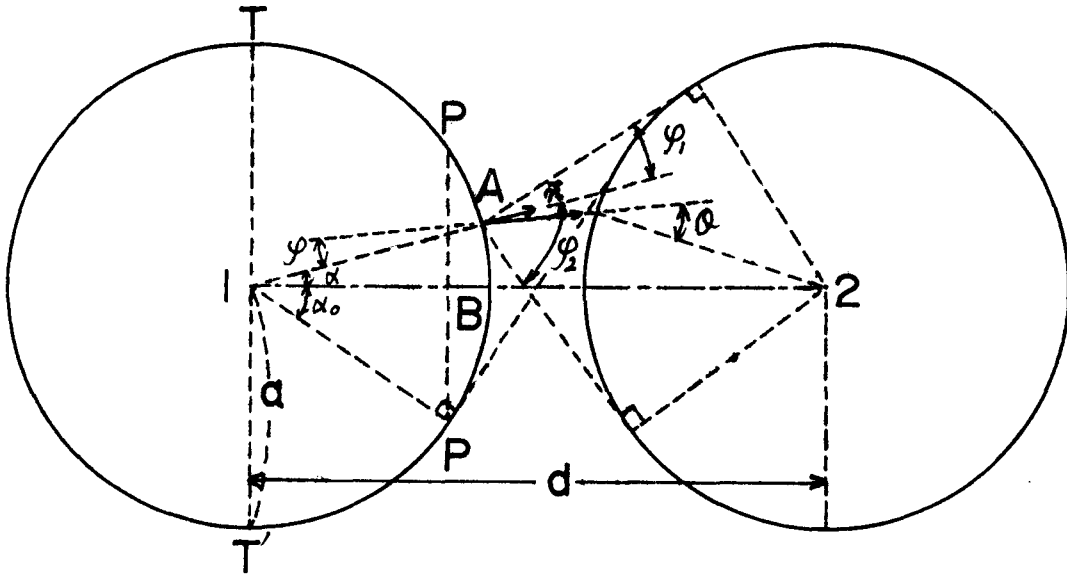


Fig. 4.2 Transition of neutron between two adjacent rods

where d is the distance between the centers of the subcells. Next we evaluate the probability Λ_{2b} for a neutron escaping from a subcell to enter an adjacent subcell (b is the radius of subcells).

$$\begin{aligned}\Lambda_{2b} &= \frac{1}{4\pi} \int_{-\pi/2}^{\pi/2} d\varphi \cos \varphi \int_{-\pi/2}^{\pi/2} d\theta \cos \theta \frac{b}{\sqrt{|d^2 - b^2(\sin \theta - \sin \varphi)^2|}} \\ &= \frac{1}{2\pi} \left(\pi - \frac{d}{b} + 2 \ln \frac{2b + \sqrt{4b^2 - d^2}}{d} - \sqrt{4 - \frac{d^2}{b^2}} \right).\end{aligned}\quad (4.14)$$

Here it is assumed that a neutron starting from a subcell along the path \vec{AE} can reach the adjacent subcell by passing through the original subcell inwardly (path \vec{AC} shown in Fig. 4.3).

Applying Eqs. (4.13) and (4.14), we can obtain the probabilities between subcells when there is coolant present between the rods. Firstly, we calculate the probability Q_{13} that a neutron escaping from the fuel rod 1 undergoes its first collision in the fuel rod 3 in Fig. 4.4. We assume that a neutron born in the fuel rod 1 escapes from the original subcell with the probability $\{1 - P_c(z, a)\}(1 - H_{12})$. It proceeds to the surface of the region 4 with the probability Λ_{2b} (b means the radius of the subcells) and has its first collision in the fuel rod 3 with the probability $(\Sigma_3 V_1 / S_2) \{1 - P_c(z, a)\}(1 - H_{12})$. After all we have

$$Q_{13} = \frac{2 \Sigma_1 a^2}{b} \Lambda_{2b} \{1 - P_c(z, a)\}^2 (1 - H_{12}). \quad (4.15)$$

In a similar manner we obtain Q_{14} and Q_{24} :

$$\begin{aligned}Q_{14} &= \frac{2 \Sigma_2 (b^2 - a^2)}{b} \Lambda_{2b} \{1 - P_c(z, a)\} \\ &\cdot (1 - H_{12})(1 - P_{22} - P_{21}),\end{aligned}\quad (4.16)$$

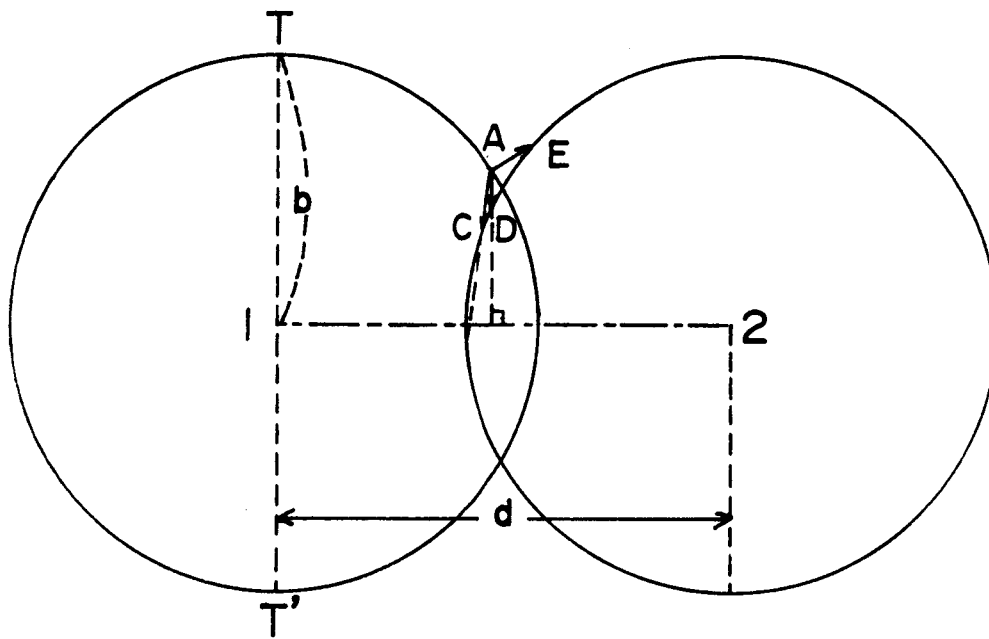


Fig. 4.3 Transition of neutron between two adjacent subcells

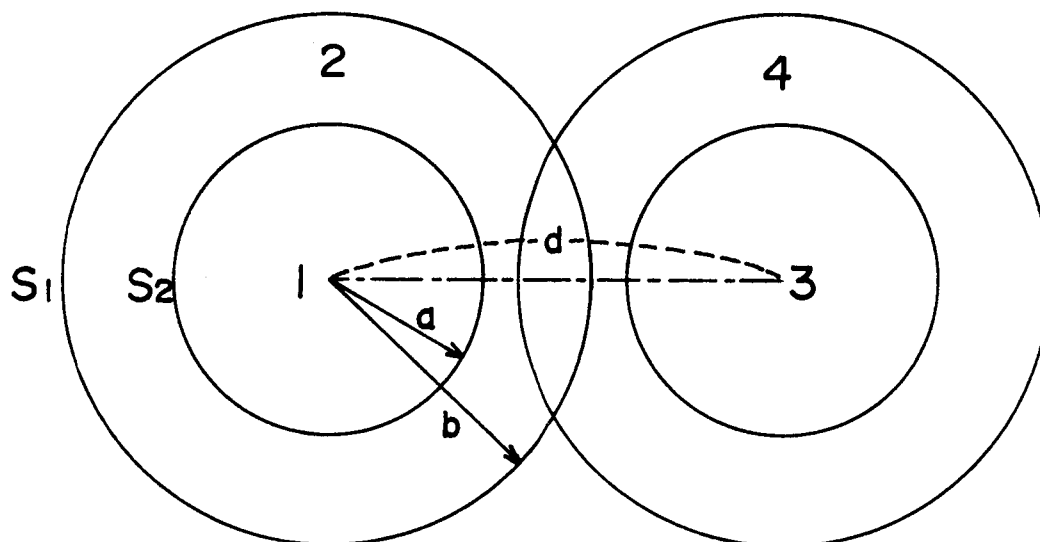


Fig. 4.4 Two adjacent subcells

$$Q_{24} = \frac{2 \Sigma_2 (b^2 - a^2)}{b} \Lambda_{2b} (1 - P_{22} - P_{21})^2 . \quad (4.17)$$

Here H_{12} , P_{21} and P_{22} have already been calculated.

The first-flight collision probabilities between subcells separated from one another by a void region between them are calculated by substituting Λ_{1b} for Λ_{2b} in Eqs. (4.15)~(4.17), and changing the distance d to an appropriate one.

Applying the equations derived up to now, we calculate the first-flight collision probability in cluster systems.

First, we derive collision probabilities in a cluster without cladding. In a hexagonal cluster we choose a ring region that is tangent, for example, to the six rods shown in Fig. 4.5. Subregions in the ring are indexed by k as is marked in Fig. 4.5, where fuel rod corresponds to $k = \text{odd}$ and coolant to $k = \text{even}$. We consider the collision probability $P_{ii}^0(l, k)$ that a neutron born in the subregion l of the ring i undergoes its first collision in the subregion k of the same ring, in the case where the internal region of the ring i is void. Here the suffixes l and k are either f (fuel) or c (coolant). The macroscopic neutron cross sections of the fuel and the coolant are denoted by Σ_f and Σ_c respectively, and the superscript 0 denotes that all the inner regions are void. We assume also that $Q(l, m)$ represents the probability for a neutron born in the subregion l (fuel) to undergo its first collision in the subregion m in the same ring when the inner region of the ring is void. Then we have

$$P_{ii}^0(f, f) = \sum_{m=1,3,\dots,M-1} Q(l, m) , \quad (4.18)$$

where $M-1$ is the maximum odd number of subregions in the ring. In the

calculation of $Q(1,m)$, $Q(1,1)$ is the probability that a neutron born in the fuel rod 1 undergoes its first collision within the same rod, and may be calculated by using Eq. (4.1). The other $Q(1,m)$'s, for example, in the 6-rod ring in a hexagonal cluster, are determined as follows: $Q(1,3)$ may be calculated by using Eq. (4.15). But in the calculations of $Q(1,5)$ and $Q(1,7)$, the intermediate medium between the subregions 1 and 5 or 7 is assumed to be void, and simultaneously the quantity Λ_{2b} is replaced by Λ_{1a} , as it was previously done, furthermore we choose a suitable length d and let $H_{12} = 0$ in Eq. (4.15).

Next we write down the probability $P_{ii}^0(f,c)$ in the form

$$P_{ii}^0(f,c) = \{1 - P_c(a z_c)\} G_{bc}, \quad (4.19)$$

where G_{bc} is the probability that a neutron escaping from one of the fuel rods in the ring collides in the coolant in the same ring when the internal region of the ring is void, and is evaluated as follows.

We replace rod and coolant areas in the ring by radial lines so as to maintain the same areas, and denote the angle of a fuel rod and coolant medium by γ_1 and γ_2 respectively (cf. Fig. 4.5). The probability $P_{ii,c}^0$ that a neutron born in the ring i ——in the case where all subregions of the ring are coolant——has its first collision in the same ring may be written as follows:

$$\begin{aligned} P_{ii,c}^0 &= \sum_{m=1}^M Q^c(1,m) \\ &= \sum_{m=1,3,\dots,(M-1)} Q^c(1,m) + \{1 - P_c(a z_c)\} G_{bc}, \end{aligned} \quad (4.20)$$

where the superscript c means that all the subregions are coolant.

Since $P_{ii,c}^0$ can be calculated by Eq. (4.5) and $Q^c(1,m)$'s by the similar way to the above $Q(1,m)$'s, we can now determine $P_{ii}^0(f,c)$ by using

Eqs. (4.19) and (4.20). By using the reciprocity relation, we have

$$P_{ii}^o(c, f) = \frac{\sum_f V_f}{\sum_c V_c} P_{ii}^o(f, c) , \quad (4.21)$$

$$P_{ii}^o(c, c) = \left(1 - \frac{V_f}{V_c}\right) P_{ii,c}^o + \frac{V_f}{V_c} \sum_{m=1, 3, \dots, N-1} Q^c(l, m) . \quad (4.22)$$

Thus the collision probabilities in one ring having internal void region are obtained by Eqs. (4.18) through (4.22).

Using $P_{ii}^0(l, k)$, the probability $P_{ii}(l, k)$ in the presence of given media in the internal regions of the ring i can be calculated by using Leslie-Jonsson's approximation for a cell containing two regions⁽⁴⁾:

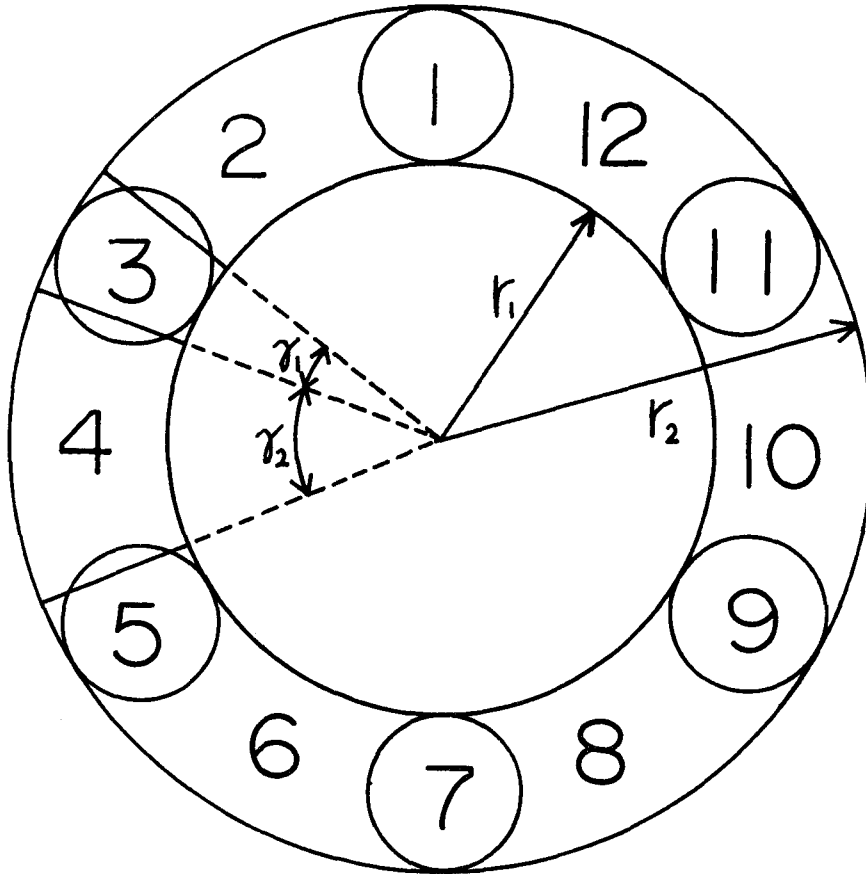


Fig. 4.5 Ring region for hexagonal cluster

$$P_{ii}(\ell, k) = P_{ii}^0(\ell, k) - P_{i, inner}(\ell, f+c) G_{inner, i} \alpha_{ki} \quad (4.23)$$

where $P_{i, inner}(\ell, f+c)$ is the probability for a neutron born in the sub-region ℓ of the ring i to have its first collision in the internal media of the ring i , $G_{inner, i}$ is the probability for a neutron escaping from the internal media outwards to undergo its first collision anywhere in the ring i , and α_{ki} is the ratio for the collision to occur in the subregion k of the ring i ; $P_{i, inner}(\ell, f+c)$ is related to the probability $P_{i, inner}$ that a neutron born uniformly in the homogenized ring i has its first collision in the internal media of the ring i by the relation:

$$P_{i, inner}(\ell, f+c) = \frac{\sum_k \Sigma_{ki} V_{ki}}{\sum_{ki} \Sigma_{ki} V_{ki}} P_{i, inner} \alpha_{ki} \quad (4.24)$$

where V_{ki} and Σ_{ki} are the volume and the total cross section in the sub-region k of the ring i . Homogenizing the ring i , we obtain

$$P_{ii} = P_{ii}^0 - P_{i, inner} G_{inner, i} \quad (4.25)$$

Using Eqs. (4.23) through (4.25), we obtain

$$P_{ii}(\ell, k) = P_{ii}^0(\ell, k) - \alpha_{ki} \alpha_{ki} \frac{\sum_k \Sigma_{ki} V_{ki}}{\sum_{ki} \Sigma_{ki} V_{ki}} (P_{ii}^0 - P_{ii}) \quad (4.26)$$

In the above equation, P_{ii} and P_{ii}^0 are calculated for the case where the ring is homogenized. We may assume for α_{ki} that

$$\alpha_{ji} = \frac{\delta_1 H_{i-1, i}(\Sigma_f)}{\delta_1 H_{i-1, i}(\Sigma_f) + \delta_2 H_{i-1, i}(\Sigma_c)} \quad , \quad (4.27a)$$

$$\alpha_{ci} = 1 - \alpha_{ji} \quad (4.27b)$$

In Eq. (4.25), when we homogenize the ring containing fuel rods and coolant, the homogenized cross section is chosen so that the probability for a neutron entering this ring inwards to undergo its first collision in the homogenized ring is the same as that for an actual heterogeneous ring:

$$H_{i-1,i}(\Sigma_{\text{hom}}) = \frac{r_1}{r_1 + r_2} H_{i-1,i}(\Sigma_f) + \frac{r_2}{r_1 + r_2} H_{i-1,i}(\Sigma_c) . \quad (4.28)$$

In the calculation of the collision probabilities P_{ij} between rings neither of which contains any fuel rod, P_{ij} may be evaluated in the scheme for an annular system, with use made of homogenized cross sections in each region. For rings both of which contain fuel rods, $P_{ij}(l,k)$ may also be evaluated by the relation

$$P_{ij}(l,k) = \alpha_{li} \alpha_{kj} \frac{\sum_i \Sigma_{li} V_{li}}{\Sigma_{li} V_{li}} P_{ij} , \quad (4.29)$$

which was introduced by Leslie and Jonsson^{(4),(23)}.

In a cluster system with cladding, we cannot use Eqs. (4.18) and (4.22). So we divide the system into subcells containing the three constituents of fuel rod, cladding and coolant, and denote the subcells by indices m, m' . We assume that $Q_{mm'}(l,k)$ is the probability for a neutron born in the subregion l in the subcell m to collide in the subregion k in the subcell m' in the same ring when the internal region of the ring is void. Then we have

$$P_{ii}^o(l,k) = \sum_{m'=1}^M Q_{mm'}(l,k) . \quad (4.30)$$

In the calculation of $Q_{mm'}(l,k)$, $Q_{mm}(l,k)$ is the probability in an annular system and can be evaluated by the previous procedure, and when $m \neq m'$,

$$Q_{mm'}(l, k) = (1 - \sum_{l'} P_{ll'}) \Lambda_{m \rightarrow m'} P_{sk} . \quad (4.31)$$

Here $P_{ll'}$ is the probability for a neutron born in a subregion l to collide in a subregion l' in the same subcell. The summation of l' is performed over all the constituents of the subcell. Further, $\Lambda_{m \rightarrow m'}$ is the probability for a neutron leaving the subcell m to reach the subcell m' , and is equal to Λ_{2b} for adjacent subcells, and to Λ_{1b} for other subcells; P_{sk} is the probability for a neutron impinging on the surface S of the subcell to collide in the subregion k in the subcell, and is given by

$$P_{sk} = \frac{4}{S} \Sigma_k V_k (1 - \sum_{l'} P_{kl'}) . \quad (4.32)$$

Using Eqs. (4.26) and (4.30), we obtain the probabilities $P_{ii}(l, k)$ for a cluster with cladding. The ratio α_{ki} for a neutron to collide in the subregion k in the subcell i is

$$\alpha_{ki} = \frac{P_{sk}}{\sum_k P_{sk}} . \quad (4.33)$$

A homogenized cross section of the ring Σ_{homo} is evaluated to satisfy the relation

$$P_{sh}(\Sigma_{\text{homo}}) = \sum_k P_{sk} , \quad (4.34)$$

where P_{sh} is the probability for a neutron impinging on the surface of the subcell to collide in the homogenized subcell, and is expressed by

$$P_{sh}(\Sigma_{\text{homo}}) = \frac{4}{S} \Sigma_{\text{homo}} V_t \{1 - P_c(b \Sigma_{\text{homo}})\} , \quad (4.35)$$

where V_t is the volume of the subcell.

Using the homogenized cross section and α_{ki} , we obtain, by using Eq. (4.29), the probabilities $P_{ij}(l, k)$ for a cluster with cladding. Thus all the probabilities in the cluster system with cladding have been derived.

In this section, the effect of finiteness of systems under consideration in the axial direction brought upon the flux distribution is investigated by deriving a new first-flight collision probability.

The neutron flux in three dimensional systems is expressed in sine series:

$$\phi(\vec{r}) = \sum_{m=0}^{\infty} \phi_m(\vec{x}) \sin B_m z, \quad (4.36)$$

where \vec{x} is a vector in the horizontal plane and z is a coordinate along the axial direction, and B_m is given by

$$B_m = \frac{(2m+1)\pi}{H}, \quad (4.37)$$

where H is the axial height. The neutron source is also expressed in sine series:

$$S(\vec{r}) = \sum_{m=0}^{\infty} S_m(\vec{x}) \sin B_m z. \quad (4.38)$$

Substituting Eqs. (4.36) and (4.38) into the integral Boltzmann equation

$$\phi(\vec{r}) = \int d\vec{r}' \frac{\bar{e}^{-\vec{r}\vec{r}'}}{4\pi R^2} \{ \Sigma_s(\vec{r}') \phi(\vec{r}') + S(\vec{r}') \}, \quad (4.39)$$

and integrating over $0 \sim H$ about z after multiplying by $\sin B_k z$, we obtain the equation

$$\begin{aligned} \frac{H}{2} \phi_k(\vec{x}) &= \int_0^H dz \sin B_k z \int d\vec{r}' \frac{\bar{e}^{-\vec{r}\vec{r}'}}{4\pi R^2} \sum_{l=0}^{\infty} \sin B_l z' \\ &\cdot \{ \Sigma_s(\vec{x}') \phi_l(\vec{x}') + S_l(\vec{x}') \}. \end{aligned} \quad (4.40)$$

Here the horizontal area is divided into some regions in each of

which the neutron cross sections are constant. In each region it is assumed that the neutron flux and source are constant and, for instance in the i -th region and in mode k , they are denoted by ϕ_{ik} and S_{ik} respectively. Integration of the above equation over the surface area V_j of the horizontal j -th region produces the equation

$$V_j \Sigma_j \phi_{jk} = \sum_i \sum_{l=0}^{\infty} P_{ij}^{lk} V_i (\Sigma_{il} \phi_{il} + S_{il}), \quad (4.41)$$

where P_{ij}^{lk} is given by

$$P_{ij}^{lk} = \frac{2 \Sigma_j}{H V_i} \int d\vec{r} \int d\vec{r}' \sin B_z z' \sin B_z z \frac{e^{-\hat{z}\vec{R}}}{4\pi R^2}. \quad (4.42)$$

If the first-flight collision probabilities P_{ij}^{lk} are obtained, the flux components ϕ_{ik} are calculated by solving the simultaneous equation (4.41). In what follows, we will calculate the probability P_{ij}^{00} for the fundamental mode. Other probabilities would be similarly obtained.

First, we calculate the fundamental mode first-flight collision probability in a slab system. Notations in the slab system are described in Fig. 4.6. The probability P_{ij}^{00} ($i \neq j$) takes the form:

$$P_{ij}^{00} = \frac{2 \Sigma_j}{H l_i} \int_0^{l_i} dx' \int_0^H dz' \sin B z' \int d\vec{r} \sin B z \frac{e^{-\hat{z}\vec{R}}}{4\pi R^2}, \quad (4.43)$$

where B is the abbreviation of B_0 and l_i is the thickness of the i -th region. Owing to the relations

$$d\vec{r} = R^2 dR d\vec{\Omega}, \quad (4.44a)$$

$$d\vec{\Omega} = \sin \alpha d\alpha d\phi, \quad (4.44b)$$

$$z = z' + l \tan \alpha \sin \phi, \quad (4.44c)$$

the above equation reduces to

$$P_{ij}^{00} = \frac{2 \Sigma_j}{\pi H l_i} \int_0^{l_i} dx' \int_0^H dz' \sin B z' \int_{l_{ij}+l_i}^{l_{ij}+l_j+l_i} dx \int_0^{\pi/2} d\phi \int_0^{\alpha^*} d\alpha \tan \alpha \cdot e^{-\hat{z}\vec{R}/\cos \alpha} \sin B (z' + l \tan \alpha \sin \phi), \quad (4.45)$$

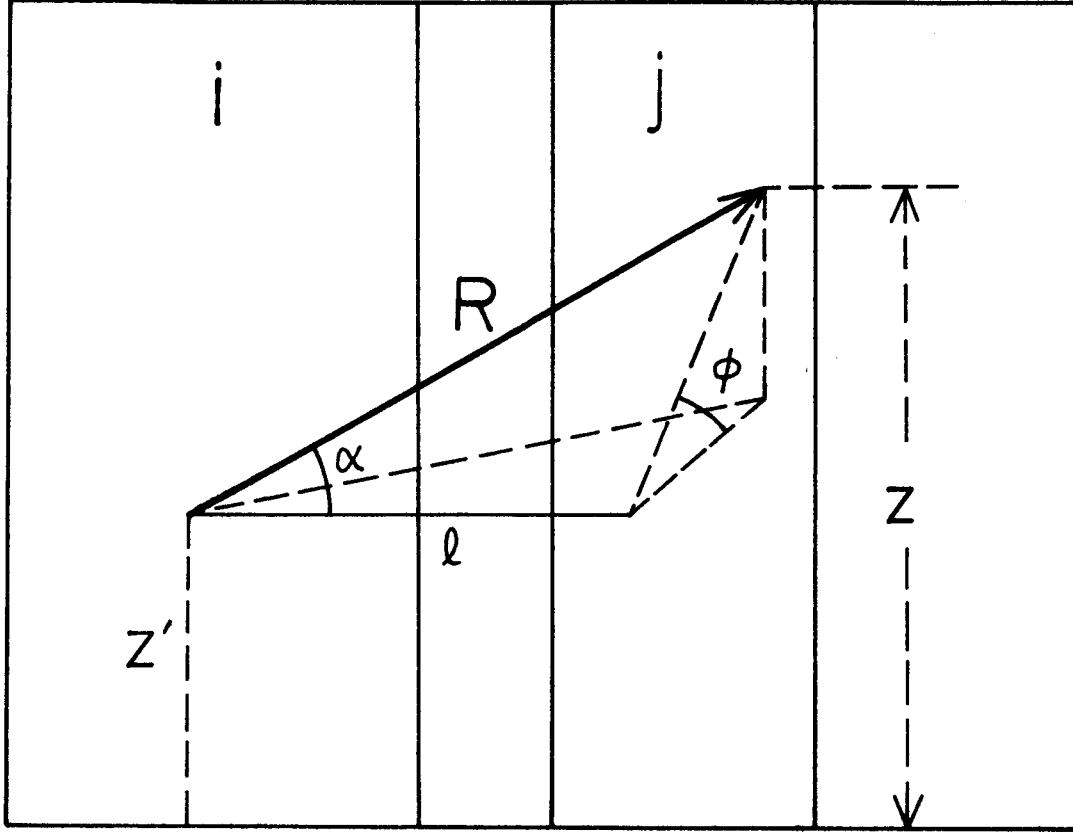


Fig. 4.6 Notations in a finite slab system

where α^* is given by the relation

$$z' + l \tan \alpha^* \sin \phi = H. \quad (4.46)$$

If we exchange the order of integration in Eq. (4.45) by

$$\int_0^H dz' \int_0^{\alpha^*} d\alpha = \int_0^{\tan^{-1}(\frac{H}{l \sin \phi})} d\alpha \int_0^{H - l \tan \alpha \sin \phi} dz', \quad (4.47)$$

and perform the integration about z' , we can reduce Eq. (4.45) in the form:

$$P_{ij}^{00} = \frac{2Z_j}{\pi l_i} \int_0^{l_i} dx' \int_{l_{ij}+l_i}^{l_{ij}+l_i+l_j} dx \int_0^{\pi/2} d\phi \int_0^{\tan^{-1}(\frac{H}{l \sin \phi})} d\alpha \tan \alpha e^{-x'/\cos \alpha} A, \quad (4.48)$$

where

$$A = \cos(B l \tan \alpha \sin \phi) \left\{ \frac{1}{2} \left(1 - \frac{l}{H} \tan \alpha \sin \phi \right) + \frac{l}{4BH} \sin(2B l \tan \alpha \sin \phi) \right\} + \frac{l}{2BH} \sin^3(B l \tan \alpha \sin \phi). \quad (4.49)$$

In a similar manner, P_{ii}^{00} is expressed in the form:

$$P_{ii}^{00} = \frac{4 \Sigma_i}{\pi l_i} \int_0^{l_i} dx' \int_{x'}^{l_i} dx \int_0^{\pi/2} d\phi \int_0^{\tan^{-1}(\frac{H}{l \sin \phi})} d\alpha \tan \alpha \bar{e}^{-x l / \cos \alpha} A, \quad (4.50)$$

where $l = x - x'$. In Eqs. (4.48) and (4.50), the double integral about x' and x can be reduced to a single integral about l . Thus we obtain the following expression for P_{ii}^{00} :

$$P_{ii}^{00} = \frac{4 \Sigma_i}{\pi l_i} \int_0^{l_i} dl (l_i - l) \int_0^{\pi/2} d\phi \int_0^{\tan^{-1}(\frac{H}{l \sin \phi})} d\alpha \tan \alpha \bar{e}^{-x l / \cos \alpha} A. \quad (4.51)$$

In the calculation of P_{ij}^{00} we first consider the case $\Sigma_i = \Sigma_j$. When

$l_i = l_j$ and $\Sigma_i = \Sigma_j$, we obtain

$$P_{ij}^{00} = \frac{2 \Sigma_j}{\pi l_i} \int_{l_{ij}}^{l_{ij}+l_i} dl (l - l_{ij}) \int_0^{\pi/2} d\phi \int_0^{\tan^{-1}(\frac{H}{l \sin \phi})} d\alpha C \\ + \frac{2 \Sigma_j}{\pi l_i} \int_{l_{ij}+l_i}^{l_{ij}+2l_i} dl (2l_i + l_{ij} - l) \int_0^{\pi/2} d\phi \int_0^{\tan^{-1}(\frac{H}{l \sin \phi})} d\alpha C, \quad (4.52)$$

where

$$C = A \tan \alpha \bar{e}^{-\frac{\Sigma l_{ij} - \Sigma_j l_{ij} + \Sigma_j l}{\cos \alpha}},$$

and l_{ij} and Σl_{ij} are the real and optical distances from the right side of the i -th region to the left side of the j -th region. When $l_i > l_j$ and $\Sigma_i = \Sigma_j$,

$$P_{ij}^{00} = \frac{2 \Sigma_j}{\pi l_i} \int_{l_{ij}}^{l_{ij}+l_j} dl (l - l_{ij}) \int_0^{\pi/2} d\phi \int_0^{\tan^{-1}(\frac{H}{l \sin \phi})} d\alpha C \\ + \frac{2 \Sigma_j}{\pi l_i} \int_{l_{ij}+l_j}^{l_{ij}+l_i} dl l_j \int_0^{\pi/2} d\phi \int_0^{\tan^{-1}(\frac{H}{l \sin \phi})} d\alpha C \\ + \frac{2 \Sigma_j}{\pi l_i} \int_{l_{ij}+l_i}^{l_{ij}+l_i+l_j} dl (l_{ij} + l_i + l_j - l) \int_0^{\pi/2} d\phi \int_0^{\tan^{-1}(\frac{H}{l \sin \phi})} d\alpha C. \quad (4.53)$$

When $l_j > l_i$ and $\Sigma_i = \Sigma_j$,

$$P_{ij}^{00} = \frac{2 \Sigma_j}{\pi l_i} \int_{l_{ij}}^{l_{ij}+l_i} dl (l - l_{ij}) \int_0^{\pi/2} d\phi \int_0^{\tan^{-1}(\frac{H}{l \sin \phi})} d\alpha C$$

$$\begin{aligned}
& + \frac{2 \Sigma_{\pm}}{\pi l_i} \int_{l_{ij}+l_i}^{l_{ij}+l_{\pm}} dl \int_0^{\pi/2} d\phi \int_0^{\tan^{-1}(\frac{H}{l \sin \phi})} d\alpha \quad C \\
& + \frac{2 \Sigma_{\pm}}{\pi l_i} \int_{l_{ij}+l_i}^{l_{ij}+l_i+l_{\pm}} dl (l_{ij}+l_i+l_{\pm}-l) \int_0^{\pi/2} d\phi \int_0^{\tan^{-1}(\frac{H}{l \sin \phi})} d\alpha \quad C .
\end{aligned} \tag{4.54}$$

Next we consider the case $\Sigma_i \neq \Sigma_{\pm}$. When $l_i = l_{\pm}$ and $\Sigma_i \neq \Sigma_{\pm}$, we obtain

$$\begin{aligned}
P_{i\pm}^{oo} &= \frac{2 \Sigma_{\pm}}{\pi l_i} \cdot \frac{1}{\Sigma_i - \Sigma_{\pm}} \int_{l_{ij}}^{l_{ij}+l_i} dl \int_0^{\pi/2} d\phi \int_0^{\tan^{-1}(\frac{H}{l \sin \phi})} d\alpha \quad D \\
&\quad \cdot \left\{ 1 - e^{-(\Sigma_i - \Sigma_{\pm})(l - l_{ij})/\cos \alpha} \right\} \\
&+ \frac{2 \Sigma_{\pm}}{\pi l_i} \cdot \frac{1}{\Sigma_i - \Sigma_{\pm}} \int_{l_{ij}+l_i}^{l_{ij}+2l_i} dl \int_0^{\pi/2} d\phi \int_0^{\tan^{-1}(\frac{H}{l \sin \phi})} d\alpha \quad D \\
&\quad \cdot \left\{ e^{-(\Sigma_i - \Sigma_{\pm})(l - l_i - l_{ij})/\cos \alpha} - e^{-(\Sigma_i - \Sigma_{\pm})l_i/\cos \alpha} \right\} ,
\end{aligned} \tag{4.55}$$

where

$$D = A \sin \alpha \, e^{-\frac{\widehat{\Sigma} l_{ij} - \Sigma_{\pm} l_{ij} + \Sigma_{\pm} l}{\cos \alpha}} .$$

When $l_i > l_{\pm}$ and $\Sigma_i \neq \Sigma_{\pm}$,

$$\begin{aligned}
P_{i\pm}^{oo} &= \frac{2 \Sigma_{\pm}}{\pi l_i} \cdot \frac{1}{\Sigma_i - \Sigma_{\pm}} \int_{l_{ij}}^{l_{ij}+l_{\pm}} dl \int_0^{\pi/2} d\phi \int_0^{\tan^{-1}(\frac{H}{l \sin \phi})} d\alpha \quad D \\
&\quad \cdot \left\{ 1 - e^{-(\Sigma_i - \Sigma_{\pm})(l - l_{ij})/\cos \alpha} \right\} \\
&+ \frac{2 \Sigma_{\pm}}{\pi l_i} \cdot \frac{1}{\Sigma_i - \Sigma_{\pm}} \int_{l_{ij}+l_{\pm}}^{l_{ij}+l_i} dl \int_0^{\pi/2} d\phi \int_0^{\tan^{-1}(\frac{H}{l \sin \phi})} d\alpha \quad D \\
&\quad \cdot \left\{ e^{-(\Sigma_i - \Sigma_{\pm})(l - l_{ij} - l_{\pm})/\cos \alpha} - e^{-(\Sigma_i - \Sigma_{\pm})(l - l_{ij})/\cos \alpha} \right\} \\
&+ \frac{2 \Sigma_{\pm}}{\pi l_i} \cdot \frac{1}{\Sigma_i - \Sigma_{\pm}} \int_{l_{ij}+l_i}^{l_{ij}+l_i+l_{\pm}} dl \int_0^{\pi/2} d\phi \int_0^{\tan^{-1}(\frac{H}{l \sin \phi})} d\alpha \quad D \\
&\quad \cdot \left\{ e^{-(\Sigma_i - \Sigma_{\pm})(l - l_{ij} - l_{\pm})/\cos \alpha} - e^{-(\Sigma_i - \Sigma_{\pm})l_i/\cos \alpha} \right\} .
\end{aligned} \tag{4.56}$$

When $l_j > l_i$ and $\Sigma_i \neq \Sigma_j$,

$$\begin{aligned}
 P_{ij}^{oo} = & \frac{2\Sigma_j}{\pi l_i} \cdot \frac{1}{\Sigma_i - \Sigma_j} \int_{l_{ij}}^{l_{ij}+l_i} d\ell \int_0^{\pi/2} d\phi \int_0^{\tan^{-1}(\frac{H}{\ell \sin \phi})} d\alpha \quad D \\
 & \cdot \left\{ 1 - e^{-(\Sigma_i - \Sigma_j)(\ell - l_{ij})/\cos \alpha} \right\} \\
 & + \frac{2\Sigma_j}{\pi l_i} \cdot \frac{1}{\Sigma_i - \Sigma_j} \int_{l_{ij}+l_i}^{l_{ij}+l_j} d\ell \int_0^{\pi/2} d\phi \int_0^{\tan^{-1}(\frac{H}{\ell \sin \phi})} d\alpha \quad D \\
 & \cdot \left\{ 1 - e^{-(\Sigma_i - \Sigma_j)\ell/\cos \alpha} \right\} \\
 & + \frac{2\Sigma_j}{\pi l_i} \cdot \frac{1}{\Sigma_i - \Sigma_j} \int_{l_{ij}+l_j}^{l_{ij}+l_i+l_j} d\ell \int_0^{\pi/2} d\phi \int_0^{\tan^{-1}(\frac{H}{\ell \sin \phi})} d\alpha \quad D \\
 & \cdot \left\{ e^{-(\Sigma_i - \Sigma_j)(\ell - l_{ij} - l_j)/\cos \alpha} - e^{-(\Sigma_i - \Sigma_j)\ell/\cos \alpha} \right\}.
 \end{aligned} \tag{4.57}$$

The probabilities P_{ij}^{oo} ($i > j$) are obtained from the reciprocity relation

$$\Sigma_i V_i P_{ij}^{oo} = \Sigma_j V_j P_{ji}^{oo}. \tag{4.58}$$

From Eqs. (4.51)~(4.58), all the probabilities necessary for the flux determination in slab systems of finite dimension or in infinite slab lattice cells are obtained.

Next, we calculate the collision probability in a cylindrical system. In a cylindrical lattice system, unlike in the slab system, the boundary condition on the cell surface must be considered.

We express the first-flight collision probability P_{ij}^{t00} in the lattice system in the following form:

$$P_{ij}^{t00} = P_{ij}^{oo} + P_{is} \frac{1}{1 - P_{ss}} P_{sj}, \tag{4.59}$$

where

P_{ij}^{oo} = the first-flight collision probability that a neutron born in the i -th region with weight $2\sin Bz'$ makes its first collision in the

j-th region in the original cell with weight $\sin Bz$.

P_{is} = the probability that a neutron born in the i-th region with weight $2 \sin Bz'$ escapes from the original cell without collision through the side surface S.

P_{ss} = the probability that a neutron entering a cell through the side surface S with an isotropic distribution and with an axial distribution $\sin Bz_s$ escapes from the cell through the side surface S again.

P_{sj} = the probability that a neutron entering a cell through the side surface S with isotropic and $\sin Bz_s$ distributions undergoes its first collision in the j-th region in the cell with weight $\sin Bz$.

They are expressed as follows:

$$P_{is} = \frac{2}{H V_i} \int_i d\vec{r}' \sin Bz' \int \frac{d\vec{\Omega}}{4\pi} e^{-\widehat{\Sigma} R_{is}}, \quad (4.60)$$

$$P_{ss} = \frac{B}{2\pi S} \int_0^H dz_s \sin Bz_s \int dS \int d\vec{\Omega}_s (\vec{n} \cdot \vec{\Omega}_s) e^{-\widehat{\Sigma} R_{ss}}, \quad (4.61)$$

$$P_{sj} = \frac{B z_+}{2\pi S} \int_0^H dz_s \sin Bz_s \int dS \int d\vec{\Omega}_s (\vec{n} \cdot \vec{\Omega}_s) \int_i dR e^{-\widehat{\Sigma} R_{js}} \sin Bz, \quad (4.62)$$

where $\widehat{\Sigma} R_{is}$ is the optical distance from the point \vec{r} in the i-th region to the cell boundary along the neutron direction $\vec{\Omega}$, and $\widehat{\Sigma} R_{ss}$ the optical distance from the side surface S to S along $\vec{\Omega}_s$, and \vec{n} the inward normal vector at S (S is the circumference of the side surface of each cell). The integration about R is performed over the line element in the j-th region along the direction $\vec{\Omega}_s$.

To begin with, we calculate the probability P_{ij}^{00} in a cell. Notations used in the calculation are described in Fig. 4.7. The technique adopted is similar to that by Kavenoky who evaluated the first-flight collision probability in an infinitely long cylindrical system. In his method, all the neutron paths are taken to be

parallel to the x-axis and the distance from the original point to the neutron path is denoted by y, and the positions of starting and end points along the neutron path are denoted by l' and l respectively.

P_{ij}^{00} ($j > i$) is expressed in the form (cf. Fig. 4.7)

$$P_{ij}^{00} = \frac{4\pi \Sigma_i}{H V_i} \int_{r_{i-1}}^{r_i} r' dr' \int_0^H dz' \int_0^\pi d\theta \frac{\sin \theta}{4\pi} \int_0^{2\pi} d\varphi \int dR e^{-\hat{z}R} \sin Bz' \cdot \sin Bz, \quad (4.63)$$

where r_i and r_{i-1} are the outer and inner radii of the i -th annular region, respectively. We introduce the relation

$$r' dr' d\varphi = -d\varphi dl', \quad (4.64)$$

in the above equation to obtain

$$P_{ij}^{00} = \frac{4\Sigma_i}{H V_i} \int_0^{r_i} d\varphi \int_{l_{i-1}}^{l_i} dl' \int_{l_{i-1}}^{l_i} dl \int_0^H dz' \int_{\tan^{-1}(\frac{l-l'}{H-z'})}^{\pi/2} d\theta e^{-\hat{z}R} \sin Bz' \cdot \sin Bz, \quad (4.65)$$

where l_i and l_{i-1} are the distances from the point O in Fig. 4.7 to the inner and outer surfaces of the i -th region along the neutron path respectively. If we change the order of integration about z and on the basis of the relation

$$\int_0^H dz' \int_{\tan^{-1}(\frac{s}{H-z'})}^{\pi/2} d\theta = \int_{\tan^{-1}(\frac{s}{H})}^{\pi/2} d\theta \int_0^{H-s/\tan \theta} dz', \quad (4.66)$$

where $s = l - l'$, and perform the integration about z' in the use of the relation

$$z = z' + s/\tan \theta, \quad (4.67)$$

we have

$$P_{ij}^{00} = \frac{4\Sigma_i}{V_i} \int_0^{r_i} d\varphi \int_{l_{i-1}}^{l_i} dl' \int_{l_{i-1}}^{l_i} dl \int_{\tan^{-1}(\frac{s}{H})}^{\pi/2} d\theta e^{-\hat{z}s/\sin \theta} A' + \frac{4\Sigma_i}{V_i} \int_0^{r_i} d\varphi \int_{-l_i}^{-l_{i-1}} dl' \int_{l_{i-1}}^{l_i} dl \int_{\tan^{-1}(\frac{s}{H})}^{\pi/2} d\theta e^{-\hat{z}s/\sin \theta} A', \quad (4.68)$$

where A' is given by

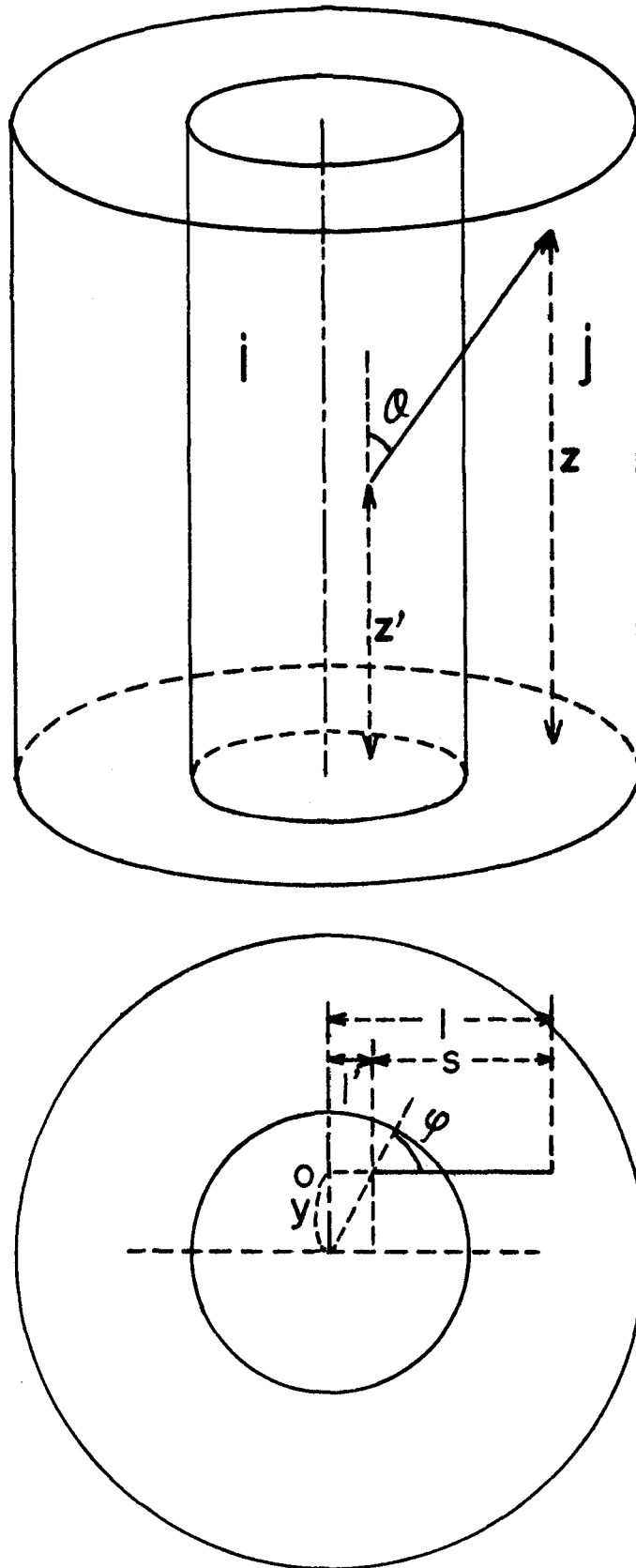


Fig. 4.7 Notations in a finite cylinder

$$A' = \cos(Bs/\tan\theta) \left\{ \frac{1}{2} \left(1 - \frac{s}{H \tan\theta} \right) + \frac{1}{4BH} \sin(2Bs/\tan\theta) \right\} \\ + \frac{1}{2BH} \sin^3(Bs/\tan\theta) . \quad (4.69)$$

In Eq. (4.68) the first term expresses the contribution of neutron current from the right side of the i -th annular region to the right side of the j -th annular region, and the second term expresses that from the left side of the i -th region to the right side of the j -th region.

In a similar manner we obtain the expression

$$P_{ii}^{oo} = \frac{4\Sigma_i}{V_i} \int_0^{r_i} d\gamma \int_{l_{i-1}}^{l_i} dl' \int_{l_{i-1}}^{l_i} dl \int_{\tan^{-1}(s/H)}^{\pi/2} d\theta e^{-\frac{\Sigma_i s}{\sin\theta}} A' \\ + \frac{4\Sigma_i}{V_i} \int_0^{r_i} d\gamma \int_{-l_i}^{-l_{i-1}} dl' \int_{l_{i-1}}^{l_i} dl \int_{\tan^{-1}(s/H)}^{\pi/2} d\theta e^{-\frac{\widetilde{\Sigma}s}{\sin\theta}} A' , \quad (4.70)$$

where $s = |l - l'|$. After the reduction of the double integral about l' and l into a single integral about s , we obtain

$$P_{ii}^{oo} = \frac{4\Sigma_i}{V_i} \int_0^{r_i} d\gamma \int_0^{l_i - l_{i-1}} ds \, 2(l_i - l_{i-1} - s) \int_{\tan^{-1}(s/H)}^{\pi/2} d\theta e^{-\Sigma_i s / \sin\theta} A' \\ + \frac{4\Sigma_i}{V_i} \int_0^{r_i} d\gamma \int_{2l_{i-1}}^{l_i + l_{i-1}} ds \, (s - 2l_{i-1}) \int_{\tan^{-1}(s/H)}^{\pi/2} d\theta e^{-(\Sigma_i s + 2\widetilde{\Sigma}l_{i-1} - 2\Sigma_i l_{i-1}) / \sin\theta} A' \\ + \frac{4\Sigma_i}{V_i} \int_0^{r_i} d\gamma \int_{l_i + l_{i-1}}^{2l_i} ds \, (2l_i - s) \int_{\tan^{-1}(s/H)}^{\pi/2} d\theta e^{-(\Sigma_i s + 2\widetilde{\Sigma}l_{i-1} - 2\Sigma_i l_{i-1}) / \sin\theta} A' . \quad (4.71)$$

Next, we calculate the probability P_{ij}^{oo} ($i < j$) from Eq. (4.68) in the use of the same technique as adopted in deriving Eq. (4.71) from Eq. (4.70). When $\Sigma_i = \Sigma_j$,

$$P_{ij}^{oo} = \frac{4\Sigma_i}{V_i} \int_0^{r_i} d\gamma \left[H(l_0 - l'_0) \left\{ \int_{l_{ij}}^{l_{ij} + l'_0} ds \, (s - l_{ij}) + \int_{l_{ij} + l'_0}^{l_{ij} + l_0} ds \, l'_0 \right. \right. \\ \left. \left. + \int_{l_{ij} + l_0}^{l_{ij} + l'_0 + l_0} ds \, (l_0 + l'_0 + l_{ij} - s) \right\} \right]$$

$$\begin{aligned}
& + H(l'_0 - l_0) \left\{ \int_{l_{ij}}^{l_{ij}+l_0} d\lambda (\lambda - l_{ij}) + \int_{l_{ij}+l_0}^{l_{ij}+l'_0} d\lambda l_0 \right. \\
& \quad \left. + \int_{l_{ij}+l'_0}^{l_{ij}+l_0+l'_0} d\lambda (l_0 + l'_0 + l_{ij} - \lambda) \right\} \\
& \cdot \int_{\tan^{-1}(\lambda/H)}^{\pi/2} d\theta e^{-\frac{\Sigma l_{ij} - \Sigma_j l_{ij} + \Sigma_j \lambda}{\sin \theta}} A', \tag{4.72}
\end{aligned}$$

where $l_0 = l_j - l_{j-1}$ and $l'_0 = l_i - l_{i-1}$, and $H(x)$ is given by

$$H(x) = \begin{cases} 1 & \text{for } x > 0 \\ 1/2 & \text{for } x = 0 \\ 0 & \text{for } x < 0 \end{cases} \tag{4.73}$$

In evaluating P_{ij}^{00} , the evaluated results of Eq. (4.72) for two possibilities of $\hat{\Sigma} l_{ij}$ and l_{ij} are added; the one corresponding to the neutron current from the right side of the i -th region to the right side of the j -th region, and the other corresponding to the neutron current from the left side of the i -th region to the right side of the j -th region.

When $\Sigma_i \neq \Sigma_j$,

$$\begin{aligned}
P_{ij}^{00} = & \frac{4 \Sigma_j}{V_i (\Sigma_i - \Sigma_j)} \int_0^{r_i} d\gamma \left[H(l_0 - l'_0) \left\{ \int_{l_{ij}}^{l_{ij}+l'_0} d\lambda \int_{\tan^{-1}(\lambda/H)}^{\pi/2} d\theta D' \right. \right. \\
& \cdot \left\{ 1 - e^{-(\Sigma_i - \Sigma_j)(\lambda - l_{ij})/\sin \theta} \right\} + \int_{l_{ij}+l'_0}^{l_{ij}+l_0} d\lambda \int_{\tan^{-1}(\lambda/H)}^{\pi/2} d\theta D' \left\{ 1 - e^{-(\Sigma_i - \Sigma_j)l'_0/\sin \theta} \right\} \\
& + \int_{l_{ij}+l_0}^{l_{ij}+l_0+l'_0} d\lambda \int_{\tan^{-1}(\lambda/H)}^{\pi/2} d\theta D' \left\{ e^{-(\Sigma_i - \Sigma_j)(\lambda - l_{ij} - l_0)/\sin \theta} - e^{-(\Sigma_i - \Sigma_j)l'_0/\sin \theta} \right\} \\
& + H(l'_0 - l_0) \left\{ \int_{l_{ij}}^{l_{ij}+l_0} d\lambda \int_{\tan^{-1}(\lambda/H)}^{\pi/2} d\theta D' \left\{ 1 - e^{-(\Sigma_i - \Sigma_j)(\lambda - l_{ij})/\sin \theta} \right\} \right. \\
& \left. + \int_{l_{ij}+l_0}^{l_{ij}+l'_0} d\lambda \int_{\tan^{-1}(\lambda/H)}^{\pi/2} d\theta D' \left\{ e^{-(\Sigma_i - \Sigma_j)(\lambda - l_{ij} - l_0)/\sin \theta} - e^{-(\Sigma_i - \Sigma_j)(\lambda - l_{ij})/\sin \theta} \right\} \right]
\end{aligned}$$

$$+ \int_{l_{ij}+l_0}^{l_{ij}+l_0+l_0'} d\Delta \int_{\tan^{-1}(\Delta/H)}^{\pi/2} d\theta D' \left\{ e^{-(z_i-z_j)(\Delta-l_{ij}-l_0)/\sin\theta} - e^{-(z_i-z_j)l_0'/\sin\theta} \right\}, \quad (4.74)$$

where $D' = A' \sin\theta e^{-\frac{\hat{x}l_{ij}-z_jl_0+z_j\Delta}{\sin\theta}}$.

The evaluation of the above equation must be performed in the same way as in evaluating Eq. (4.72). From Eqs. (4.71) ~ (4.74), and the reciprocity relation (4.58), all the probabilities in the cylindrical cell can be obtained. Next, in order to extend the probability to lattice systems, we calculate the probabilities P_{is} , P_{sj} and P_{ss} . The probability P_{is} reduces to

$$P_{is} = \frac{4}{\pi V_i} \int_0^{r_i} d\gamma \int_{\Delta_1}^{\Delta_2} d\Delta \int_{\tan^{-1}(\Delta/H)}^{\pi/2} d\theta \sin\theta e^{-\hat{x}\Delta/\sin\theta} \{1 + \cos(B\Delta/\tan\theta)\}, \quad (4.75)$$

where s is the distance from the cell surface to the starting point in the i -th region (see Fig. 4.8). In terms of the relation

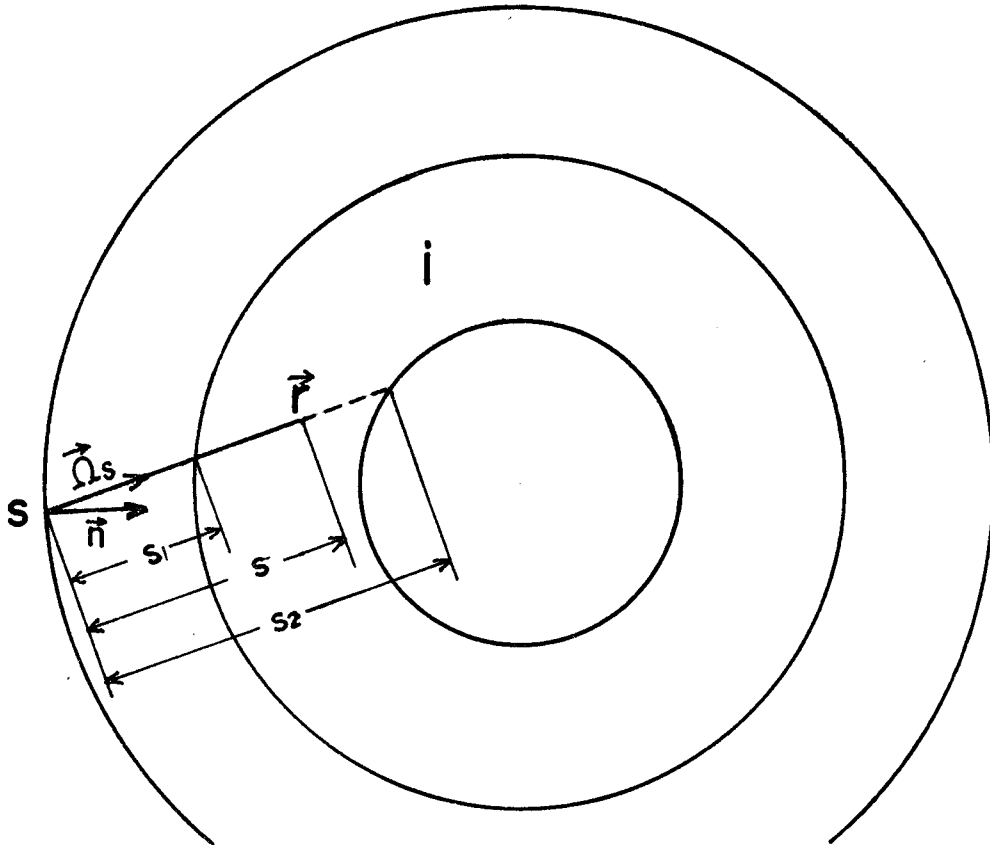


Fig. 4.8 Neutron injection from the cell boundary

$$dz dS d\vec{\Omega}_s (\vec{n} \cdot \vec{\Omega}_s) dR = d\vec{\Omega} d\vec{r}, \quad (4.76)$$

the quantity P_{sj} is given by

$$P_{sj} = \frac{4\pi \Sigma_j}{S} \int_0^{r_i} dz \int_{A_1}^{A_2} dS \int_{\tan^{-1}(A/H)}^{\pi/2} d\theta \sin \theta e^{-\hat{z}\Delta/\sin \theta} A'. \quad (4.77)$$

P_{ss} is transformed into the form

$$\begin{aligned} P_{ss} &= 1 - \frac{B}{2\pi S} \int_0^H dz_s \sin B z_s \int dS \int d\vec{\Omega}_s (\vec{n} \cdot \vec{\Omega}_s) \int_0^{R_s} dR \Sigma e^{-\hat{z}R} \\ &= 1 - \sum_i \frac{g \Sigma_i}{S} \int_0^{r_i} dz \int_{A_1}^{A_2} dS \int_{\tan^{-1}(A/H)}^{\pi/2} d\theta \sin \theta e^{-\hat{z}\Delta/\sin \theta} \cos(B\Delta/\tan \theta), \end{aligned} \quad (4.78)$$

where R_s is the chord length in the cell along the neutron direction

$\vec{\Omega}_s$. In terms of Eqs. (4.75) ~ (4.78), the first-flight collision probability in Eq. (4.59) in the case of cylindrical lattice can be obtained.

§4.4 Neutron Spectra in a Resonance⁽²⁵⁾

In this section we derive an improved expression of the correction of the moderator flux for an isolated wide resonance with use made of the Greuling-Goertzel approximation⁽¹⁷⁾. An analytic expression of the resonance integral is also obtained, which takes into account the flux decrement in the moderator. We treat a two-region cell, of which the moderator is not very large compared with the neutron mean free path in the region. In such a system we can use the flat flux approximation in both fuel and moderator regions. For a cell with large moderator, we can use the concept in §2.4, or the effective volume of the moderator, as shown by Iijima⁽²⁶⁾.

The neutron balance equations are written in terms of the first-flight collision probabilities P_{ij} in the forms

$$\phi_f(u) \Sigma_f(u) V_f = P_{ff}(u) K_f \phi_f \Sigma_{fs} V_f + P_{mf}(u) K_m \phi_m \Sigma_{ms} V_m + S(u), \quad (4.79)$$

$$\phi_m(u) \Sigma_m(u) V_m = P_{fm}(u) K_f \phi_f \Sigma_{fs} V_f + P_{mm}(u) K_m \phi_m \Sigma_{ms} V_m. \quad (4.80)$$

The leading suffixes f and m in Σ stand for fuel and moderator, and the tail suffixes s and a stand for scattering and absorption, respectively; V_f and V_m are the volumes of the fuel rod and the moderator in a cell; K_i is an integral operator of the slowing down in the i-th region, and is given by

$$K_i \phi = \int_{u-g_i}^u du' \frac{1}{1-\alpha_i} e^{-(u-u')} \phi(u'). \quad (4.81)$$

We use the Greuling-Goertzel approximation for the kernel of the moderator, and the wide resonance approximation for the kernel of the fuel:

$$K_f \phi = \phi, \quad (4.82a)$$

$$K_m \phi = \int_{-\infty}^u du' \left\{ \frac{\Sigma_m}{\Sigma_m^2} e^{-\frac{u-u'}{\sigma_m}} + \left(1 - \frac{\Sigma_m}{\Sigma_m^2}\right) S(u'-u) \right\} \phi(u'). \quad (4.82b)$$

Adding Eqs. (4.79) and (4.80), we have

$$\begin{aligned} & \phi_f(u) \Sigma_f V_f + \phi_m(u) \Sigma_m V_m \\ &= \mathcal{K}_f \phi_f \Sigma_{fs} V_f + \mathcal{K}_m \phi_m \Sigma_m V_m + \delta(u), \end{aligned} \quad (4.83)$$

where we assume that absorption in the moderator is negligible, and that the scattering cross section in the moderator is constant.

The lattice system considered is assumed to be so large that the leakage of neutrons from the system can be neglected.

Applying Eq. (4.82) to Eq. (4.83), we obtain

$$\begin{aligned} \phi_m(u) \Sigma_m V_m &= \frac{1}{\xi_m} \left\{ 1 - \Sigma_{fa}(u) \phi_f(u) V_f \right\} \\ &\quad - \int_0^u du' \Sigma_{fa}(u') \phi_f(u') V_f. \end{aligned} \quad (4.84)$$

Under the assumption of constant flux in the moderator, $\phi_f(u)$ is expressed by the first order approximation of Eq. (4.79):

$$\phi_f(u) = \frac{1}{\xi_m V_f} \cdot \frac{P_{mf}(u)}{\Sigma_f(u) - P_{ff}(u) \Sigma_{fs}(u)}. \quad (4.85)$$

Thus Eq. (4.84) becomes

$$\begin{aligned} \phi_m(u) \Sigma_m V_m &= \frac{1}{\xi_m} \left[1 - \frac{\Sigma_{fa}(u) P_{mf}(u)}{\xi_m \{ \Sigma_{fa}(u) + \Sigma_{fs}(u) P_{fm}(u) \}} \right. \\ &\quad \left. - \int_0^u du' \frac{P_{mf}(u') \Sigma_{fa}(u')}{\xi_m \{ \Sigma_{fa}(u') + \Sigma_{fs}(u') P_{fm}(u') \}} \right]. \end{aligned} \quad (4.86)$$

A rational approximation for collision probabilities is introduced, as in the paper by Goldstein *et al.*⁽¹⁰⁾:

$$P_{ff}(u) = \frac{\Sigma_f(u)}{S + \Sigma_f(u)}, \quad P_{fm}(u) = \frac{S}{S + \Sigma_f(u)}. \quad (4.87)$$

Neutron cross sections are also expressed by the Breit-Wigner formula⁽²⁷⁾

which neglects the interference between potential and resonance scatterings:

$$\sigma_a = \frac{\Gamma_r}{\Gamma} \cdot \frac{\sigma_0}{1+x^2} , \quad (4.88a)$$

$$\sigma_s = \frac{\Gamma_n}{\Gamma} \cdot \frac{\sigma_0}{1+x^2} + \sigma_{p0} , \quad (4.88b)$$

where $x = \frac{2}{\Gamma} (E - E_r) .$

Using the relations (4.87) and (4.88) and the reciprocity relation for the collision probabilities, Eq. (4.86) may be reduced to

$$\begin{aligned} \phi_m(u) \sum_m V_m = & \frac{1}{\sum_m} \left\{ 1 - \frac{\sigma_m \Gamma_r \sigma_0}{\sum_m \Gamma \sigma_m} \cdot \frac{1}{x^2 + \beta_0^2} \right. \\ & \left. - \frac{I_0}{\sum_m \sigma_m} \left(\frac{1}{2} - \frac{1}{\pi} \tan^{-1} \frac{x}{\beta_0} \right) \right\} , \end{aligned} \quad (4.89)$$

where $\sigma_m = \frac{\sum_m V_m}{N_f V_f}$, $\beta_0^2 = 1 + \frac{\sigma_0 \Gamma_r}{S \Gamma}$, $I_0 = I^{(0)}/\beta_0$, $I^{(0)} = \frac{\pi \sigma_0 \Gamma_r}{2 E_r}$,

and I_0 is the resonance integral in the W.R. limit; N_f is the number density of the fuel element. From Eq. (4.79), we obtain

$$\phi_f(x) = \frac{S}{S + \sigma_{fa}(x)} \kappa_m \phi_m . \quad (4.90)$$

Inserting Eq. (4.89) into Eq. (4.90) and using the approximation

$$\kappa_m \phi = \frac{1}{\delta_m} \int_x^{x+\delta_m} \phi(x') dx' , \quad (\delta_m = \frac{2 E_r}{\Gamma} (1 - \alpha_m)) \quad (4.91)$$

which was used by Goldstein *et al.*, we obtain the second order approximation of the flux in the fuel:

$$\phi_f(x) = \frac{1}{\sum_m \sum_m V_m} \cdot \frac{1+x^2}{\beta_0^2+x^2} \{ 1 - f(x) \} , \quad (4.92)$$

where

$$\begin{aligned} f(x) = & \frac{I_0}{\sum_m \sigma_m} \left[\frac{1}{2} - \frac{1}{\pi} \left\{ \frac{x+\delta_m}{\delta_m} \tan^{-1} \frac{x+\delta_m}{\beta_0} \right. \right. \\ & \left. \left. - \frac{x}{\delta_m} \tan^{-1} \frac{x}{\beta_0} - \frac{\beta_0}{2 \delta_m} \ln \frac{\beta_0^2 + (x+\delta_m)^2}{\beta_0^2 + x^2} \right\} \right] \end{aligned}$$

$$+ \frac{\delta_m \sigma_o}{\Sigma_m \sigma_m} \cdot \frac{P_r}{P} \cdot \frac{1}{\beta_o \delta_m} \left(\tan^{-1} \frac{x + \delta_m}{\beta_o} - \tan^{-1} \frac{x}{\beta_o} \right) . \quad (4.93)$$

Eqs. (4.92) and (4.89), which express the fluxes in the fuel and the moderator in second order approximation, tend to the exact limit when $x \rightarrow -\infty$. In other words, the asymptotic distribution far below the resonance is equal to the resonance escape probability. Using these expressions for the fluxes, we obtain the resonance integral.

This is given from Eq. (4.90) by

$$I_{G0} = \frac{P_r \sigma_o}{2 E_r} \int_{-\infty}^{\infty} dx \frac{1}{\beta_o^2 + x^2} \mathcal{K}_m \phi_m . \quad (4.94)$$

From Eq. (4.83), $\mathcal{K}_m \phi_m$ is also given by

$$\mathcal{K}_m \phi_m = \phi_m + \frac{\Sigma_{fa} V_f}{\Sigma_m V_m} \phi_f . \quad (4.95)$$

Substituting Eq. (4.92) (for $f(x) = 0$) and Eq. (4.89) into the right-hand side of the above equation, we get

$$\begin{aligned} \mathcal{K}_m \phi_m = & \frac{1}{\Sigma_m \Sigma_m V_m} \left\{ 1 - \frac{I_o}{\Sigma_m \sigma_m} \left(\frac{1}{2} - \frac{1}{\pi} \tan^{-1} \frac{x}{\beta_o} \right) \right. \\ & \left. + \frac{P_r \sigma_o}{P \sigma_m} \cdot \frac{1}{\beta_o^2 + x^2} \left(1 - \frac{\delta_m}{\Sigma_m} \right) \right\} . \end{aligned} \quad (4.96)$$

Using this equation, Eq. (4.94) reduces to

$$I_{G0} = I_o \left\{ 1 - \frac{I_o}{2 \Sigma_m \sigma_m} + \frac{P_r \sigma_o}{P \sigma_m} \cdot \frac{1}{2 \beta_o^2} \left(1 - \frac{\delta_m}{\Sigma_m} \right) \right\} . \quad (4.97)$$

The second and third terms of this equation show the deviation of the resonance integral from the W.R. approximation. The correction for $f(x) \neq 0$ to this expression is very small. Although we assumed the flat flux in the whole cell, the effect of flux change in each region is easily taken into account by introducing the probabilities Q and R defined in chapter 3.

§4.5 Numerical Results and Conclusions

First we calculate the first-flight collision probabilities in cluster systems by the method in §4.2. It requires a large amount of computer time to evaluate collision probabilities in a complex system with the true geometry. Using the present method, the probabilities in a cluster may be calculated in a short time. For example, making use of a NEAC-2200 (model 500), it takes 15 sec by the present method, 10 sec by Bonalumi's, and 3 min by the exact method for an annular system containing 4 different media. The present method coincides precisely with Bonalumi's for an annular system containing only two media, and is superior to his result for a system

Table 4.1 Collision probabilities for a cell containing four annular regions

$r_1=0.5$ cm $r_2=0.61$ cm
 $r_3=0.8$ cm $r_4=4.55$ cm
 $\Sigma_1=2.0$ cm⁻¹ $\Sigma_2=0.5$ cm⁻¹
 $\Sigma_3=1.5$ cm⁻¹ $\Sigma_4=1.5$ cm⁻¹

Probabilities	Exact	Our method	Bonalumi
$P_{1,1}$	0.5951	0.5938	0.5938
$P_{1,2}$	0.0336	0.0336	0.0336
$P_{1,3}$	0.1201	0.1173	0.1173
$P_{1,4}$	0.2535	0.2553	0.2553
$P_{2,1}$	0.2749	0.2748	0.2748
$P_{2,2}$	0.0896	0.0729	0.0729
$P_{2,3}$	0.2536	0.2567	0.2610
$P_{2,4}$	0.3863	0.3956	0.3913
$P_{3,1}$	0.1495	0.1460	0.1459
$P_{3,2}$	0.0385	0.0390	0.0396
$P_{3,3}$	0.3455	0.3369	0.3350
$P_{3,4}$	0.4781	0.4780	0.4794
$P_{4,1}$	0.0042	0.0042	0.0042
$P_{4,2}$	0.00079	0.00080	0.00079
$P_{4,3}$	0.00638	0.00638	0.00640
$P_{4,4}$	0.9886	0.9886	0.9886

Table 4.2 Collision probabilities between two adjacent rods

a : Radius of fuel rod
 b : Equivalent radius of subcell
 Σ_f : Total cross section of fuel rod
 Σ_c : Total cross section of coolant

a (cm)	b (cm)	Σ_f (cm ⁻¹)	Σ_c (cm ⁻¹)	Exact	Eq. (4.15)
0.2	0.61	5.0	2.0	0.0028	0.0026
0.2	0.61	2.0	1.0	0.0072	0.0075
0.5	0.61	5.0	2.0	0.0157	0.0154
0.5	0.61	2.0	1.0	0.0378	0.0383
0.5	0.61	1.0	1.0	0.0402	0.0410
0.5	0.61	0.5	1.0	0.0320	0.0328
0.5	0.61	1.0	0.8	0.0429	0.0440
0.5	0.61	1.0	0.6	0.0459	0.0471
0.5	0.61	1.0	0.4	0.0492	0.0505
0.5	0.61	1.0	0.2	0.0529	0.0542
0.5	0.61	0.5	0.5	0.0382	0.0389
0.5	0.61	0.1	0.5	0.0122	0.0121
0.5	0.61	0.05	0.5	0.0065	0.0064
0.5	0.61	0.02	0.5	0.0027	0.0026
0.5	0.61	1.0	0.5	0.0475	0.0488
0.5	0.61	2.0	0.5	0.0446	0.0455
0.5	0.61	3.0	0.5	0.0369	0.0375
0.5	0.61	5.0	0.5	0.0254	0.0256
1.0	1.5	1.0	1.0	0.0113	0.0105
1.0	2.0	1.0	1.0	0.0027	0.0023
1.0	3.0	1.0	1.0	0.0002	0.0001

containing more media, as it may be seen from Table 4.1. The probability for a neutron born in a rod to undergo its first collision in an adjacent fuel rod is shown in Table 4.2 for various geometries and cross sections. It is apparent that Eq. (4.15) is a good approximation.

In the case of a hexagonal cluster containing 7 fuel rods without cladding (see Fig. 4.9), the heterogeneity around the outer rods may be estimated in more detail since we did not divide the system into subcells. The results evaluated by the present method are in good agreement with those of exact calculation and PIJE code⁽²⁸⁾ (see Table 4.3) except the probability that a neutron born in the outer fuel rods undergoes its

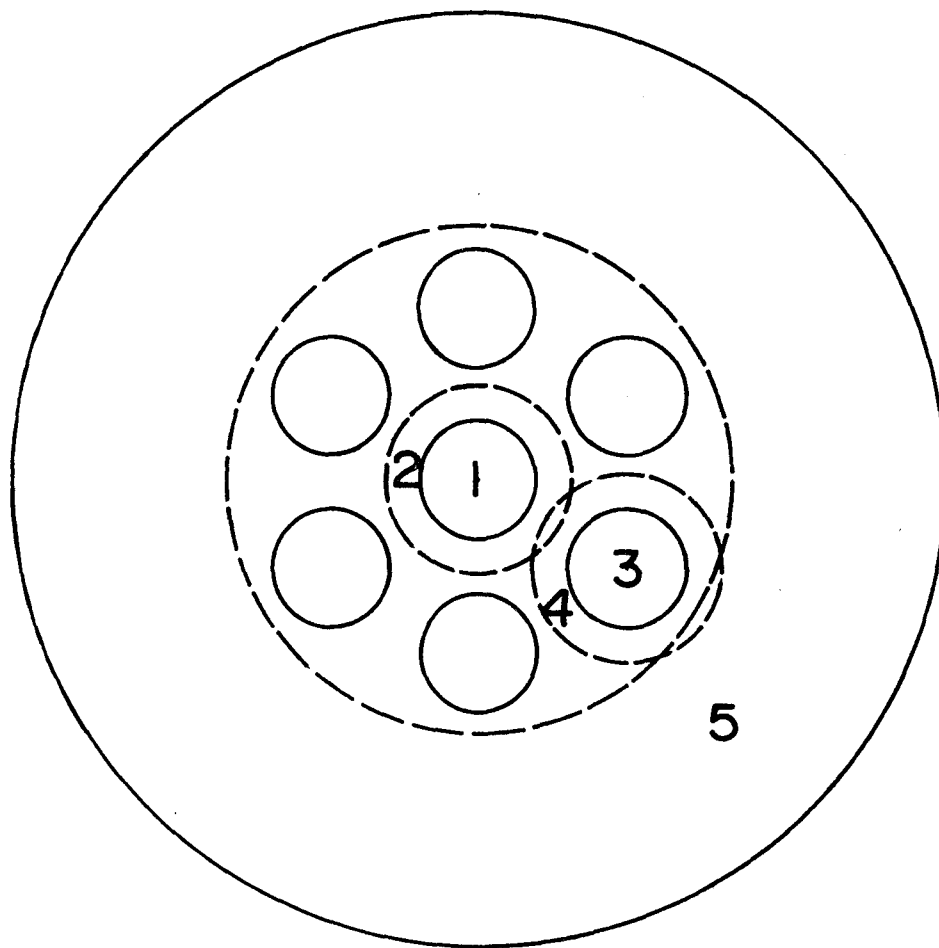


Fig. 4.9 Cluster geometry containing 7 fuel rods

Table 4.3 Collision probabilities for hexagonal cluster containing 7 fuel rods (c.f. Fig. 4.9)

Total cross section of fuel: 2.63 cm^{-1}
 Total cross section of coolant: 1.52 cm^{-1}
 Scattering cross section of fuel: 0.3637 cm^{-1}
 Scattering cross section of coolant: 1.48 cm^{-1}

Probabilities	Our method	Exact	PIJE
P_{11}	0.7104	0.7104	0.7106
P_{12}	0.2627	0.2681	0.2682
P_{13}	0.00069	0.00066	0.00043
P_{14}	0.0204	0.0230	0.0207
P_{15}	0.0057	†	0.00005
P_{21}	0.0450	0.0458	0.0459
P_{22}	0.7835	0.7809	0.7805
P_{23}	0.0034	0.0039	0.0036
P_{24}	0.1659	0.1666	0.1696
P_{25}	0.0021		0.00039
P_{31}	0.00011	0.00011	0.00007
P_{32}	0.0033	0.0038	0.0035
P_{33}	0.7180	0.7108	0.7108
P_{34}	0.2560	0.2759	0.2762
P_{35}	0.0224		0.0095
P_{41}	††	0.00065	0.00059
P_{42}		0.0277	0.0283
P_{43}		0.0472	0.0473
P_{44}		0.8377	0.8460
P_{45}			0.0778
P_{51}	0.0001		0.0000
P_{52}	0.0002		0.00004
P_{53}	0.0023		0.0010
P_{54}	0.0455		0.0472
P_{55}	0.9517		0.9518

† The moderator region 5 is not taken into account in the exact method.

†† The coolant region 4 is divided in more detail in our method.

Table 4.4 Collision probabilities for a cluster containing 28 fuel rods (c.f. Fig. 4.11)

Total cross section of fuel: 0.3604 cm^{-1}
 Total cross section of cladding: 0.2067 cm^{-1}
 Total cross section of coolant and moderator: 0.4316 cm^{-1}
 Scattering cross section of fuel: 0.2 cm^{-1}
 Scattering cross section of cladding: 0.15 cm^{-1}
 Scattering cross section of coolant and moderator: 0.4 cm^{-1}

Probabilities	Our method	CLUP	PIJE
$P_{1,1}$	0.2430	0.2349	0.2501
$P_{1,2}$	0.0885	0.0936	0.0905
$P_{1,3}$	0.0553	0.0601	0.0532
$P_{1,4}$	0.0470	0.0425	0.0437
$P_{1,5}$	0.0256	0.0273	0.0238
$P_{1,6}$	0.0160	0.0172	0.0136
$P_{1,7}$	0.1775	0.1488	0.1719
$P_{1,8}$	0.1240	0.1409	0.1301
$P_{1,9}$	0.0775	0.0971	0.0809
$P_{1,10}$	0.0139	0.0143	0.0133
$P_{1,11}$	0.0249	0.0251	0.0234
$P_{1,12}$	0.0244	0.0238	0.0224
$P_{1,13}$	0.0249	0.0234	0.0222
$P_{1,14}$	0.0267	0.0241	0.0231
$P_{1,15}$	0.0311	0.0266	0.0259
$P_{7,7}$	0.2619	0.2737	0.2332
$P_{7,8}$	0.1323	0.2044	0.1420
$P_{7,9}$	0.0820	0.1211	0.0833
$P_{7,1}$	0.1341	0.1138	0.1314
$P_{7,4}$	0.0453	0.0359	0.0443

first collision in the coolant around the fuel rods. The exact calculation is performed by dividing the system into subcells and obtaining collision probabilities between subcells numerically.

In Fig. 4.10 is shown the one-group flux distribution with constant sources within coolant and moderator. The hexagonal cluster adopted consists of 7 fuel rods with radius 0.5 cm, 7 coolant regions with equivalent outer radius of 2 cm, and an outermost moderator region of

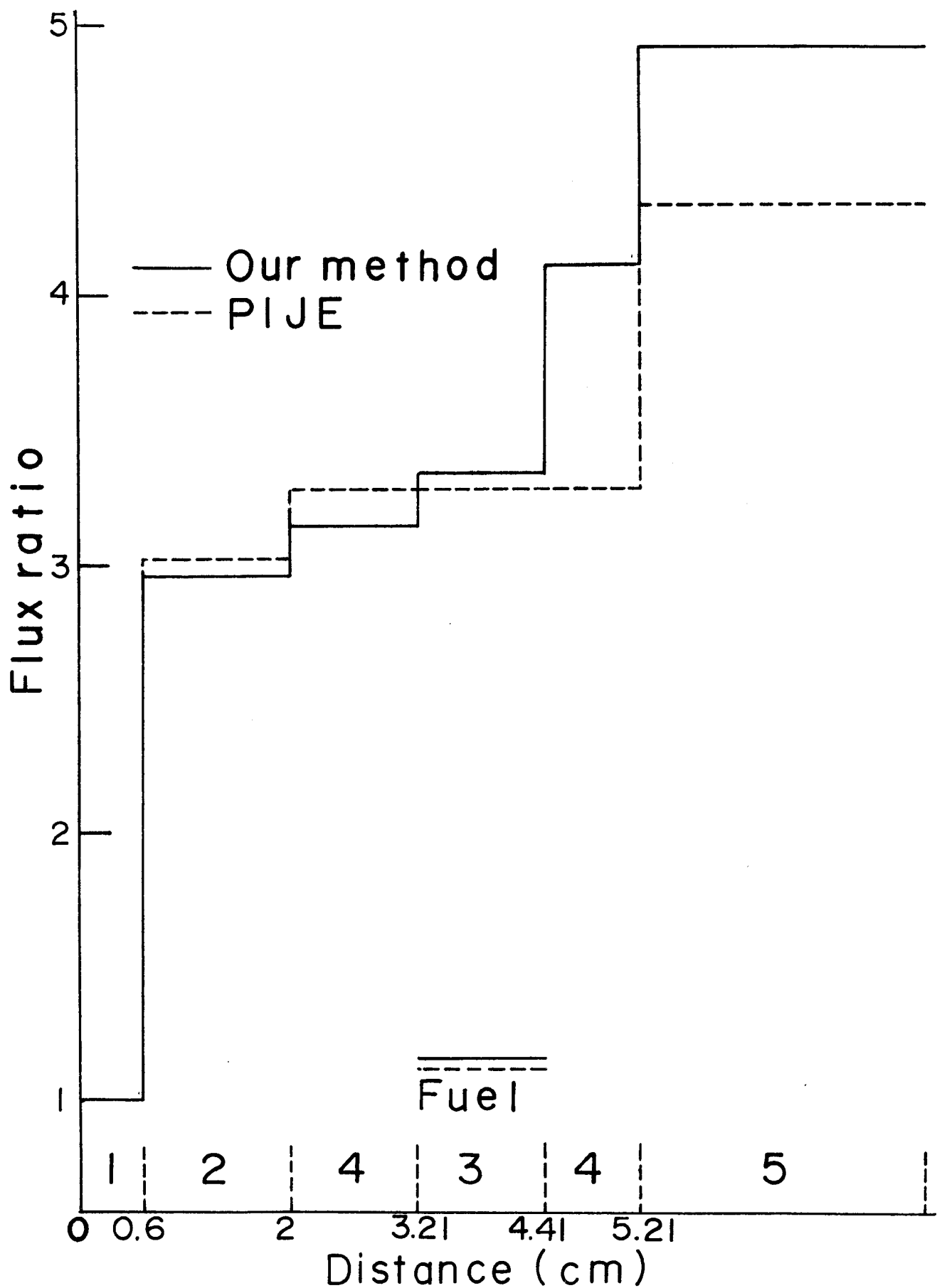


Fig. 4.10 Flux distribution for cluster containing 7 fuel rods

2.71 cm thick. It may be seen that there is a sudden change of flux through the coolant region 4 in the outer ring. Inner regions, from region 2 to region 4, however, the change is quite gradual. This is due to the fact that neutrons starting from the moderator are shielded by the outer fuel region 3.

Next we treat a square cluster containing 28 fuel rods of 0.5 cm radius, 28 sheathes of 0.61 cm external radius, 28 coolant media of 0.8 cm equivalent outer radius, and a pressure tube of 0.3 cm thickness (see Fig. 4.11). The collision probabilities evaluated from the present method that a neutron born in the fuel rods in the central ring undergoes its first collision in the external moderator region are in agreement with those by the CLUP code⁽²⁹⁾ as we will show in Table 4.4.

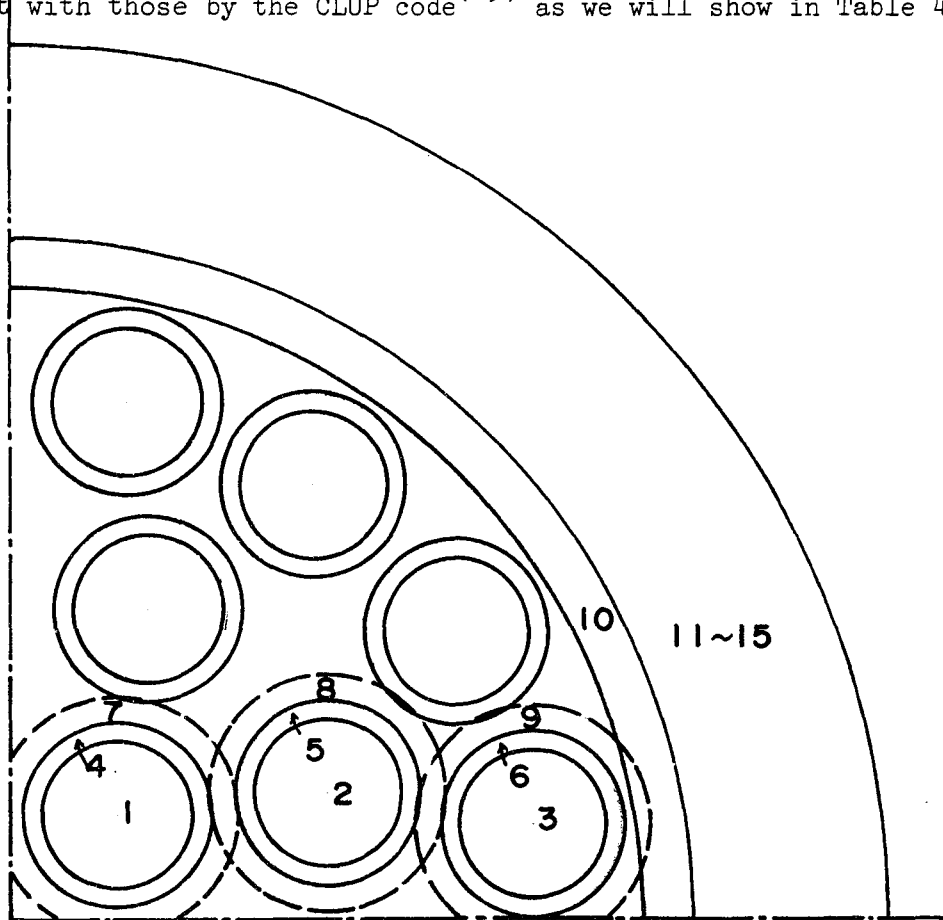


Fig. 4.11 Cluster geometry containing 28 fuel rods

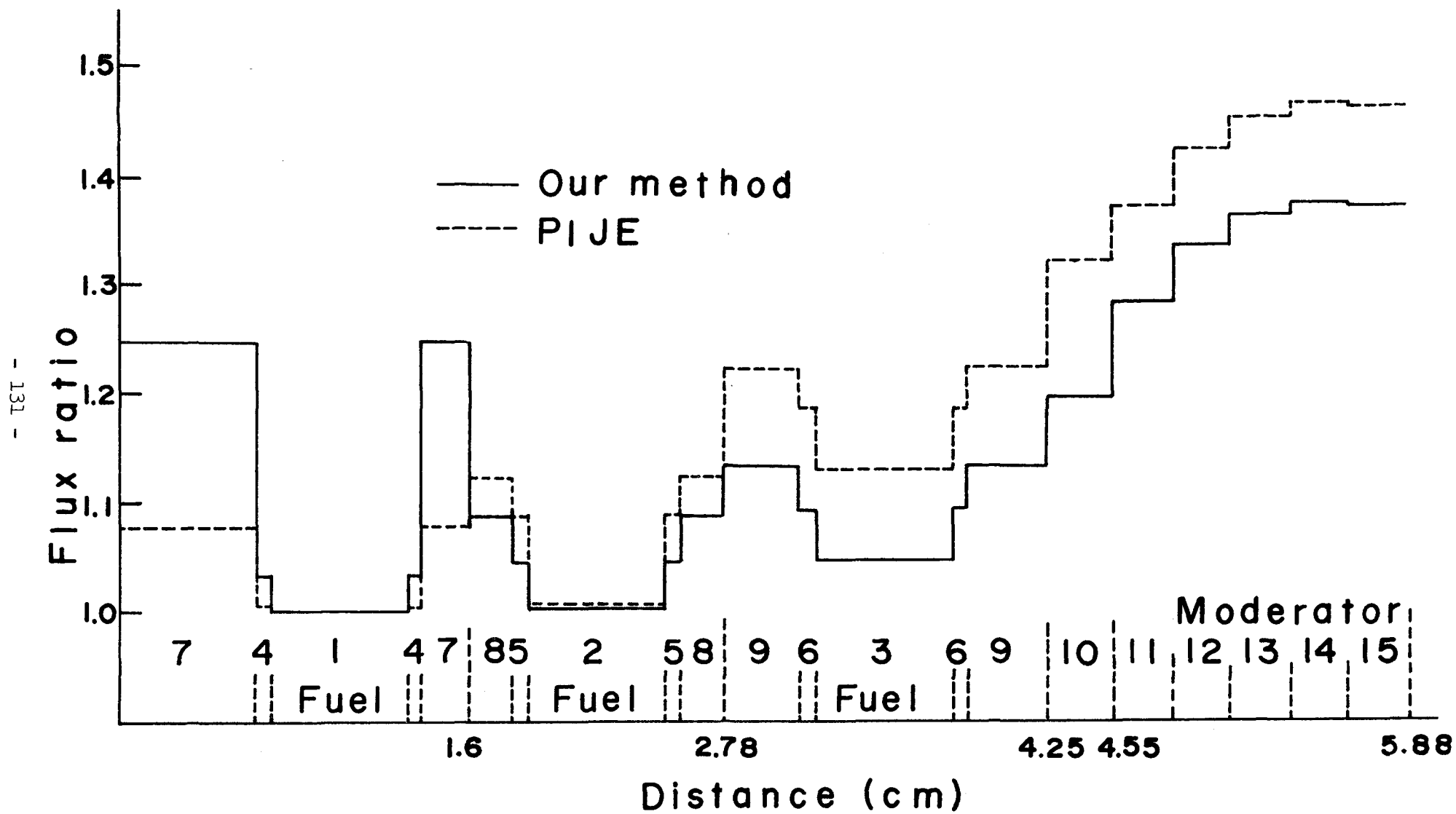


Fig. 4.12 Flux distribution for cluster containing 28 fuel rods

The probabilities for a neutron born in the central fuel rods to have its first collision in the coolant media are in agreement with those by the PIJE code. The flux distribution is shown in Fig. 4.12. The curves from the two methods show the same tendency in the moderator, but different tendency in the inner region of the pressure tube.

In what follows, we evaluate the effect of finiteness of the systems based on the method in §4.3. Since the finiteness of a cell system in the axial direction is assumed to have the same effect as in a bare system, we evaluate the flux distributions in finite systems both in the axial and radial directions.

At first a slab system has been treated. The slab is divided into 4 regions, in all of which the total and scattering cross sections and the thickness are 1.0 cm⁻¹, 1.0 cm⁻¹ and 1.0 cm, respectively. These regions are numbered by 1~4 from the right side to the left. In calculating the flux distribution, the uniform source is assumed over the system. The flux distribution by the present method is presented in Table 4.5 for various axial lengths, together with that by the buckling approximation. As is seen from the table, the difference between the present method and the buckling approximation becomes apparent for a system with smaller axial length than 10 cm.

According to the discussion in Ref. (8), the assumption

Table 4.5 Flux distribution in a finite slab for various axial lengths

Axial length (cm)	Flux distribution			
	Present method		Buckling approximation	
	ϕ_1	ϕ_2	ϕ_1	ϕ_2
5	3.8961	5.3680	3.2637	4.4532
10	5.3992	7.5484	5.2004	7.2571
20	6.1598	8.6503	6.1221	8.5942
40	6.4124	9.0160	6.4071	9.0078
100	6.4911	9.1299	6.4918	9.1308
500	6.5063	9.1518	6.5075	9.1536

of the flux form $\sin Bz$ is justified in the case of 10 cm axial length. Therefore the present method is considered to be still accurate for such a case. For a system with axial length larger than 20 cm, the difference of the flux distributions between both methods is within 1 %. For a fast reactor such as JEZEABEL, which is only of the order of 2 mean free path in diameter, the buckling approximation cannot be adopted⁽³⁰⁾.

In Table 4.6 are shown the values of the first-flight collision probabilities for the systems corresponding to the cases in Table 4.5. A large difference of the values of P_{11} between both methods is seen in the case of small axial length.

Next, a cylindrical system has been treated. The cylinder is divided into 3 regions. Then each region is numbered from the center to the outermost side by 1~3. The outer radii of the regions 1, 2 and 3 are taken to be 1.0, 1.5 and 2.0 cm respectively. The total and scattering cross sections are all 1.0 cm^{-1} . As in the slab system, a large difference between the flux distributions based on both methods is seen from Table 4.7 in the case of small axial length.

Lastly, as an example of the wide resonance problem, we calculate the resonance integral and neutron spectra for a 6.68 eV ^{238}U resonance. The system considered is a square lattice, which is composed of a

Table 4.6 First-flight collision probabilities
in a finite slab

Axial length (cm)	First-flight collision probabilities							
	Present method				Buckling approximation			
	P_{11}	P_{12}	P_{13}	P_{14}	P_{11}	P_{12}	P_{13}	P_{14}
5	0.5804	0.1384	0.0230	0.0054	0.6394	0.1493	0.0239	0.0053
10	0.6007	0.1499	0.0270	0.0067	0.6175	0.1539	0.0277	0.0069
20	0.6072	0.1539	0.0286	0.0073	0.6117	0.1550	0.0288	0.0074
40	0.6090	0.1550	0.0290	0.0075	0.6102	0.1553	0.0291	0.0075
100	0.6096	0.1553	0.0292	0.0075	0.6098	0.1554	0.0292	0.0075
500	0.6097	0.1553	0.0292	0.0075	0.6097	0.1554	0.0292	0.0075

Table 4.7 Flux distribution in a finite cylinder
for various axial lengths

Axial length (cm)	Flux distribution					
	Present method			Buckling approximation		
	ϕ_1	ϕ_2	ϕ_3	ϕ_1	ϕ_2	ϕ_3
5	3.6241	3.0374	2.1295	3.2324	2.7247	1.8911
10	4.3732	3.6305	2.5256	4.3074	3.5779	2.4513
20	4.6680	3.8642	2.6822	4.6899	3.8807	2.6500
50	4.7673	3.9431	2.7352	4.8089	3.9748	2.7118
100	4.7827	3.9553	2.7434	4.8263	3.9886	2.7208
500	4.7878	3.9594	2.7461	4.8320	3.9931	2.7238

^{238}U metal fuel rod with a radius 0.5 cm, and a graphite moderator with an equivalent external radius of 2 cm. Then the second and third terms in the brackets of Eq. (4.97) become -0.09752 and 0.01959, respectively. Therefore the usual W.R. approximation overestimates the resonance integral by a factor about 0.078. The neutron spectra in the fuel and the moderator are shown in Fig. 4.13. From the figure large asymmetry about the resonance energy is seen. Far below the resonance the curves based on the present method approach to the value which corresponds to the resonance escape probability.

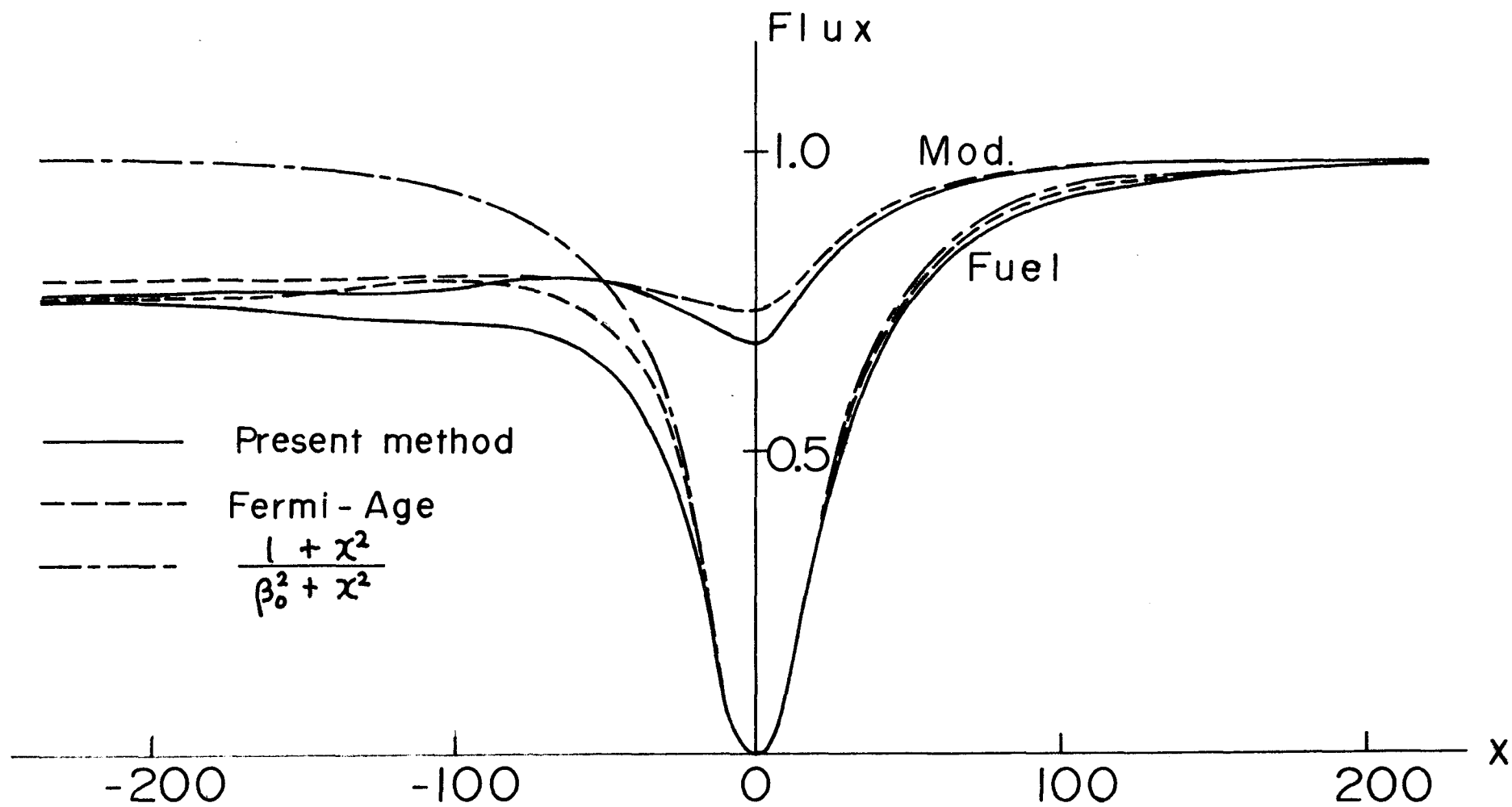


Fig. 4.13 Neutron spectra in a 6.68 eV ^{238}U resonance

References

- (1) BONALUMI, R.: Energ. Nucl., 8, 71 (1961).
- (2) BONALUMI, R.: ibid., 8, 826 (1961).
- (3) BONALUMI, R.: ibid., 12, 1 (1965).
- (4) LESLIE, D.C., JONSSON, A.: Nucl. Sci. Eng., 23, 272 (1965).
- (5) DANCOFF, S.M., GINSBURG, M.: CP-2157, (1944).
- (6) THIE, J.A.: Nucl. Sci. Eng., 5, 75 (1959).
- (7) FUKAI, Y.: ibid., 9, 370 (1961).
- (8) GOLAY, M.W., CADY, K.B.: ibid., 43, 303 (1971).
- (9) CARLVIK, I.: ibid., 30, 150 (1967).
- (10) GOLDSTEIN, R., COHEN, E.R.: ibid., 13, 132 (1962).
- (11) GOLDSTEIN, R.: ibid., 19, 359 (1964).
- (12) GOLDSTEIN, R., BROOKS, H.: ibid., 20, 331 (1964).
- (13) GOLDSTEIN, R.: ibid., 22, 387 (1965).
- (14) CHERNICK, J., VERNON, P.: ibid., 4, 649 (1958).
- (15) SPINNEY, K.T.: J. Nucl. Energy, 6, 53 (1957).
- (16) GAST, P.F.: Nucl. Sci. Eng., 21, 121 (1964).
- (17) GOERTZEL, G., GREULING, E.: ibid., 7, 69 (1960).
- (18) TAKEDA, T., SEKIYA, T.: J. Nucl. Sci. Technol., 8, 503 (1971).
- (19) CASE, K.M., DE HOFFMANN, F., PLACZEK, G.: "Introduction to the
Theory of Neutron Diffusion", Vol. 1, (1953), Los Alamos
Sci. Lab.
- (20) DI PASQUANTONIO, F.: Reactor Sci. Technol., 17, 67 (1963).
- (21) FUKAI, Y.: ibid., 17, 115 (1963).
- (22) LEWIS, E.E., ADLER, F.T.: Nucl. Sci. Eng., 31, 117 (1965).
- (23) JONSSON, A.: Reactor Sci. Technol., 17, 511 (1963).
- (24) TAKEDA, T., SEKIYA, T.: To be published in Technol. Report, Osaka
Univ.

- (25) TAKEDA,T., SEKIYA,T.: J. Nucl. Sci. Technol., 8, 649 (1971).
- (26) IIJIMA,S.: Nucl. Sci. Eng., 7, 69 (1960).
- (27) NORDHEIM,L.W.: Proc. Symp. Appl. Math., 6, 58 (1961).
- (28) YAMAMOTO,K.: Private Communication, (1970).
- (29) TSUCHIHASHI,K.: JAERI-1196, (1971).
- (30) STACEY,W.M.: "Modal Approximations", Research Monograph No. 41, The M.I.T. Press, Cambridge, Massachusetts, (1967).

CHAPTER 5

APPLICATION TO THE CALCULATION OF THE ANISOTROPIC DIFFUSION COEFFICIENTS

§5.1 Introduction

In this chapter the anisotropic diffusion coefficients in slab and square lattice cells are calculated by the integral transport theory with use made of Benoist's formula⁽¹⁾. In his theory, the quantity $P_{ij,k}^*$ appears in the principal term of the diffusion coefficient. This quantity is expanded into the Neumann series in which the n -th term corresponds to the n -fold collision processes suffered by a neutron in the course of flight from the region i to the region j . As he pointed out, the convergency of the series is very slow for slab lattice systems and also for cylindrical lattice systems though the latter converges a little faster than the former. On the basis of the integral transport theory, Benoist calculated only the first two terms in the expansion of $P_{ij,k}^*$ in the case of cylindrical cells⁽²⁾. In his calculation the scattering has, in almost every time, been assumed to be isotropic.

Leslie derived a formula of the diffusion coefficient in a cylindrical lattice cell starting from the calculation of the mean square displacement of neutron^{(3),(4),(5)}. His formula exactly corresponds to the principal term of the Benoist formula. His calculation, however, was limited to the P_1 -approximation.

In this chapter we introduce a new calculational method of the anisotropic diffusion coefficient defined by Benoist which is based on the integral transport theory. This method can be applied to slab and square lattices composed of many heterogeneous regions. Because of the effect of anisotropic scattering we adopted the generalized first-flight collision probability which contains an anisotropy of scattering. The contributions of all the expansion terms of $P_{ij,k}^*$ are taken into consideration by solving simultaneous equations in which the generalized collision probability is included.

We will also discuss on the origin of the difference between theoretical and experimental values of the anisotropic diffusion coefficients. Most experiments^{(6),(7)} for determining the anisotropic diffusion coefficients have been based on the pulsed neutron technique. However, there is theoretically no reason why the experimental value of the diffusion coefficient thus determined should be identical with the theoretical one which appears in the neutron leakage factor from the system.

Deniz⁽⁸⁾ derived the expression of the anisotropic diffusion coefficient which corresponds to the experimental results in the pulsed source measurement. This formula corresponds to the principal term of Benoist's formula except the weighting function in the case where the flux is decreasing with the asymptotic mode $e^{-\lambda t}$ in time. The difference between Benoist's and Deniz's diffusion coefficients has never been evaluated. Especially the evaluation of the additional term of Benoist's formula in time dependent problem is supposed to be of much interest. Then we will evaluate the perpendicular diffusion coefficient in slab cells, adopting the formulae by Benoist and Deniz

in time dependent problem on the basis of the method in §5.3.

The difference of the values D_1 between the two methods is also investigated. In the following section, we will try to introduce the Benoist formula more concisely than he originally derived.

§5.2 Derivation of the Benoist Formula of Anisotropic

Diffusion Coefficient

Here the Benoist formula of the anisotropic diffusion coefficient will be derived by a technique which differs from the original Benoist method.

In the first step, the anisotropic diffusion coefficient in steady state is introduced. Here the diffusion coefficient is defined in the expression which represents the neutron leakage from the whole system under consideration. Namely the neutron leakage \mathcal{F} is written in the form:

$$\mathcal{F} \equiv \int_{(\text{reactor surface})} d\mathbf{s} \quad (\vec{n} \cdot \vec{j}) = \sum_k D_k B_k^2 \int_{(\text{reactor})} d\vec{r} \quad \phi(\vec{r}), \quad (5.1)$$

where $\phi(\vec{r})$ and \vec{j} are the neutron flux and current, and D_k and B_k are the anisotropic diffusion coefficient and the buckling in the k-axis respectively. The neutron angular flux $\phi(\vec{r}, \vec{\Omega})$ satisfies the integro-differential transport equation

$$\mathcal{H} \phi(\vec{r}, \vec{\Omega}) = S(\vec{r}, \vec{\Omega}), \quad (5.2)$$

where

$$\mathcal{H} \phi(\vec{r}, \vec{\Omega}) = \vec{\Omega} \cdot \text{grad} \phi(\vec{r}, \vec{\Omega}) + \Sigma \phi(\vec{r}, \vec{\Omega}) - \int d\vec{\Omega}' \Sigma_s(r, \vec{\Omega} \rightarrow \vec{\Omega}') \phi(\vec{r}, \vec{\Omega}'). \quad (5.3)$$

Here we assume that the source distribution is written in the form:

$$S(\vec{r}, \vec{\Omega}) = S_0(\vec{r}, \vec{\Omega}) e^{i\vec{B} \cdot \vec{r}}, \quad (5.4)$$

where $S_0(\vec{r}, \vec{\Omega})$ is the source for an infinite lattice. If we denote the neutron angular flux due to the source $S_0(\vec{r}, \vec{\Omega})$ by $\phi_0(\vec{r}, \vec{\Omega})$, the real angular flux $\phi(\vec{r}, \vec{\Omega})$ is expressed in the form⁽⁹⁾:

$$\phi(\vec{r}, \vec{\Omega}) = \phi_0(\vec{r}, \vec{\Omega}) e^{i\vec{B} \cdot \vec{r}} - \mathcal{M}^{-1}(i\vec{B} \cdot \vec{\Omega}) e^{i\vec{B} \cdot \vec{r}} \phi_0(\vec{r}, \vec{\Omega}) . \quad (5.5)$$

From the above equation, the neutron current becomes as follows:

$$\vec{J}(\vec{r}) = \vec{j}_0 e^{i\vec{B} \cdot \vec{r}} - \int d\vec{\Omega} \vec{\Omega} \mathcal{M}^{-1}(i\vec{B} \cdot \vec{\Omega}) e^{i\vec{B} \cdot \vec{r}} \phi_0(\vec{r}, \vec{\Omega}) , \quad (5.6)$$

where

$$\vec{j}_0(\vec{r}) = \int d\vec{\Omega} \vec{\Omega} \phi_0(\vec{r}, \vec{\Omega}) . \quad (5.7)$$

Since the leakage \mathcal{F} is rewritten in the form

$$\mathcal{F} = \int_{(reactor)} d\vec{r} \operatorname{div} \vec{J}(\vec{r}) , \quad (5.8)$$

we need to calculate the integrand $\operatorname{div} \vec{J}(\vec{r})$. Replacing the inverse operator \mathcal{M}^{-1} by the Green function $G(\vec{r}, \vec{\Omega}; \vec{r}', \vec{\Omega}')$, which is the angular flux at the position \vec{r} and along the direction $\vec{\Omega}$, produced by a neutron born at the position \vec{r}' and along the direction $\vec{\Omega}'$, we obtain

$$\begin{aligned} \operatorname{div} \vec{J}(\vec{r}) &= \operatorname{div} (\vec{j}_0(\vec{r}) e^{i\vec{B} \cdot \vec{r}}) \\ &- \int d\vec{\Omega} \vec{\Omega} \cdot \vec{\operatorname{grad}} \int d\vec{r}' \int d\vec{\Omega}' G(\vec{r}, \vec{\Omega}; \vec{r}', \vec{\Omega}') (i\vec{B} \cdot \vec{\Omega}') e^{i\vec{B} \cdot \vec{r}'} \phi_0(\vec{r}', \vec{\Omega}') . \end{aligned} \quad (5.9)$$

Approximating $e^{i\vec{B} \cdot \vec{r}'}$ in the second term in the right-hand side of the above equation by

$$e^{i\vec{B} \cdot \vec{r}'} = e^{i\vec{B} \cdot \vec{r}} \{ 1 + i(\vec{r}' - \vec{r}) \cdot \vec{B} \} \quad (5.10)$$

and $e^{i\vec{B} \cdot \vec{r}}$ in Eq. (5.10) by

$$e^{i\vec{B} \cdot \vec{r}} = e^{i\vec{B} \cdot \vec{r}_0} \{ 1 + i(\vec{r} - \vec{r}_0) \cdot \vec{B} \} \quad (5.11)$$

(\vec{r}_0 is the center of the cell in which \vec{r} is included), we obtain

$$\begin{aligned}
\operatorname{div} \vec{j}(\vec{r}) &= \operatorname{div} \left(\vec{j}_0(\vec{r}) e^{i\vec{B} \cdot \vec{r}} \right) \\
&+ e^{i\vec{B} \cdot \vec{r}_0} \int d\vec{\Omega} (\vec{B} \cdot \vec{\Omega}) \int d\vec{r}' \int d\vec{\Omega}' G(\vec{r}, \vec{\Omega}; \vec{r}', \vec{\Omega}') (\vec{B} \cdot \vec{\Omega}') \\
&\quad \cdot \phi_0(\vec{r}', \vec{\Omega}') \\
&- e^{i\vec{B} \cdot \vec{r}_0} \int d\vec{\Omega} \vec{\Omega} \cdot \overrightarrow{\operatorname{grad}} \left\{ \int d\vec{r}' \int d\vec{\Omega}' G(\vec{r}, \vec{\Omega}; \vec{r}', \vec{\Omega}') (i\vec{B} \cdot \vec{\Omega}') \phi_0(\vec{r}', \vec{\Omega}') \right\} \\
&+ e^{i\vec{B} \cdot \vec{r}_0} \int d\vec{\Omega} (\vec{B} \cdot \vec{r} - \vec{r}_0) \vec{\Omega} \cdot \overrightarrow{\operatorname{grad}} \left\{ \int d\vec{r}' \int d\vec{\Omega}' G(\vec{r}, \vec{\Omega}; \vec{r}', \vec{\Omega}') \right. \\
&\quad \cdot (\vec{B} \cdot \vec{\Omega}') \phi_0(\vec{r}', \vec{\Omega}') \left. \right\} \\
&+ e^{i\vec{B} \cdot \vec{r}_0} \int d\vec{\Omega} \vec{\Omega} \cdot \overrightarrow{\operatorname{grad}} \left\{ \int d\vec{r}' \int d\vec{\Omega}' G(\vec{r}, \vec{\Omega}; \vec{r}', \vec{\Omega}') (\vec{B} \cdot \vec{\Omega}') \right. \\
&\quad \cdot \vec{B} \cdot (\vec{r} - \vec{r}') \phi_0(\vec{r}', \vec{\Omega}') \left. \right\} .
\end{aligned} \tag{5.12}$$

If we integrate the above equation over the cell in which the point \vec{r} is included, the first and the fifth terms vanish since the integrands become zero at the cell boundary through the integration about $\vec{\Omega}$. The third term also vanishes because of the symmetries about the x- and y-axes. Furthermore, only the terms with $k = k'$ in the terms $B_k B_{k'}$, remain in the second and the fourth terms in Eq. (5.12). Then we obtain

$$\begin{aligned}
\int_{\text{cell}} d\vec{r} \operatorname{div} \vec{j}(\vec{r}) &= \sum_k B_k^2 e^{i\vec{B} \cdot \vec{r}_0} \left\{ \int_{\text{cell}} d\vec{r} \int d\vec{\Omega} \Omega_k j_k(\vec{r}, \vec{\Omega}) \right. \\
&+ \left. \int_{\text{cell}} d\vec{r} \int d\vec{\Omega} (r_k - r_{0k}) \vec{\Omega} \cdot \overrightarrow{\operatorname{grad}} j_k(\vec{r}, \vec{\Omega}) \right\} ,
\end{aligned} \tag{5.13}$$

where

$$j_k(\vec{r}, \vec{\Omega}) = \int d\vec{r}' \int d\vec{\Omega}' G(\vec{r}, \vec{\Omega}; \vec{r}', \vec{\Omega}') \Omega'_k \phi_0(\vec{r}', \vec{\Omega}') . \tag{5.14}$$

From the definition of D_k in Eq. (5.1), we obtain

$$D_k = \frac{\int_{\text{cell}} d\vec{r} \int d\vec{\Omega} \{ \Omega_k j_k(\vec{r}, \vec{\Omega}) + (\gamma_k - r_{0k}) \vec{\Omega} \cdot \vec{\text{grad}} j_k(\vec{r}, \vec{\Omega}) \}}{\int_{\text{cell}} d\vec{r} \int d\vec{\Omega} \phi_0(\vec{r}, \vec{\Omega})} \quad (5.15)$$

This corresponds to the well-known Benoist's formula.

In the next step, we consider the time dependent behaviour of the anisotropic diffusion coefficient in the case where a pulsed source is injected into the heterogeneous lattice. Here we treat an asymptotic time region where the flux is decreasing by a factor $e^{-\lambda t}$. The neutron angular flux satisfies the equation

$$\left(\frac{1}{v} \frac{\partial}{\partial t} + \vec{\Omega} \cdot \vec{\text{grad}} + \Sigma \right) \phi(\vec{r}, \vec{\Omega}, t) = S(\vec{r}, \vec{\Omega}) \delta(t) - \int d\vec{\Omega}' \Sigma_s(\vec{r}, \vec{\Omega}' \rightarrow \vec{\Omega}) \phi(\vec{r}, \vec{\Omega}', t) \quad (5.16)$$

where v is the neutron velocity. Under the above assumption, we expand the flux in the form:

$$\phi(\vec{r}, \vec{\Omega}, t) = e^{-\lambda t} e^{i\vec{B} \cdot \vec{r}} \left\{ \phi_0(\vec{r}, \vec{\Omega}) + \sum_k B_k \phi_{1k}(\vec{r}, \vec{\Omega}) + \sum_{k, k'} B_k B_{k'} \phi_{2kk'}(\vec{r}, \vec{\Omega}) + \dots \right\} \quad (5.17)$$

where

$$\lambda = \lambda_0 + \sum_k \lambda_{1k} B_k + \sum_{k, k'} \lambda_{2kk'} B_k B_{k'} + \dots \quad (5.18)$$

Inserting the above equation into Eq. (5.16) and equating the same order B^m terms ($m \leq 2$) in both sides of the resulting equation, we obtain

$$H' \phi_0(\vec{r}, \vec{\Omega}) = 0 \quad (5.19)$$

$$\mathcal{M}' \phi_{1k}(\vec{r}, \vec{\Omega}) = -i \Omega_k \phi_0(\vec{r}, \vec{\Omega}) , \quad (5.20)$$

$$\begin{aligned} \mathcal{M}' \phi_{2kk'}(\vec{r}, \vec{\Omega}) &= \frac{1}{v} \lambda_{2kk'} \phi_0(\vec{r}, \vec{\Omega}) \\ &- (i \Omega_k \phi_{1k'} + i \Omega_{k'} \phi_{1k})(2 - \delta_{kk'})/2 , \end{aligned} \quad (5.21)$$

where \mathcal{M}' is defined by

$$\begin{aligned} \mathcal{M}' \phi_0(\vec{r}, \vec{\Omega}) &= \vec{\Omega} \cdot \vec{\nabla} \phi_0(\vec{r}, \vec{\Omega}) + \left(\Sigma - \frac{\lambda_0}{v} \right) \phi_0(\vec{r}, \vec{\Omega}) \\ &- \int d\vec{\Omega}' \Sigma_s(\vec{r}, \vec{\Omega}' \rightarrow \vec{\Omega}) \phi_0(\vec{r}, \vec{\Omega}') , \end{aligned} \quad (5.22)$$

and eigenvalue $\lambda_{2kk'}$ is given by

$$\frac{\lambda_{2kk'}}{v} = \frac{\int d\vec{r} \int d\vec{\Omega} \phi_0^*(\vec{r}, \vec{\Omega}) i \Omega_k \phi_{1k}(\vec{r}, \vec{\Omega})}{\int d\vec{r} \int d\vec{\Omega} \phi_0^*(\vec{r}, \vec{\Omega}) \phi_0(\vec{r}, \vec{\Omega})} , \quad (5.23)$$

where $\phi_0^*(\vec{r}, \vec{\Omega})$ is the adjoint flux; the eigenvalues λ_{1k} and $\lambda_{2kk'}$ ($k = k'$)

become zero owing to the symmetries about the x- and y-axes:

$$\frac{\lambda_{1k}}{v} = \frac{\int d\vec{r} \int d\vec{\Omega} \phi_0^*(\vec{r}, \vec{\Omega}) (i \Omega_k) \phi_0(\vec{r}, \vec{\Omega})}{\int d\vec{r} \int d\vec{\Omega} \phi_0^*(\vec{r}, \vec{\Omega}) \phi_0(\vec{r}, \vec{\Omega})} = 0 , \quad (5.24)$$

$$\frac{\lambda_{2kk'}}{v} = \frac{\int d\vec{r} \int d\vec{\Omega} \phi_0^*(\vec{r}, \vec{\Omega}) \{ (i \Omega_k) \phi_{1k'}(\vec{r}, \vec{\Omega}) + i \Omega_{k'} \phi_{1k}(\vec{r}, \vec{\Omega}) \}}{\int d\vec{r} \int d\vec{\Omega} \phi_0^*(\vec{r}, \vec{\Omega}) \phi_0(\vec{r}, \vec{\Omega})} = 0 . \quad (5.25)$$

The neutron leakage at time t is given by

$$\mathcal{F} = e^{-\lambda t} \int_{(reactor)} d\vec{r} \operatorname{div} \left\{ \int d\vec{\Omega} \vec{\Omega} \phi(\vec{r}, \vec{\Omega}) \right\} . \quad (5.26)$$

Substituting Eq. (5.17) possessing the B^m terms for $m \leq 2$ into the above equation, we have

$$\begin{aligned} \mathcal{F} &= e^{-\lambda t} \left[\int_{(reactor)} d\vec{r} \operatorname{div} \left\{ e^{i \vec{B} \cdot \vec{r}} \int d\vec{\Omega} \vec{\Omega} \phi_0(\vec{r}, \vec{\Omega}) \right. \right. \\ &\quad \left. \left. + \int_{(reactor)} d\vec{r} \operatorname{div} \left\{ e^{i \vec{B} \cdot \vec{r}} \int d\vec{\Omega} \sum_k B_k \phi_{1k}(\vec{r}, \vec{\Omega}) \right\} \right] \end{aligned}$$

$$+ \int_{(reactor)} d\vec{r} \operatorname{div} \left\{ e^{i\vec{B} \cdot \vec{r}} \int d\vec{\Omega} \vec{\Omega} \sum_{k,k'} B_k B_{k'} \phi_{2kk'}(\vec{r}, \vec{\Omega}) \right\} . \quad (5.27)$$

The first term in the above equation vanishes because the term in the bracket expresses the neutron current in infinite lattice. The third term becomes also zero because the term in the bracket vanishes on the cell boundary after the integration about $\vec{\Omega}$. From the remaining term we obtain the equation:

$$\begin{aligned} \mathcal{F} = \sum_{cell\ 0} e^{-\lambda t} & \left[e^{i\vec{B} \cdot \vec{r}_0} \int d\vec{r} \{ 1 + i\vec{B} \cdot (\vec{r} - \vec{r}_0) \} \operatorname{div} \int d\vec{\Omega} \vec{\Omega} \sum_k B_k \phi_{1k}(\vec{r}, \vec{\Omega}) \right. \\ & \left. + i\vec{B} e^{i\vec{B} \cdot \vec{r}_0} \cdot \int d\vec{r} \int d\vec{\Omega} \vec{\Omega} \sum_k B_k \phi_{1k}(\vec{r}, \vec{\Omega}) \right] . \end{aligned} \quad (5.28)$$

Since the first term of the above equation vanishes, Eq. (5.28) reduces to

$$\begin{aligned} \mathcal{F} = \sum_{cell\ 0} e^{-\lambda t} e^{i\vec{B} \cdot \vec{r}_0} & \sum_k i B_k^2 \left\{ \int d\vec{r} \int d\vec{\Omega} \vec{\Omega} \phi_{1k}(\vec{r}, \vec{\Omega}) \right. \\ & \left. + \int d\vec{r} (r_k - r_{0k}) \operatorname{div} \left(\int d\vec{\Omega} \vec{\Omega} \phi_{1k}(\vec{r}, \vec{\Omega}) \right) \right\} . \end{aligned} \quad (5.29)$$

This is equal to

$$\mathcal{F} = \sum_{cell\ 0} \sum_k e^{-\lambda t} e^{i\vec{B} \cdot \vec{r}_0} D_k B_k^2 \int d\vec{r} \int d\vec{\Omega} \phi_0(\vec{r}, \vec{\Omega}) . \quad (5.30)$$

From this we obtain the same expression for the anisotropic diffusion coefficient as Eq. (5.15) in the case of steady state, except that, in the pulse problems, the equation determining the flux is homogeneous and the usual total cross section must be replaced by $\Sigma - \alpha/v$.

In what follows, we consider the anisotropic diffusion coefficient obtained from the pulsed neutron technique. In this case, D_k is obtained from the relation

$$\lambda = (\lambda_0 + \sum_k D_k B_k^2) v . \quad (5.31)$$

Then from Eq. (5.23), we obtain

$$D_k = \frac{\int d\vec{r} \int d\vec{R} \phi_0^*(\vec{r}, \vec{R}) \Omega_k j_k(\vec{r}, \vec{R})}{\int d\vec{r} \int d\vec{R} \phi_0^*(\vec{r}, \vec{R}) \phi_0(\vec{r}, \vec{R})} \quad (5.32)$$

This expression was first introduced by Deniz, and corresponds to the principal term of the Benoist formula except the weighting function.

§5.3 Calculation of the Diffusion Coefficients⁽¹⁰⁾

First we calculate the anisotropic diffusion coefficient in a slab lattice system. In order to evaluate Eq. (5.15), we calculate the quantity $j_k(\vec{r}, \vec{\Omega})$. In slab system a phase point $(\vec{r}, \vec{\Omega})$ is expressed by (x, μ) ; x being the spatial coordinate in the axis which is perpendicular to the slab surface, and μ being the projection of $\vec{\Omega}$ onto the x -axis. Since the diffusion coefficient parallel to the slab surface is easily calculated^{(3),(11),(12),(13),(14)}, we treat only the perpendicular diffusion coefficient D_x , namely we put $k = x$ in Eq. (5.15). We expand $j_x(x, \mu)$, $\phi(x, \mu)$ and the scattering cross section $\Sigma_s(x, \vec{\Omega}' \rightarrow \vec{\Omega})$ into the Legendre series as follows:

$$j_x(x, \mu) = \sum_{n=0}^{\infty} \frac{2n+1}{4\pi} j_x^n(x) P_n(\mu), \quad (5.33)$$

$$\phi(x, \mu) = \sum_{n=0}^{\infty} \frac{2n+1}{4\pi} \phi^n(x) P_n(\mu), \quad (5.34)$$

$$\begin{aligned} \Sigma_s(x, \vec{\Omega}' \rightarrow \vec{\Omega}) &= \sum_{n=0}^{\infty} \frac{2n+1}{4\pi} \Sigma_s^n(x) \{ P_n(\mu') P_n(\mu) \\ &+ 2 \sum_{m=1}^n \frac{(l-m)!}{(l+m)!} P_n^m(\mu') P_n^m(\mu) \cos m(\varphi - \varphi') \}, \end{aligned} \quad (5.35)$$

where φ is the azimuthal angle. From the definition of $j_x(\vec{r}, \vec{\Omega})$ in Eq. (5.14), this quantity satisfies the equation:

$$j_x(\vec{r}, \vec{\Omega}) = \int_0^{\infty} dR \, e^{-\vec{r} \cdot \vec{R}} \left\{ \mu \phi(\vec{r}, \vec{\Omega}) + \int_{4\pi} d\vec{\Omega}' \Sigma_s(\vec{r}, \vec{\Omega}' \rightarrow \vec{\Omega}) j_x(\vec{r}, \vec{\Omega}') \right\}. \quad (5.36)$$

In order to obtain the coefficients in Eq. (5.33), we divide a slab cell into many regions, and assume that $j_x^n(x)$ and $\phi^n(x)$ are constant in each region, and, in the j -th region, express them by j_{jx}^n and ϕ_j^n respectively. Here we retain the terms with $n \leq 1$ in Eqs. (5.33) ~

(5.35). Namely we limit our treatment up to the anisotropic scattering of the first order about cosine of the scattering angle. When we substitute Eqs. (5.33)~(5.35) into Eq. (5.36) and perform the integration about the azimuthal angle φ' in the scattering term, there remains only the term with $m = 0$. And then integrating the resulting equation about $\vec{\Omega}$ over the whole solid angle 4π and about x over the volume V_j of the j -th region, we obtain

$$\begin{aligned} \sum_i V_i j_{ix}^0 = \sum_i \{ \sum_i V_i j_{ix}^0 c_i^0 P_{ij}^{00} + \sum_i V_i j_{ix}^1 c_i^1 P_{ij}^{10} \\ + \frac{1}{3} V_i \phi_i^0 P_{ij}^{10} + \frac{1}{3} V_i \phi_i^1 P_{ij}^{20} \} , \end{aligned} \quad (5.37)$$

where c_i^0 and c_i^1 are defined by

$$c_i^0 = \frac{\sum_{is}^0}{\sum_i} , \quad c_i^1 = \frac{\sum_{is}^1}{\sum_i} . \quad (5.38)$$

Next, we multiply Eq. (5.36) by μ and integrate about $\vec{\Omega}$ and x over the whole solid angle 4π and V_j , respectively. Then we obtain

$$\begin{aligned} \sum_i V_i j_{ix}^1 = \sum_i \{ \sum_i V_i j_{ix}^0 c_i^0 P_{ij}^{01} + \sum_i V_i j_{ix}^1 c_i^1 P_{ij}^{11} \\ + \frac{1}{3} V_i \phi_i^0 P_{ij}^{11} + \frac{1}{3} V_i \phi_i^1 P_{ij}^{21} \} . \end{aligned} \quad (5.39)$$

In Eqs. (5.37) and (5.39) we adopted the generalized first-flight collision probabilities. If an operator \mathcal{H}_{ij} is defined by

$$\mathcal{H}_{ij} \mu^n = \frac{\sum_i V_i}{V_i} \int_{V_i} d\vec{r}' \int_{V_j} d\vec{r} \frac{e^{-\hat{s}R}}{4\pi R^2} \mu^n , \quad (5.40)$$

the generalized first-flight collision probabilities are expressed in the forms

$$\begin{aligned} P_{ij}^{00} &= \mathcal{H}_{ij} \mu^0 , \\ P_{ij}^{10} &= 3 \mathcal{H}_{ij} \mu , \end{aligned}$$

$$\begin{aligned}
P_{ij}^{20} &= 9 H_{ij} \mu^2, \\
P_{ij}^{01} &= \frac{1}{3} P_{ij}^{10}, \\
P_{ij}^{11} &= \frac{1}{3} P_{ij}^{20}, \\
P_{ij}^{21} &= 9 H_{ij} \mu^3.
\end{aligned} \tag{5.41}$$

Explicit expressions for them are presented in Appendix 5A.

If we put

$$y_j^0 = 3 \sum_i \nabla_i j_{ix}^0, \quad y_j^1 = 3 \sum_i \nabla_i j_{ix}^1, \tag{5.42}$$

Eqs. (5.37) and (5.39) reduce to

$$y_j^0 = \sum_i (y_i^0 c_i^0 P_{ij}^{00} + y_i^1 c_i^1 P_{ij}^{10} + S_i^0 P_{ij}^{10} + S_i^1 P_{ij}^{20}), \tag{5.43}$$

$$y_j^1 = \sum_i (y_i^0 c_i^0 P_{ij}^{01} + y_i^1 c_i^1 P_{ij}^{11} + S_i^0 P_{ij}^{11} + S_i^1 P_{ij}^{21}), \tag{5.44}$$

where

$$S_i^0 = \nabla_i \phi_i^0, \quad S_i^1 = \nabla_i \phi_i^1. \tag{5.45}$$

We express Eq. (5.15) by the sum of D_1 and D_2 , where D_1 and D_2 correspond to the first and second terms in the brackets in the equation, respectively. Then the principal term D_1 of the diffusion coefficient

D_x is obtained from the definition in the form

$$D_1 = \frac{\sum_j j_{jx}^1 \nabla_j}{\sum_j \phi_j^0 \nabla_j} = \frac{\sum_i y_i^1 / 3 \sum_i}{\sum_i \phi_i^0 \nabla_i}. \tag{5.46}$$

The well-known formula by Benoist is derived as follows. If we put

$S_i^0 = \delta_{ik}$, $S_i^1 = 0$ (δ_{ik} being the Kronecker delta function) in Eqs. (5.43) and (5.44), and represent the solutions y_j^1 by P_{kj}^* , Eq. (5.46)

may be rewritten in the form

$$D_1 = \frac{\sum_i \sum_k V_k \phi_k^0 P_{ki}^* / 3 \Sigma_i}{\sum_k V_k \phi_k^0}, \quad (5.47)$$

which is Benoist's formula. As easily seen from Eq. (5.44), P_{kj}^{11} corresponds to the first order contribution to P_{kj}^* . Since we divide the cell system into many regions, which are denoted by suffixes i and j in Eqs. (5.43) and (5.44), the contribution of infinite number of collisions of a neutron traveling from the k -th region to the j -th region is taken into account for the calculation of P_{kj}^* .

In what follows, we calculate the additional term D_2 . The quantity $j_x(\vec{r}, \vec{\Omega})$ satisfies the integro-differential equation

$$\begin{aligned} \vec{\Omega} \cdot \vec{\text{grad}} j_x(\vec{r}, \vec{\Omega}) + \Sigma j_x(\vec{r}, \vec{\Omega}) &= \int d\vec{\Omega}' \Sigma_s(\vec{r}, \vec{\Omega}' \rightarrow \vec{\Omega}) j_x(\vec{r}, \vec{\Omega}') \\ &+ \mu \phi(\vec{r}, \vec{\Omega}). \end{aligned} \quad (5.48)$$

Integration of the above equation about the solid angle $\vec{\Omega}$ leads to

$$\int_{4\pi} d\vec{\Omega} \vec{\Omega} \cdot \vec{\text{grad}} j_x(\vec{r}, \vec{\Omega}) = \phi'(\vec{r}) - \Sigma_a j_x^0(\vec{r}). \quad (5.49)$$

Then, from the definition of D_2 , we obtain

$$D_2 = \frac{\sum_i \frac{1}{2} (r_{i+1}^2 - r_i^2) (\phi'_i - \Sigma_{ia} j_{ix}^0)}{\sum_i V_i \phi_i^0}, \quad (5.50)$$

where r_{i+1} and r_i are distances from the center of a cell to the outer and inner surfaces of the i -th region.

Next, we calculate the anisotropic diffusion coefficient D_x in a square lattice. In the system, we choose the z -axis in the axial direction and assume that θ is the polar angle between the neutron

direction $\vec{\Omega}$ and the z-axis, and α is the azimuthal angle between the projection of $\vec{\Omega}$ on the x-y plane and the x-axis. Then we expand $j_x(\vec{r}, \vec{\Omega})$, $\phi(\vec{r}, \vec{\Omega})$ and $\Sigma_s(\vec{r}, \vec{\Omega} \rightarrow \vec{\Omega})$ into the spherical harmonics series:

$$j_x(\vec{r}, \vec{\Omega}) = \sum_{n=0}^{\infty} (H_n^0)^2 j_x^{(n0)} P_n(\cos \theta) + 2 \sum_{n=1}^{\infty} \sum_{m=1}^n (H_n^m)^2 \cdot \left\{ j_x^{(n1)} \cos m\alpha + j_x^{(n2)} \sin m\alpha \right\} P_n^m(\cos \theta) , \quad (5.51)$$

$$\phi(\vec{r}, \vec{\Omega}) = \sum_{n=0}^{\infty} (H_n^0)^2 \phi^{(n0)} P_n(\cos \theta) + 2 \sum_{n=1}^{\infty} \sum_{m=1}^n (H_n^m)^2 \cdot \left\{ \phi^{(n1)} \cos m\alpha + \phi^{(n2)} \sin m\alpha \right\} P_n^m(\cos \theta) , \quad (5.52)$$

$$\Sigma_s(\vec{r}, \vec{\Omega} \rightarrow \vec{\Omega}) = \sum_{n=0}^{\infty} (H_n^0)^2 \Sigma_s^n P_n(\cos \theta') P_n(\cos \theta) + 2 \sum_{n=1}^{\infty} \sum_{m=1}^n (H_n^m)^2 \Sigma_s^n P_n^m(\cos \theta') P_n^m(\cos \theta) \cos m(\alpha - \alpha') , \quad (5.53)$$

where H_n^m has been defined in Eq. (2.12b). We calculate the quantity $j_x(\vec{r}, \vec{\Omega})$, which satisfies the equation

$$j_x(\vec{r}, \vec{\Omega}) = \int_0^\infty dR \, e^{-\hat{\Sigma}R} \left\{ \Omega_x \phi(\vec{r}, \vec{\Omega}) + \int d\vec{\Omega}' \Sigma_s(\vec{r}, \vec{\Omega}' \rightarrow \vec{\Omega}) j_x(\vec{r}, \vec{\Omega}') \right\} , \quad (5.54)$$

where $\Omega_x = \sin\theta \cos\alpha$. Substituting Eqs. (5.51) ~ (5.53) into the above equation, retaining only the terms with $n = 0$ and 1, and using the similar means to that used in deriving Eqs. (5.37) and (5.39), as well as the definitions

$$\begin{aligned} \varphi_i^0 &= 3 \Sigma_i \nabla_i j_i^{(00)} , \\ \varphi_i^{1x} &= 3 \Sigma_i \nabla_i j_i^{(11)} , \\ \varphi_i^{1y} &= 3 \Sigma_i \nabla_i j_i^{(12)} , \end{aligned} \quad (5.55)$$

we obtain the three equations

$$\begin{aligned} \mathcal{Y}_i^0 = \sum_j \{ & \mathcal{Y}_i^0 c_i^0 P_{ij}^{0,0} + \mathcal{Y}_i^{1x} c_i^1 P_{ij}^{1x,0} + \mathcal{Y}_i^{1g} c_i^1 P_{ij}^{1g,0} \\ & + S_i^0 P_{ij}^{1x,0} + S_i^{1x} P_{ij}^{2x,0} + S_i^{1g} P_{ij}^{1x1g,0} \} , \end{aligned} \quad (5.56)$$

$$\begin{aligned} \mathcal{Y}_i^{1x} = \sum_j \{ & \mathcal{Y}_i^0 c_i^0 P_{ij}^{0,1x} + \mathcal{Y}_i^{1x} c_i^1 P_{ij}^{1x,1x} + \mathcal{Y}_i^{1g} c_i^1 P_{ij}^{1g,1x} \\ & + S_i^0 P_{ij}^{1x,1x} + S_i^{1x} P_{ij}^{2x,1x} + S_i^{1g} P_{ij}^{1x1g,1x} \} , \end{aligned} \quad (5.57)$$

$$\begin{aligned} \mathcal{Y}_i^{1g} = \sum_j \{ & \mathcal{Y}_i^0 c_i^0 P_{ij}^{0,1g} + \mathcal{Y}_i^{1x} c_i^1 P_{ij}^{1x,1g} + \mathcal{Y}_i^{1g} c_i^1 P_{ij}^{1g,1g} \\ & + S_i^0 P_{ij}^{1x,1g} + S_i^{1x} P_{ij}^{2x,1g} + S_i^{1g} P_{ij}^{1x1g,1g} \} , \end{aligned} \quad (5.58)$$

where

$$S_i^0 = \nabla_i \phi_i^{(0,0)} , \quad S_i^{1x} = \nabla_i \phi_i^{(1,1)} , \quad S_i^{1g} = \nabla_i \phi_i^{(1,2)} . \quad (5.59)$$

Here we used the following generalized first-flight collision probabilities:

$$\begin{aligned} P_{ij}^{0,0} &= \mathcal{N}_{ij} \quad , & P_{ij}^{1x,0} &= 3 \mathcal{N}_{ij} \Omega_x , \\ P_{ij}^{1g,0} &= 3 \mathcal{N}_{ij} \Omega_g , & P_{ij}^{1x1g,0} &= 9 \mathcal{N}_{ij} \Omega_x \Omega_g , \\ P_{ij}^{2x,0} &= 9 \mathcal{N}_{ij} \Omega_x^2 , & P_{ij}^{0,1x} &= \frac{1}{3} P_{ij}^{1x,0} , \\ P_{ij}^{1x,1x} &= \frac{1}{3} P_{ij}^{2x,0} , & P_{ij}^{1g,1x} &= \frac{1}{3} P_{ij}^{1x1g,0} , \\ P_{ij}^{1x1g,1x} &= 9 \mathcal{N}_{ij} \Omega_x^2 \Omega_g , & P_{ij}^{2x,1x} &= 9 \mathcal{N}_{ij} \Omega_x^3 , \\ P_{ij}^{0,1g} &= \frac{1}{3} P_{ij}^{1g,0} , & P_{ij}^{1x,1g} &= P_{ij}^{1g,1x} , \end{aligned}$$

$$P_{ij}^{1g, 1g} = 3 H_{ij} \Omega_y^2, \quad P_{ij}^{1x1g, 1g} = 9 H_{ij} \Omega_x \Omega_y^2,$$

$$P_{ij}^{2x, 1g} = P_{ij}^{1x1g, 1x}.$$

(5.60)

Their approximate expressions are given in Appendix 5B. They have also the properties:

$$\begin{aligned} \sum_{j=1}^{\infty} P_{ij}^{0,0} &= 1, \\ \sum_{j=1}^{\infty} P_{ij}^{1x,0} &= \sum_{j=1}^{\infty} P_{ij}^{1g,0} = \sum_{j=1}^{\infty} P_{ij}^{1x1g,0} = \sum_{j=1}^{\infty} P_{ij}^{1x1g,1x} \\ &= \sum_{j=1}^{\infty} P_{ij}^{2x,1x} = \sum_{j=1}^{\infty} P_{ij}^{1x,1g} = \sum_{j=1}^{\infty} P_{ij}^{1x1g,1g} = 0, \\ \sum_{j=1}^{\infty} P_{ij}^{1x,1x} &= \sum_{j=1}^{\infty} P_{ij}^{1g,1g} = 1. \end{aligned} \quad (5.61)$$

These relations can be used in order to calculate the probabilities that a neutron born in a region undergoes its first collision within the same region.

Since the quantities \mathcal{P}_i^0 , \mathcal{P}_i^{1x} and \mathcal{P}_i^{1g} have some symmetries about the x- and y- axes as shown in Table 5.1, it will suffice to

Table 5.1 Symmetries about \mathcal{P}_i^0 , \mathcal{P}_i^{1x} and \mathcal{P}_i^{1g}

	Quadrant			
	1 [†]	2	3	4
\mathcal{P}_i^0	+	-	-	+
\mathcal{P}_i^{1x}	+	+	+	+
\mathcal{P}_i^{1g}	+	-	+	-

[†]All the values of \mathcal{P}_i^0 , \mathcal{P}_i^{1x} and \mathcal{P}_i^{1g} are taken positive in the first quadrant

treat the quantities only in the first quadrant. Then Eqs. (5.56)

~ (5.58) reduce to

$$\begin{aligned} \mathcal{G}_{j1}^0 = \sum_{i1} \{ & \mathcal{G}_{i1}^0 c_i^0 P_{i,j1}^{0,0} + \mathcal{G}_{i1}^{1x} c_i^{1x} P_{i,j1}^{1x,0} + \mathcal{G}_{i1}^{1y} c_i^{1y} P_{i,j1}^{1y,0} \\ & + S_{i1}^0 P_{i,j1}^{1x,0} + S_{i1}^{1x} P_{i,j1}^{2x,0} + S_{i1}^{1y} P_{i,j1}^{1x1y,0} \} , \end{aligned} \quad (5.62)$$

$$\begin{aligned} \mathcal{G}_{j1}^{1x} = \sum_{i1} \{ & \mathcal{G}_{i1}^0 c_i^0 P_{i,j1}^{0,1x} + \mathcal{G}_{i1}^{1x} c_i^{1x} P_{i,j1}^{1x,1x} + \mathcal{G}_{i1}^{1y} c_i^{1y} P_{i,j1}^{1y,1x} \\ & + S_{i1}^0 P_{i,j1}^{1x,1x} + S_{i1}^{1x} P_{i,j1}^{2x,1x} + S_{i1}^{1y} P_{i,j1}^{1x1y,1x} \} , \end{aligned} \quad (5.63)$$

$$\begin{aligned} \mathcal{G}_{j1}^{1y} = \sum_{i1} \{ & \mathcal{G}_{i1}^0 c_i^0 P_{i,j1}^{0,1y} + \mathcal{G}_{i1}^{1x} c_i^{1x} P_{i,j1}^{1x,1y} + \mathcal{G}_{i1}^{1y} c_i^{1y} P_{i,j1}^{1y,1y} \\ & + S_{i1}^0 P_{i,j1}^{1x,1y} + S_{i1}^{1x} P_{i,j1}^{2x,1y} + S_{i1}^{1y} P_{i,j1}^{1x1y,1y} \} . \end{aligned} \quad (5.64)$$

Here $i1$ is a point in the first quadrant and $i2$, $i3$ and $i4$ are the symmetric points to $i1$ in the second, third and fourth quadrants, respectively. Furthermore, in the above equations, the following probabilities are used:

$$P_{i,j1}^{0,t} = P_{i1,j1}^{0,t} - P_{i2,j1}^{0,t} - P_{i3,j1}^{0,t} + P_{i4,j1}^{0,t} , \quad (5.65)$$

$$P_{i,j1}^{1x,t} = P_{i1,j1}^{1x,t} + P_{i2,j1}^{1x,t} + P_{i3,j1}^{1x,t} + P_{i4,j1}^{1x,t} , \quad (5.66)$$

$$P_{i,j1}^{1y,t} = P_{i1,j1}^{1y,t} - P_{i2,j1}^{1y,t} + P_{i3,j1}^{1y,t} - P_{i4,j1}^{1y,t} , \quad (5.67)$$

$$P_{i,j1}^{2x,t} = P_{i1,j1}^{2x,t} - P_{i2,j1}^{2x,t} - P_{i3,j1}^{2x,t} + P_{i4,j1}^{2x,t} , \quad (5.68)$$

$$P_{i,j1}^{1x1y,t} = P_{i1,j1}^{1x1y,t} + P_{i2,j1}^{1x1y,t} - P_{i3,j1}^{1x1y,t} - P_{i4,j1}^{1x1y,t} , \quad (5.69)$$

where t denotes 0 or $1x$ or $1y$.

In terms of the solution of Eqs. (5.62) ~ (5.64), the principal

term D_1 of the diffusion coefficient D_x is calculated:

$$D_1 = \frac{\sum_i y_i^2 / 3 \Sigma_i}{\sum_i V_i \phi_i^{(00)}} , \quad (5.70)$$

where region i is taken only over the first quadrant. And the additional term D_2 becomes

$$D_2 = \frac{\sum_i x_i \{ V_i \phi_i^{(11)} - \Sigma_{ia} y_i^2 / 3 \Sigma_i \}}{\sum_i V_i \phi_i^{(00)}} , \quad (5.71)$$

where x_i is the x -coordinate of the center of the i -th region.

In Table 5.2 the principal terms of the perpendicular diffusion coefficient D_{\perp} are presented for slab lattice cells consisting of a moderator and a void channel. They are calculated for various total cross sections Σ of the moderator and for various c (the number of secondary neutrons per collision in the moderator). In the calculation we divided a moderator in a cell into 70 regions for the case of isotropic scattering and 50 regions for the case of anisotropic

Table 5.2 Diffusion coefficient in slab cell with void channel

Values of $\frac{D_{\perp}}{\frac{\lambda_m}{3}}$

Isotropic scattering (mesh 70)

$\Sigma \backslash c$	0.98	0.999	0.9999	0.99999
0.05	1.1000	1.1000	1.1000	1.1000
0.1	1.1000	1.1000	1.1000	1.1000
0.5	1.1003	1.1000	1.1000	1.1000
1.0	1.1011	1.1001	1.1000	1.1000
2.0	1.1041	1.1003	1.1000	1.1000
5.0	1.1191	1.1017	1.1004	1.1003

Values of $\frac{D_{\perp}}{\frac{\lambda_m}{3(1-c\mu)}}$

Anisotropic scattering (mesh 50) $\mu = 1/3$

$\Sigma \backslash c$	0.98	0.999	0.9999	0.99999
0.05	1.1002	1.1017	1.1036	1.1041
0.1	1.1004	1.1030	1.1041	1.1042
0.5	1.1036	1.1060	1.1061	1.1062
1.0	1.1088	1.1112	1.1125	1.1125
2.0	1.1219	1.1295	1.1305	1.1305
5.0	1.1613	1.1769	1.1819	1.1825

Thickness of void channel: 0.5 cm

Thickness of moderator: 5.0 cm

c : scattering ratio in moderator

Σ : total cross section of moderator

scattering in the moderator. The thickness of the void channel and the moderator are taken to be 0.5 and 5.0 cm respectively.

For the case of isotropic scattering, the value $\frac{D_1}{\lambda_m/3}$ approaches 1.1 as c approaches 1 (λ_m is the mean free path in the moderator). For the case where $c = 1$, the value of D_1 can be calculated analytically, and corresponds to the homogeneous limit exactly⁽¹¹⁾. In this case the homogeneous limit of $\frac{D_1}{\lambda_m/3}$ becomes 1.1 and this justifies the present results. When there is absorption in the moderator, the values of $\frac{D_1}{\lambda_m/3}$ become larger than 1.1 and this tendency is appreciable for large Σ .

For the case of anisotropic scattering in the moderator, the transport mean free path in the moderator is $\frac{\lambda_m}{1 - c\mu}$, where μ is the average cosine of the scattering angle and is now assumed to be 1/3. The value $D_1 / (\frac{1}{3} \cdot \frac{\lambda_m}{1 - c\mu})$ does not approach 1.1 (value of homogeneous limit) when c approaches 1 unlike the case of isotropic scattering. And this discrepancy from 1.1 becomes larger for $c \approx 1$.

In Table 5.3 the principal and the additional terms D_1 and D_2 of the perpendicular diffusion coefficient in slab cells are shown together with those calculated by the usual approximate methods. They are evaluated for various scattering cross sections in a fuel Σ_{fs} and in a moderator Σ_{ms} and for various thicknesses of the fuel l_f and of the moderator l_m . The average cosine of the scattering angle in the moderator μ_m is taken as 1/3 and that in the fuel μ_f is taken as 0 or 1/3. The total cross sections in the fuel and the moderator are assumed to be 1.0 and 2.0 cm^{-1} , respectively. In calculating D_1 and D_2 , we divided all lattice cells into 20 regions (4 regions in the fuel and 16 regions in the moderator). The quantity D_{iso} is evaluated

Table 5.3 Diffusion coefficient in slab cells

Total cross section in fuel: 1.0 cm^{-1}

Total cross section in moderator: 2.0 cm^{-1}

$^t \Sigma_{sf}$	Σ_{sm}	l_f	l_m	μ_f	D_1	D_2	D_{iso}	D_{homo}^1	D_{homo}^2
0.3	2.0	2	8	0	0.2665	-0.1126	0.2600	0.1706	0.2529
0.5	2.0	2	8	0	0.2671	-0.1074	0.2607	0.1717	0.2537
0.8	2.0	2	8	0	0.2673	-0.08171	0.2621	0.1756	0.2565
0.3	1.5	2	8	0	0.2358	0.04094	0.2328	0.1722	0.2271
0.5	1.5	2	8	0	0.2366	0.03393	0.2338	0.1735	0.2283
0.8	1.5	2	8	0	0.2386	0.01414	0.2367	0.1777	0.2318
0.3	2.0	1	4	0	0.2672	-0.07301	0.2625	0.1742	0.2555
0.5	2.0	1	4	0	0.2669	-0.06274	0.2627	0.1758	0.2567
0.8	2.0	1	4	0	0.2655	-0.03561	0.2631	0.1798	0.2594
0.3	1.5	1	4	0	0.2395	0.00405	0.2362	0.1754	0.2299
0.5	1.5	1	4	0	0.2396	0.00091	0.2369	0.1770	0.2312
0.8	1.5	1	4	0	0.2397	-0.00581	0.2382	0.1807	0.2344
0.3	2.0	1	4	1/3	0.2731	-0.07418	0.2667	0.1742	0.2572
0.5	2.0	1	4	1/3	0.2764	-0.06420	0.2699	0.1758	0.2601
0.8	2.0	1	4	1/3	0.2795	-0.03651	0.2751	0.1798	0.2675
0.3	1.5	1	4	1/3	0.2438	0.00058	0.2397	0.1754	0.2315
0.5	1.5	1	4	1/3	0.2471	-0.00497	0.2431	0.1770	0.2344
0.8	1.5	1	4	1/3	0.2519	-0.01516	0.2493	0.1807	0.2414

[†] Σ_{sf} , Σ_{sm} are scattering cross sections in fuel and moderator
 l_f , l_m are thicknesses of fuel and moderator
 μ_f is average cosine of the scattering angle in fuel

by the calculation of D_1 assuming that $\mu = 0$ and adopting the transport cross section instead of the total cross section. And D_{homo}^1 and D_{homo}^2 are evaluated by

$$D_{homo}^1 = 1 / (3 \bar{\Sigma}_t) , \quad D_{homo}^2 = 1 / (3 \bar{\Sigma}_{tr})$$

where $\bar{\Sigma}_t$ and $\bar{\Sigma}_{tr}$ are the homogenized total and transport cross sections averaged over a cell by weighting with the product of volume and flux.

From the table, we can see that, in so far as the principal term D_1 is concerned, D_{iso} is a good approximation for D_1 and that D_{homo}^2 underestimates the value a little. When we take into account the additional term D_2 , however, the diffusion coefficient $D_1 = D_1 + D_2$ shows a great change especially for a cell containing a fuel with

large absorption ratio (ratio of absorption cross section to total cross section). In such a system, $D_1 + D_2$ approaches the value of D_{homo}^1 instead of D_{homo}^2 . For a cell with small absorption ratio and with small lattice pitch, the additional term D_2 is usually small. This is especially the case for a system containing a moderator with absorption. This is based on the fact that, for such a system, the neutron flux approaches flat over a cell and the current becomes small and the D_2 evaluated from Eq. (5.50) becomes small.

In Table 5.4 the principal and the additional terms of the radial diffusion coefficient are presented together with the values of D_{homo}^2 for a square lattice. In a square cell containing a fuel and a moderator, the additional term has a significant contribution to the diffusion coefficient especially for $\mu = 0$ (μ = average cosine of the scattering angle in the moderator). But the ratio of D_2 to D_1 is not so large as in the slab cell. Though the additional term does not vary appreciably with μ , this term decreases a little for large μ . The homogeneous transport approximation for the diffusion coefficient

Table 5.4 Diffusion coefficient in a square cell

Total cross section in fuel : 1.0 cm^{-1}
 Total cross section in moderator : 2.0 cm^{-1}
 Scattering cross section in fuel : 0.5 cm^{-1}
 Scattering cross section in moderator : 2.0 cm^{-1}
 Fuel radius : 1.0 cm
 Lattice pitch : 3.5 cm

Average cosine of scattering angle	D_1	D_2	D_{homo}^2
0	0.1936	-0.03617	0.1814
1/3	0.2648	-0.03309	0.2620
2/3	0.4468	-0.02839	0.4559

becomes good for the square cell.

In the next place⁽¹⁵⁾, we treat the anisotropic diffusion coefficient in slab systems in a time dependent problem. In Table 5.5 are presented the values of the perpendicular diffusion coefficient in a slab lattice with absorbing fuel in the cell center. A cell is composed of a central fuel region with thickness 1.0 cm and the surrounding left and right moderator regions with thickness 2.0 cm respectively. The total cross section in the fuel is taken to be 1.0 cm^{-1} . In the first 5 cases the total cross section in the moderator is assumed to be 1.33333 cm^{-1} and the absorption in the moderator is taken to be zero and the scattering cross section in the fuel is changed from 0.3 to 0.99 cm^{-1} . In the following 5 cases the absorption in the moderator is taken into consideration. The total and scattering

Table 5.5 Diffusion coefficient D_{\perp} in slab cells

Σ_{mt}	Σ_{fs}	Σ_{ms}	D_1	Benoist D_2	D_{\perp}	Deniz	Homogeneous limit
1.33333	0.3	1.33333	0.2838	-0.1082	0.1756	0.2347	0.2702
1.33333	0.5	1.33333	0.2804	-0.08492	0.1955	0.2466	0.2692
1.33333	0.8	1.33333	0.2722	-0.03779	0.2344	0.2634	0.2666
1.33333	0.9	1.33333	0.2682	-0.01907	0.2491	0.2656	0.2652
1.33333	0.99	1.33333	0.2638	-0.00188	0.2619	0.2637	0.2634
1.5	0.3	1.0	0.3890	-0.03542	0.3535	0.3803	0.3753
1.5	0.5	1.0	0.3705	-0.10416*	0.3705	0.3705	0.3703
1.5	0.8	1.0	0.3305	0.04046	0.3710	0.2994	0.3538
1.5	0.9	1.0	0.3148	0.04182	0.3566	0.2618	0.3446
1.5	0.99	1.0	0.3003	0.03566	0.3360	0.2278	0.3346

Total cross section in the fuel: 1.0 cm^{-1}

Σ_{mt} : Total cross section in the moderator (cm^{-1})

Σ_{fs} : Scattering cross section in the fuel (cm^{-1})

Σ_{ms} : Scattering cross section in the moderator (cm^{-1})

Fuel thickness in a cell: 1.0 cm

Moderator thickness in a cell: 4.0 cm

cross sections in the moderator are taken to be 1.5 and 1.0 cm^{-1} , respectively. The scattering cross section in the fuel is changed from 0.3 to 0.99 cm^{-1} . For these 10 cases, values of the perpendicular diffusion coefficients D_{\perp} by Benoist are compared with those by Deniz and homogeneous approximation in the 4~8 columns. It is seen from this table that if the absorption both in the moderator and the fuel are small, the value of D_{\perp} from the Benoist formula is similar to that from the Deniz formula. When the absorption in the fuel increases, the difference between the values from Benoist's and Deniz's increases even if the absorption cross section in the moderator is zero. Even in these cases, the values from the Deniz formula are closer to those from the Benoist formula than those of homogeneous limit. If only the principal term of the Benoist formula is taken into account for the calculation of D_{\perp} , the values based on the Deniz formula are superior to those based on the principal term of Benoist in order to express the leakage rate of neutrons. When there is absorption in the moderator (last 5 cases), there can be seen a large difference between the values of D_{\perp} from the Benoist formula and those from the Deniz formula even if the absorption in the fuel is negligible. In these cases, the homogeneous limit of D_{\perp} is much closer to the values from the Benoist formula than those from the Deniz formula. Then the values from the Deniz formula are not desirable to adopt for the calculation of D_{\perp} in such a case.

In Tables 5.6 and 5.7 are shown the eigenvalues α/ν for various scattering cross sections in the fuel, which are adopted in the calculation of D_{\perp} in Table 5.5. The self-shielding effect on α/ν by the fuel is seen when the absorption in the fuel becomes large.

Table 5.6 Values of the decay constant

Total cross section in the fuel: 1.0 cm⁻¹
 Total cross section in the moderator: 1.33333 cm⁻¹
 Scattering cross section in the moderator: 1.33333 cm⁻¹
 Thickness of the fuel in a cell: 1.0 cm
 Thickness of the moderator in a cell: 4.0 cm

Scattering cross section in the fuel	Decay constant (α/ν)
0.1	0.07480
0.2	0.07141
0.3	0.06745
0.4	0.06276
0.5	0.05713
0.6	0.05028
0.7	0.04181
0.8	0.03117
0.9	0.01758
0.99	0.00197

Table 5.7 Values of the decay constant

Total cross section in the fuel: 1.0 cm⁻¹
 Total cross section in the moderator: 1.5 cm⁻¹
 Scattering cross section in the moderator: 1.0 cm⁻¹
 Thickness of the fuel in a cell: 1.0 cm
 Thickness of the moderator in a cell: 4.0 cm

Scattering cross section in the fuel	Decay constant (α/ν)
0.1	0.5519
0.2	0.5423
0.3	0.5311
0.4	0.5170
0.5	0.5000
0.6	0.4782
0.7	0.4496
0.8	0.4138
0.9	0.3700
0.99	0.3239

In Table 5.8 the values of D_1 from these three methods are presented for slab cells with central void region instead of the fuel. The geometrical arrangement and the cross sections in the moderator are the same as those in Table 5.5. In these cases, the additional term of Benoist's formula is very small and the very good agreement between the values by Benoist and Deniz can be seen. The values by the homogenized method slightly overestimates the value of D_1 .

In conclusion, the value from the Deniz formula (experimentally determined anisotropic diffusion coefficient from the pulsed neutron technique) approaches to the value from the Benoist formula if the absorption cross sections in the fuel and the moderator are small.

Table 5.8 Diffusion coefficient D_1 in slab cells with void region

Σ_{vs}	D_1	Benoist D_2	D_1	Deniz	Homogeneous limit
0.0003	0.3100	-0.1113×10^{-3}	0.3100	0.3101	0.3123
0.0005	0.3103	-0.8012×10^{-4}	0.3102	0.3103	0.3124
0.0008	0.3106	-0.2929×10^{-4}	0.3105	0.3106	0.3124
0.0009	0.3106	-0.1618×10^{-4}	0.3106	0.3106	0.3124
0.00099	0.3107	0.7989×10^{-6}	0.3107	0.3107	0.3124

Σ_{vs} : Scattering cross section in the void region (cm^{-1})

Total cross section in the void region: 0.001 cm^{-1}

Total cross section in the moderator: 1.33333 cm^{-1}

Scattering cross section in the moderator: 1.33333 cm^{-1}

Void thickness in a cell: 1.0 cm

Moderator thickness in a cell: 4.0 cm

Appendix 5A

Generalized Collision Probabilities in a Slab Cell

We use the following symbols:

l_i : thickness of the i -th region

$\hat{\Sigma}_{i,j}$: optical thickness from the i -th region to the j -th region,

including the both end regions i and j

N : number of regions in a cell

Then P_{ij}^{00} which corresponds to the usual first-flight collision probability is expressed by

$$P_{ij}^{00} = \frac{1}{2l_i \Sigma_i} \int_0^1 d\mu \mu \left(1 - e^{-\frac{\Sigma_i l_i}{\mu}}\right) \left(1 - e^{-\frac{\Sigma_j l_j}{\mu}}\right) \cdot \left\{ e^{-\frac{\hat{\Sigma}_{i+1,j-1}}{\mu}} + e^{-\frac{\hat{\Sigma}_{i,i-1} + \hat{\Sigma}_{j+1,N}}{\mu}} \right\} / \left(1 - e^{-\frac{\hat{\Sigma}_{i,N}}{\mu}}\right),$$

(for $j > i$) (5A.1)

$$P_{ij}^{00} = 1 - \frac{1}{2l_i \Sigma_i} + \frac{1}{l_i \Sigma_i} \int_0^1 d\mu \mu \left\{ e^{-\frac{\Sigma_i l_i}{\mu}} + \left(1 - e^{-\frac{\Sigma_i l_i}{\mu}}\right)^2 e^{-\frac{\hat{\Sigma}_{i,N} - \Sigma_i l_i}{\mu}} / \left(1 - e^{-\frac{\hat{\Sigma}_{i,N}}{\mu}}\right) \right\},$$

(for $j = i$) (5A.2)

$$P_{ij}^{00} = \frac{\Sigma_j l_j}{\Sigma_i l_i} P_{ji}^{00}.$$

(for $j < i$) (5A.3)

The quantity P_{ij}^{10} becomes

$$P_{ij}^{10} = \frac{3}{2l_i \Sigma_i} \int_0^1 d\mu \mu^2 \left(1 - e^{-\frac{\Sigma_i l_i}{\mu}}\right) \left(1 - e^{-\frac{\Sigma_j l_j}{\mu}}\right) \cdot \left\{ e^{-\frac{\hat{\Sigma}_{i+1,j-1}}{\mu}} - e^{-\frac{\hat{\Sigma}_{i,i-1} + \hat{\Sigma}_{j+1,N}}{\mu}} \right\} / \left(1 - e^{-\frac{\hat{\Sigma}_{i,N}}{\mu}}\right),$$

(for $j > i$) (5A.4)

$$P_{ij}^{10} = 0,$$

(for $j = i$) (5A.5)

$$P_{ij}^{10} = - \frac{\Sigma_j l_j}{\Sigma_i l_i} P_{ji}^{10}.$$

(for $j < i$) (5A.6)

The quantity P_{ij}^{20} becomes

$$P_{ij}^{20} = \frac{9}{2 l_i \Sigma_i} \int_0^1 d\mu \mu^3 (1 - e^{-\frac{\Sigma_i l_i}{\mu}}) (1 - e^{-\frac{\Sigma_j l_j}{\mu}}) \cdot \left\{ e^{-\frac{\widehat{\Sigma} l_{i+1, j-1}}{\mu}} + e^{-\frac{\widehat{\Sigma} l_{1, i-1} + \widehat{\Sigma} l_{j+1, N}}{\mu}} \right\} / (1 - e^{-\frac{\widehat{\Sigma} l_{1, N}}{\mu}}),$$

(for $j > i$) (5A.7)

$$P_{ij}^{20} = 3 \left(1 - \frac{3}{4 \Sigma_i l_i}\right) + \frac{9}{l_i \Sigma_i} \int_0^1 d\mu \mu^3 \left\{ e^{-\frac{\Sigma_i l_i}{\mu}} + (1 - e^{-\frac{\Sigma_i l_i}{\mu}})^2 \frac{e^{-\frac{\widehat{\Sigma} l_{1, N} - \Sigma_i l_i}{\mu}}}{1 - e^{-\frac{\widehat{\Sigma} l_{1, N}}{\mu}}} \right\},$$

(for $j = i$) (5A.8)

$$P_{ij}^{20} = -\frac{\Sigma_j l_j}{\Sigma_i l_i} P_{ji}^{20}.$$

(for $j < i$) (5A.9)

And the quantity P_{ij}^{21} becomes

$$P_{ij}^{21} = -\frac{9}{2 l_i \Sigma_i} \int_0^1 d\mu \mu^3 (1 - e^{-\frac{\Sigma_i l_i}{\mu}}) (1 - e^{-\frac{\Sigma_j l_j}{\mu}}) \cdot \left\{ e^{-\frac{\widehat{\Sigma} l_{i+1, j-1}}{\mu}} - e^{-\frac{\widehat{\Sigma} l_{1, i-1} + \widehat{\Sigma} l_{j+1, N}}{\mu}} \right\} / (1 - e^{-\frac{\widehat{\Sigma} l_{1, N}}{\mu}}),$$

(for $j > i$) (5A.10)

$$P_{ij}^{21} = 0,$$

(for $j = i$) (5A.11)

$$P_{ij}^{21} = -\frac{\Sigma_j l_j}{\Sigma_i l_i} P_{ji}^{21}.$$

(for $j < i$) (5A.12)

Other quantities P_{ij}^{01} and P_{ij}^{11} are calculated by the relations in

Eq. (5.41).

Appendix 5B

Generalized Collision Probabilities in a Square Cell

In the calculation of the probabilities P_{ij} ($i \neq j$), for convenience, we assume that the neutron starts from the center of the i -th region and reaches the center of the j -th region. Then we obtain⁽⁶⁾

$$P_{ij}^{00} = \frac{V_i \Sigma_j}{2\pi \rho_{ij}^2} K_{i1}(\tau_{ij}), \quad (5B.1)$$

$$P_{ij}^{1x,0} = \frac{3 V_i \Sigma_j (x_j - x_i)}{2\pi \rho_{ij}^3} K_{i2}(\tau_{ij}), \quad (5B.2)$$

$$P_{ij}^{1y,0} = \frac{3 V_i \Sigma_j (y_j - y_i)}{2\pi \rho_{ij}^3} K_{i2}(\tau_{ij}), \quad (5B.3)$$

$$P_{ij}^{1x,1x} = \frac{3 V_i \Sigma_j (x_j - x_i)^2}{2\pi \rho_{ij}^3} K_{i3}(\tau_{ij}), \quad (5B.4)$$

$$P_{ij}^{1y,1x} = \frac{3 V_i \Sigma_j (x_j - x_i)(y_j - y_i)}{2\pi \rho_{ij}^3} K_{i3}(\tau_{ij}), \quad (5B.5)$$

$$P_{ij}^{1y,1y} = \frac{3 V_i \Sigma_j (y_j - y_i)^2}{2\pi \rho_{ij}^3} K_{i3}(\tau_{ij}), \quad (5B.6)$$

$$P_{ij}^{2x,1x} = \frac{9 V_i \Sigma_j (x_j - x_i)^3}{2\pi \rho_{ij}^4} K_{i4}(\tau_{ij}), \quad (5B.7)$$

$$P_{ij}^{2x,1y} = \frac{9 V_i \Sigma_j (x_j - x_i)^2 (y_j - y_i)}{2\pi \rho_{ij}^4} K_{i4}(\tau_{ij}), \quad (5B.8)$$

$$P_{ij}^{1x,1y,1y} = \frac{9 V_i \Sigma_j (x_j - x_i)(y_j - y_i)^2}{2\pi \rho_{ij}^4} K_{i4}(\tau_{ij}). \quad (5B.9)$$

References

- (1) BENOIST,P.: CEA-R 2278, (1964)
- (2) BENOIST,P.: J. Nucl. Energy, Pt A, 13, 97 (1961).
- (3) LESLIE,D.C.: Reactor Sci. Tech., 16, 1 (1962).
- (4) SEKIYA,T., TAKEDA,T.: Technol. Report, Osaka Univ., 18,
303 (1968).
- (5) TAKEDA,T., SEKIYA,T.: ibid., 22, 11 (1972)
- (6) DANCE,K.D., CONNOLLY,T.J.: J. Nucl. Energy, 25, 155 (1971).
- (7) BULL,S.R., CONNOLLY,T.J.: ibid., 25, 179 (1971).
- (8) DENIZ,V.: Nucl. Sci. Eng., 32, 201 (1968).
- (9) BONALUMI,R.A.: CISE-N-146, (1971).
- (10) TAKEDA,T., SEKIYA,T.: To be published in J. Nucl. Sci. Technol.
- (11) GRANT,I.S.: AERE R/R 2568, (1958).
- (12) SELENGUT,D.S.: HW-60220, 65 (1959).
- (13) WILLIAMS,M.M.R.: Atomkernenergie, 18, 31 (1971).
- (14) SPINRAD,B.I.: J. Appl. Physics, 26, 548 (1955).
- (15) TAKEDA,T., SEKIYA,T.: J. Nucl. Sci. Technol., 9, 682 (1972).

CHAPTER 6

SUMMARY AND CONCLUSIONS

The purpose of this thesis is to improve the collision probability method and to apply it to various lattice systems. The fundamental assumptions included in the usual first-flight collision probability method are as follows:

- (1) isotropic scattering in the laboratory system,
- (2) isotropic source distribution,
- (3) flat flux in each region.

All these assumptions were removed in Chap. 2 by introducing a generalized first-flight collision probability. Thus the method has been made to permit the treatment of the neutron behaviour in a fast energy region, where scattering shows remarkable anisotropy.

Usually it is assumed that the real boundary may be replaced by a circular one — Wigner Seitz cell method. This assumption, however, becomes inadequate for tightly packed lattice cells. The improvement on this assumption was performed in Chap. 3 by extending the multiple collision probability method. Thereby the effect of the cell boundary for arbitrary polygonal cells upon the flux distribution could concisely be taken into account through an extended Dancoff factor.

Chap. 4 was devoted to the applications of the usual first-flight collision probability method to the flux calculations in cluster

systems, in finite systems and in an isolated resonance energy region.

In Chap. 5 the anisotropic diffusion coefficients were calculated by using the generalized first-flight collision probability.

Concerning the integral transport theory, there remain some problems. Some important problems are

- (1) the treatment of complicated three-dimensional systems,
- (2) the calculation of the neutron spectra in terms of appropriate group constants,
- (3) time dependent problems.

The calculation of the first-flight collision probability in three dimensional systems requires a large amount of computer time. In more complicated systems than the finite systems treated in §4.3, the synthesis method seems to be most promising. Usually the synthesis method is used for the integro-differential transport equation. Its application to the integral transport theory will make it possible to treat a highly heterogeneous three-dimensional system.

The extension of the methods included in this thesis to the multi-group theory is easily done if the group constants or the neutron cross sections are known. These constants are, however, still dependent on the neutron spectra. Usually they are obtained iteratively; first, the neutron spectra are calculated by using approximately chosen group constants, and then, group constants are recalculated from the spectra obtained and so on. This process is very troublesome. Therefore, appropriate choice of cross sections, for example by a variational method for the integral transport theory, is needed.

Treatments of the time dependent problems are necessary for the study of the pulsed neutrons as well as the fuel burn-up. If only

the asymptotic mode of neutron behaviour in time is needed, the problem is reduced to that of obtaining the eigenvalue in homogeneous equations in which the first-flight collision probability is included as in §5.2. If the neutron cross sections change with time, the problem becomes very complicated and some approximations, such as the synthesis method, are required.

ACKNOWLEDGEMENT

The author would like to express his greatest appreciation to Professor T. Sekiya who has guided the author to the present study and has been giving valuable suggestions and criticisms.

The author would also like to express his gratitude to Mr. K. Azekura, Mr. K. Nakamura and Mr. T. Ogawa for their assistances in making this thesis.

The author would also like to express his deep appreciation to Dr. P. Benoist, Dr. Y. Fukai and Dr. K. Tsuchihashi for their helpful comments.

The author also wishes to express his appreciation to Dr. T. Kobayashi for his correction of this thesis.

LIST OF PUBLICATIONS BY THE AUTHOR

- (1) Effect of Anisotropic Hole Systems on the Neutron Streaming in a Moderator (1),
Technol. Report, Osaka Univ., 18, 303 (1968).
- (2) Asymptotic Neutron Distribution in a Finite Cylinder,
J. Nucl. Sci. Technol., 8, 133 (1971).
- (3) Improvement to the Calculation of Collision Probabilities in Annular System and Its Application to Cluster Geometry,
J. Nucl. Sci. Technol., 8, 503 (1971).
- (4) Disadvantage Factor in a Cell with Thin Moderator,
J. Nucl. Sci. Technol., 8, 539 (1971).
- (5) Moderator Correction for a Wide Resonance by the Greuling-Goertzel Approximation,
J. Nucl. Sci. Technol., 8, 649 (1971).
- (6) Anisotropic Collision Probabilities in Cell Problems,
J. Nucl. Sci. Technol., 8, 663 (1971).
- (7) Effect of Anisotropic Scattering in a Square Cell with Thin Moderator,
J. Nucl. Sci. Technol., 9, 53 (1972).
- (8) Effect of Higher Order Anisotropy on Disadvantage Factor in a Cell,
J. Nucl. Sci. Technol., 9, 249 (1972).
- (9) Effects of Anisotropic Hole Systems on the Neutron Streaming in a Moderator II,
Technol. Report, Osaka Univ., 22, 11 (1972).
- (10) Neutron Flux in Polygonal Cells,
Technol. Report, Osaka Univ., 22, 345 (1972).

- (11) Comparison of the Anisotropic Diffusion Coefficient Based on
the Benoist and Deniz Formulae,
J. Nucl. Sci. Technol., 9, 682 (1972).
- (12) Finiteness of Cell Systems in the Axial Direction,
To be published in Technol. Report, Osaka Univ.
- (13) Space and Angle Dependent Collision Probability in Cell Problems,
To be published in J. Nucl. Energy.
- (14) Calculation of the Anisotropic Diffusion Coefficient,
To be published in J. Nucl. Sci. Technol.